No. 231

Shortwave Propagation

—including the Rider Global Time Conversion Simplifier—

by Stanley Leinwoll

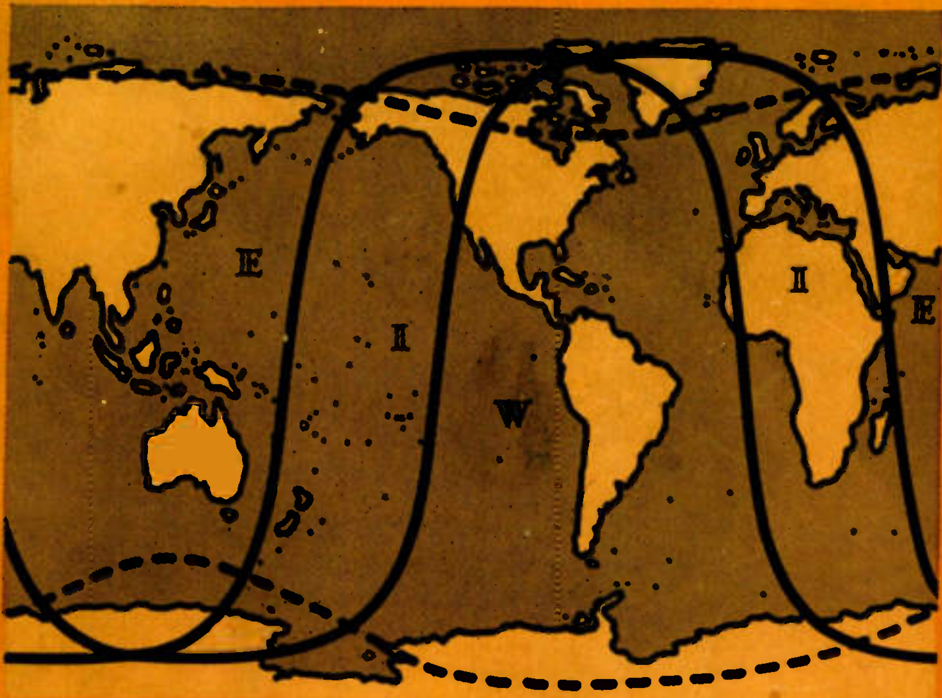

a RIDER publication

Shortwave Propagation

$3.90

Shortwave Propagation

by Stanley Leinwoll

Manager, Radio Frequency and Propagation
Radio Free Europe

JOHN F. RIDER PUBLISHER, INC.
NEW YORK

Library of Congress Catalog Card No. 59-15080

Printed in the United States of America

Preface

All present radio communication is brought about by the propagation of radio waves from transmitter to receiver. The medium which carries these radio waves is called the ionosphere. In general, long-distance radio communication is carried on almost exclusively in the shortwave bands, at frequencies ranging from 3 to 30 megacycles, on wavelengths from 100 to 10 meters.

This book presents in a straightforward manner the basic principles of shortwave radio propagation and the method in which they are used to help solve the everyday problems of long-distance shortwave radio communications.

We have attempted to present in a simple and concise manner all of the important theoretical, as well as the practical, aspects and applications of shortwave radio propagation. The chapters on Circuit Analysis, MUF Curves, and Forecasting Ionospheric Conditions are geared to the practical approach.

This book is of special interest to those interested in long-distance shortwave radio communications. For the communications engineer this interest is professional. For the amateur radioman—the ham—the interest may be that of a hobby, but because of his efforts, significant advances have been made in the field of radio communications.

We have, wherever possible, avoided the use of mathematics and have attempted to set forth all concepts in the simplest possible manner. At one or two points where the explanation of a particular concept was extremely complex, we have drawn analogies to clarify the principles involved.

Acknowledgment is made to the Central Radio Propagation Laboratories of the National Bureau of Standards for permission to use the charts and nomograms included in Chapter 8.

PREFACE

A great many people contributed to the preparation of this book; but I would like to thank the several people to whom I am especially grateful: Claude Harris, Director of Engineering at Radio Free Europe, George Jacobs and Edgar Martin of the Voice of America, John Nelson of RCA Communications, Jim Weldon, Chief Forecaster of the North Atlantic Radio Warning Service of the Bureau of Standards, Dr. Carl Gartlein of Cornell University, and my wife, Miriam, without whose patience, understanding, encouragement, and assistance this book would not have been written.

Stanley Leinwoll

New York, New York
October, 1959

Contents

Chapter 1

THE IONOSPHERE

INTRODUCTION

All radio communication takes place because radio waves travel from a transmitter to a receiver. These waves are electromagnetic in nature and are produced by rapidly oscillating currents in the transmitting antenna.

The medium through which the waves are transported through space for reception at great distances is known as the *ionosphere*. Without this medium, which is a region of ionized gases in the upper atmosphere, long-distance radio communication around the spherically shaped earth would, at best, be exceedingly difficult.

This book covers primarily the behavior of these electromagnetic radio waves from the time they leave the transmitting antenna to the time they arrive at the receiving antenna, and particularly when the receiving antenna lies far from the transmitter, at a considerable distance around the curvature of the earth.

At the present time, long-distance radio communication is carried almost exclusively on shortwave—on frequencies ranging from 3 to 30 megacycles (mc) on wavelengths of 100 to 10 meters.

It is generally not possible to carry out such long-distance communication on medium-wave frequencies, which range from 300 to 3000 kilocycles (kc) on wavelengths of 1000 to 100 meters, or on frequencies above 30 mc on wavelengths of 10 meters or below.

Although it is possible to carry out long-distance communication on some frequencies in the long- and very-long-wave bands (frequencies below 300 kc and wavelengths above 1000 meters), the size and cost of plant and equipment involved are prohibitive in comparison to similar services available in the shortwave bands.

As a result of the foregoing, utilization of shortwave frequencies and their medium of transportation, the ionosphere, represents the almost exclusive means by which long-distance radio communication is carried on by modern man.

A BRIEF HISTORY

In 1901, Guglielmo Marconi successfully completed one of the most significant experiments in the history of mankind: the transmission of a radio signal, without wires, across 2000 miles of ocean. But the experiment, however successful, posed quite a problem.

In picking up in Newfoundland radio signals transmitted from England, Marconi had done what had previously been shown to be impossible. Prior to 1901, it had been proved mathematically that the ground wave could not possibly travel along the earth's surface to such distances and produce the signal received in Newfoundland. It had also been shown that radio waves traveling through the air moved in straight lines. Heinrich Hertz, a great German physicist, demonstrated that the direction of radio signals could be altered by interposing an obstacle in their path. This meant that Marconi's signal had to pass through the atmosphere and into outer space, *unless* something had been put in the way of the signal—something about 200 miles up. But what kind of obstacle could possibly exist 200 miles above the surface of the earth? The problem kept the scientific world in a dither for a year.

In 1902, Arthur Kennelly in the United States and Oliver Heaviside in Great Britain suggested, in independent and almost simultaneous scientific papers, that the condition of the air in the upper atmosphere was sufficiently different from the air at ground level to render possible the reflection of radio waves back to earth. If the air in the upper atmosphere were actually capable of conduction, instead of being a good insulator as is the air on earth, then it was possible, they reasoned, for this region to guide radio signals back to earth at great distances from the transmitter. It was two decades before the theories of Kennelly and Heaviside could be verified.

The first experiments which positively proved the existence of a conducting region far above the surface of the earth were conducted in 1924 and 1925 by Sir Edward Appleton and his associates, using

British Broadcasting Corporation facilities. (During the years between 1902 and 1924, the BBC was a leader in the great expansion and development of the science of radio communication.)

Appleton and his co-workers performed numerous experiments indicating that radio waves from a distant transmitting station were coming down at an angle. They also found that the structure of this conducting region, which they named the *ionosphere,* was much more complex than could have been expected, that it consisted of several ionized layers of gas lying one above the other in the atmosphere, beginning at a height of about 50 miles above the surface of the earth. In addition, the characteristics of the ionosphere were found to vary from hour to hour and from day to day, as well as over longer periods.

Still another series of historic experiments was performed in 1925 by two American physicists, Breit and Tuve, of the National Bureau of Standards, who sent short pulsed waves straight up, then measured the time between the transmission of the original pulse and the return to earth of its reflected echo. Using this method, they were able to determine the heights of the reflecting regions, as well as such other characteristics as conductivity, and diurnal and seasonal changes.

A seemingly unrelated series of experiments conducted a short time later by Dr. Edison Pettit of the Mount Wilson Observatory contributed greatly to our knowledge of the ionosphere and long-distance radio communications. Dr. Pettit and his associates discovered that the intensity of ultraviolet radiation from the sun varies in direct proportion to sunspot activity, with the greatest ultraviolet intensity occurring during periods of maximum sunspot activity. Since ionospheric characteristics were seen to vary with sunspot activity, it was concluded from Dr. Pettit's discovery that ultraviolet radiation was of prime importance in the formation and behavior of the ionosphere.

Further evidence that the sun's energy primarily governs the characteristics of the ionosphere was gathered during the total eclipse of 1927. Figure 1-1 shows the relationship between solar radiation and ionization in the upper atmosphere. At the outset of the eclipse, when the moon begins to cut off the rays of the sun, the degree of ionization begins to fall. This decrease continues until the moon has totally eclipsed the sun, when ionization is at a minimum. Thereafter it increases again until it reaches normal levels a short time after the conclusion of the eclipse. Because the decrease in ionization begins at the same time that the cutoff of heat and light commences, it must be concluded that all three agents—light, heat, and ionization radiation—reach the earth simultaneously.

FORMATION OF THE IONOSPHERE

The gases constituting the earth's atmosphere are composed mainly of oxygen, nitrogen, hydrogen, and helium. At distances relatively close to the earth, these gases occur in a rather homogeneous mixture, being kept uniformly mixed by the action of the weather. In the upper regions of the atmosphere, however, these weather effects do not occur.

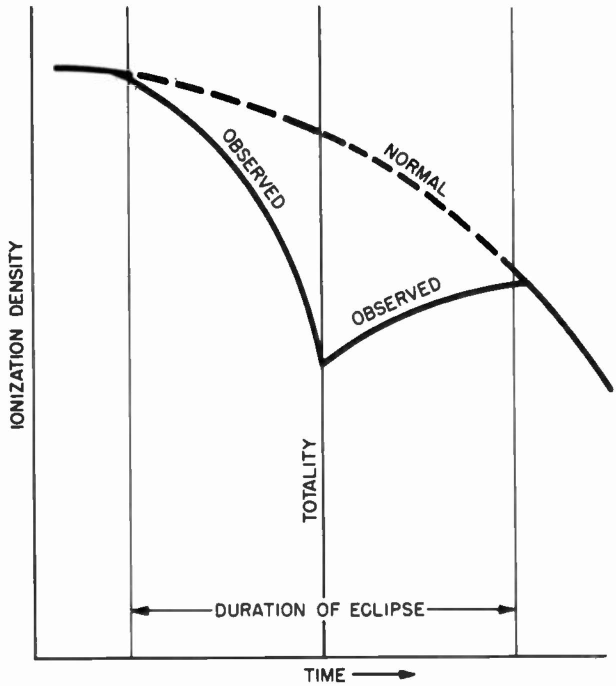

Fig. 1-1. Effects of eclipse of the sun on ionization density in the ionosphere. Cutoff of solar radiation resulted in sharp drop in ionization.

Consequently, the gases tend to become separated, with the lighter ones rising higher than the heavier ones. This results in a tendency for particular gases to exist at certain levels. In addition, gas density increases as the lower of these gas levels is approached; ultraviolet intensity decreases as density increases.

Like all matter, gases are composed of atoms. The *atom* is a fundamental unit of matter, made up of a positively charged *nucleus* surrounded by units of negative electricity called *electrons*. The entire system is in electrical equilibrium and is said to be neutral.

The ionosphere is formed by ultraviolet light from the sun bombarding these various gas atoms high in the upper atmosphere. Energy from these ultraviolet rays is absorbed by the atoms, which are set into such a state of agitation that electrons are dislodged from the formerly neutral atoms. This interaction between gas atoms and ultraviolet radiation produces free electrons and atoms which have lost one or more electrons. These are called *ions*. Because they have lost negative charge, the net charge remaining on the previously neutral atom is positive; it is therefore referred to as a positive ion (see Fig. 1-2).

Since gases of different densities are encountered at different heights above the earth by the descending ultraviolet rays, several distinct layers of ionized gas are formed in the upper atmosphere. Since the free electrons within the layers are capable of movement independent of the surrounding ions, each layer of ionized gas has the property of a

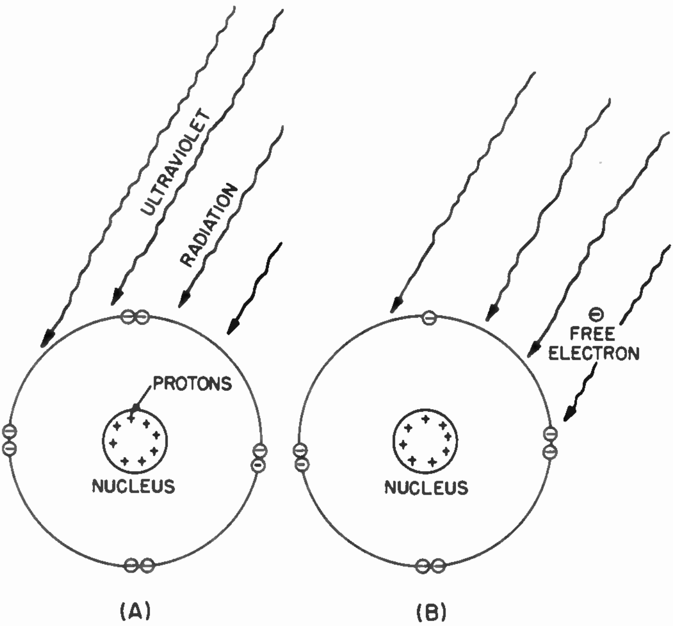

Fig. 1-2. Ionization. (A) Neutral atom: charge of +8 balanced by charge of −8 planetary electrons. (B) Positive ion: ultraviolet radiation has dislodged an electron, leaving a net charge of +1 on the nucleus.

metallic conductor and is therefore capable of returning radio waves to earth.

THE STRUCTURE OF THE IONOSPHERE

The most important layer of the ionosphere is the *F* layer. It is the primary layer for the reflection of long-distance shortwave radio signals. It occurs at heights between 100 and 250 miles above the surface of the earth. The assignment of letters to the various layers was inaugurated by Sir Edward Appleton, who discovered and named the *D, E,* and *F* layers. He considerately left the letters *A, B,* and *C* for the designation of other layers, which, he felt, might be discovered at some future time. As yet, no one has made use of these letters, and it seems unlikely that anyone will.

During the daylight hours the highly important *F* layer divides into two distinct layers; the lower one is designated the F_1, the upper F_2. During the day, the F_2 is the most important refracting layer for shortwave signals.

Below the F_1 layer, approximately 60 miles above the earth, is the *E* layer. Though capable of reflecting some shortwave radio signals during the daylight hours, its importance is secondary to the *F*, and it

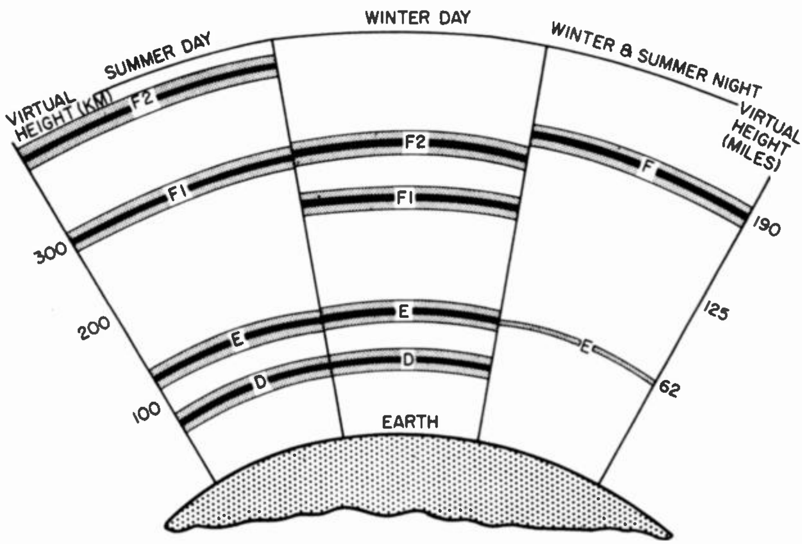

Fig. 1-3 Daily and seasonal variations in virtual ionospheric layer heights.

is generally limited to short-haul circuits. The *D* layer occurs at the lower limits of the *E* layer during the daylight hours only. Most of the absorption of short radio waves occurs in this region.

We have mentioned before that it is the rays of the sun, in particular ultraviolet radiation, which are responsible for the breakup of neutral gas atoms in the upper atmosphere, thereby causing the formation of the ionosphere. It follows that when the sun's rays are cut off—during an eclipse (see Fig. 1-1) or at night—a reversal or recombination of ions and free electrons should, and actually does, occur. This reversal affects the height and characteristics of the nighttime ionosphere.

Seasonal changes also affect the structure and behavior of the ionosphere. During the wintertime, with the earth significantly closer to the sun, ultraviolet radiation is much more intense. Consequently, ionization during the daylight hours proceeds more rapidly and extensively in the northern hemisphere than during the summertime. On the other hand, since winter nights in this hemisphere are considerably longer than during the summer, recombination, or de-ionization, takes place to a much greater extent, and ionospheric characteristics are profoundly affected. Figure 1-3 shows typical layer heights in the northern hemisphere for winter and summer, day and night.

We have seen thus far how ultraviolet radiation is of profound importance in the formation and structure of the ionosphere and how normal diurnal and seasonal changes in ultraviolet radiation affect the behavior and characteristics of the ionosphere. In addition, there are long-term normal changes, as well as various abnormal changes in radiation from the sun, which profoundly affect man's "mirror" in the heavens. All of these variations will be treated in greater detail in subsequent chapters.

Chapter 2

RADIO WAVES

THE NATURE OF RADIO WAVES

In a transmitting antenna, electrons can be made to oscillate rapidly. Because electrons in motion constitute an electric current, we actually have in the transmitting antenna minute electric currents which are rapidly changing direction as the direction of motion of the vibrating electrons is changing. The rapidly changing electric currents give rise to electric and magnetic fields which are vibrating and changing. These electric and magnetic fields radiate outward from the antenna into space at the speed of light (186,000 miles per second; 300 million meters per second) and, taken together, constitute the electromagnetic radio wave.

If we examine one such radio wave, we find that it is actually made up of two distinct parts, or components—the electric field and the magnetic field. Figure 2-1(A) illustrates the electric and magnetic component of a radio wave which is traveling outward from point *O* on the page toward the reader. The electric field, the direction of motion of the wave, and the magnetic field are all perpendicular to one another. In addition, the magnitude and direction of both the electric and magnetic fields are varying. Figure 2-1, (B) and (C), shows only the electric component of the wave at different times after it has left the transmitting antenna. We can see that the electric field has changed from a maximum in one direction, through zero at point *O′*, to a maximum in the other direction, through zero again, and back to the original magnitude and direction shown in Fig. 2-1(A).

The change in E from Fig. 2-1(A) to 2-1(C) is known as a "cycle." During this cycle, every possible value and direction of E has been traversed. If we draw a smooth curve joining every possible value of E, we get a *sine* curve, as shown, and E is said to vary *sinusoidally*. The magnetic (H) component of the radio wave also varies sinusoidally.

Figure 2-1 has illustrated the simplest type of radio wave—one in which the E and H components are fixed and vary in "phase," with

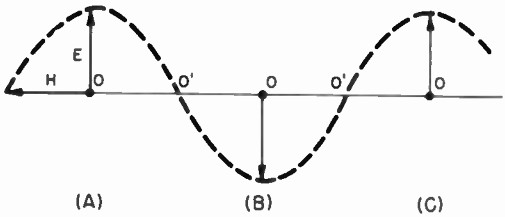

Fig. 2-1. Electric and magnetic components of a radio wave traveling out of the page toward the reader. Variations in electric component through one cycle are shown.

the relative magnitude and direction remaining fixed. Actually, very complex relationships between E and H are possible.

In Fig. 2-1, the E component varies in an up-and-down (vertical) direction. If this variation is with respect to the earth, the wave is said to be vertically polarized. If the E component varies horizontally, the wave is said to be horizontally polarized.

The number of cycles traversed in a given time is known as the *frequency*. Usually the unit of time used is the *second*. Thus, if the time taken during a complete cycle is 1 second, the frequency is 1 cycle per second.

Since the electromagnetic wave oscillates at astronomically high rates, it is more convenient to use kilocycles and megacycles:

$$1 \text{ kilocycle (kc)} = 1000 \text{ cycles},$$
$$1 \text{ megacycle (mc)} = 1000 \text{ kc} = 1{,}000{,}000 \text{ cycles}.$$

RELATIONSHIP BETWEEN FREQUENCY AND WAVELENGTH

The velocity of a radio wave traveling in free space is 186,000 miles, or 300 million meters, per second. The metric system, because it is so much more convenient and easy to handle, with all its units related in terms of tens, hundreds, or thousands, is used throughout this book.

For a brief review:

$$1 \text{ meter} = 39.37 \text{ inches}$$
$$1 \text{ kilometer} = 1000 \text{ meters}.$$
$$1 \text{ kilometer} = 0.62 \text{ mile}$$

The relationship connecting the velocity of a radio wave, its frequency, and its wavelength is

$$\text{Frequency (in kc/sec)} = \frac{300{,}000 \text{ km/sec}}{\text{wavelength (in meters)}}$$

Frequency is generally abbreviated by using the letter f; for wavelength, the Greek letter lambda (λ) is generally used. Thus,

$$f = \frac{300{,}000}{\lambda}, \tag{1}$$

or transposing,

$$\lambda = \frac{300{,}000}{f}. \tag{2}$$

A picture of the relationship between frequency, wavelength, and velocity of a radio wave may assist us in our understanding of this concept. Figure 2-2 depicts a radio wave that has left its antenna at point O 1 second ago and has completed 3 cycles. It has traveled 300 million meters (the velocity of a radio wave per second in space).

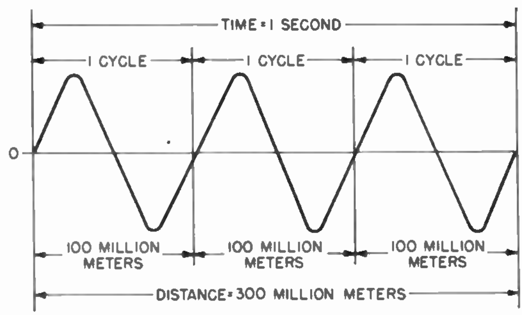

Fig. 2-2. Pictorial representation of relationships among frequency, wavelength, and velocity of a radio wave.

Since 3 full cycles have been completed, the length of the wave, or the wavelength (one wave is radiated for each complete cycle), equals 300 million meters per second, divided by 3 cycles, equals 100 million meters. This is quite a wavelength!

To solve a problem involving the conversion of frequency to wavelength, or vice versa, one of the quantities f or λ must be given. For example, suppose we have a wavelength of 10.15 meters, and we want to solve for frequency. Using equation (1), we get

$$f = \frac{300{,}000}{10.15} = 29{,}557 \text{ kc/sec}$$

$$= 29.557 \text{ mc/sec}$$

where kc/sec stands for kilocycles per second and mc/sec for megacycles per second.

If we were given a frequency of 7063 kc/sec and wished to find the wavelength, we would use equation (2):

$$\lambda = \frac{300{,}000}{7063} = 42.47 \text{ meters}$$

THE GROUND WAVE

Figure 2-3 shows the direction of travel of a radio wave as it leaves its transmitting antenna, point *T*. Figure 2-3 (A) gives a side view of the antenna and radio waves, and Fig. 2-3(B) a top view.

Although the radio wave is shown traveling in all directions (both outward and upward), it should be pointed out that the characteristics of the transmitting antenna can be altered so that much of the radiation is concentrated in a given direction. Such an antenna is called a "directional" antenna, as opposed to the "omnidirectional" antenna we have chosen in our illustration. Actually, Fig. 2-3 is intended to show only the direction of travel of the radio waves and not their magnitude, since it would be quite an accomplishment to construct an antenna that radiated equal amounts of energy in all directions.

We can see from Fig. 2-3 that there are potentially many paths a radio wave can take in traveling from transmitter to antenna. Essentially though, there are three primary modes of transmission of the radio wave. We shall first consider the *ground wave.*

Inspection of Fig. 2-3(A) shows that some of the energy radiated is traveling in directions parallel or nearly parallel to the ground. Ground-wave propagation refers to the transmission of radio waves which remain in contact with the ground, being guided by the earth and moving parallel to it, throughout their journey from transmitter to receiver. This contact with the ground causes the wave to set up minute electric currents in the earth. These "earth currents" cause a weakening in the wave, because energy is required to produce them, and energy is taken from the wave itself.

What we have then is a downward conduction of energy from the wave itself to the ground to replace that part of the energy which has

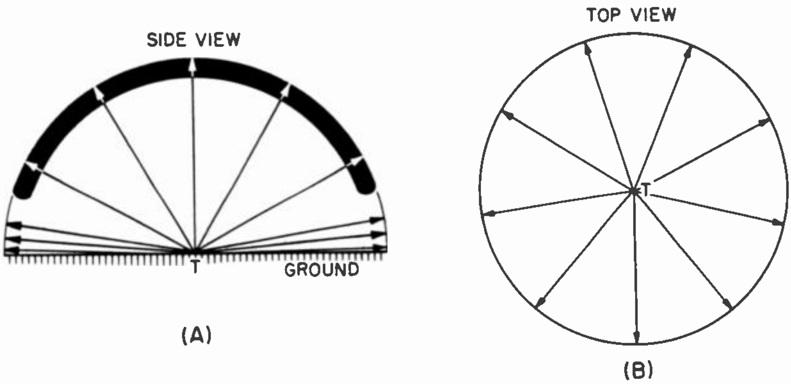

Fig. 2-3. Horizontal and vertical projection of a radio wave leaving a transmitting antenna at point *T*.

gone into the production of the earth current. As this transfer of energy continues, the wave continues to weaken and ultimately disappears completely. This weakening or "attenuation" of the ground wave varies considerably. It is dependent, among other things, on the type of terrain over which the wave travels, as well as on the frequency of the wave.

When the conductivity of the earth over which the wave travels is high, ground losses, sometimes referred to as "ground-absorption losses" are relatively low, as, for example, over sea water. As the conductivity of the earth decreases, ground absorption increases, and attenuation of the ground-propagated signal becomes more rapid. Because of ground absorption, that part of the wave which is in contact with the ground tends to lag somewhat behind the parts of the wave above it. Consequently, the wave tends to acquire a forward tilt, which is of prime importance in guiding it along the curved surface of the earth. Since a radio wave in air travels in perfectly straight lines, the ground wave, were it not for this tilting effect, would escape into space instead of following the curvature of the earth.

In addition to ground losses due to the nature of the terrain over which the wave travels, there are losses which vary with the frequency of the wave. As a matter of fact, frequency of the wave primarily determines the characteristics of the ground-wave signal.

As the frequency increases, the wavelength decreases. With decreasing wavelength, the resistance of the earth, and consequently the ground loss, increases. Figure 2-4 shows this relationship. For a constant

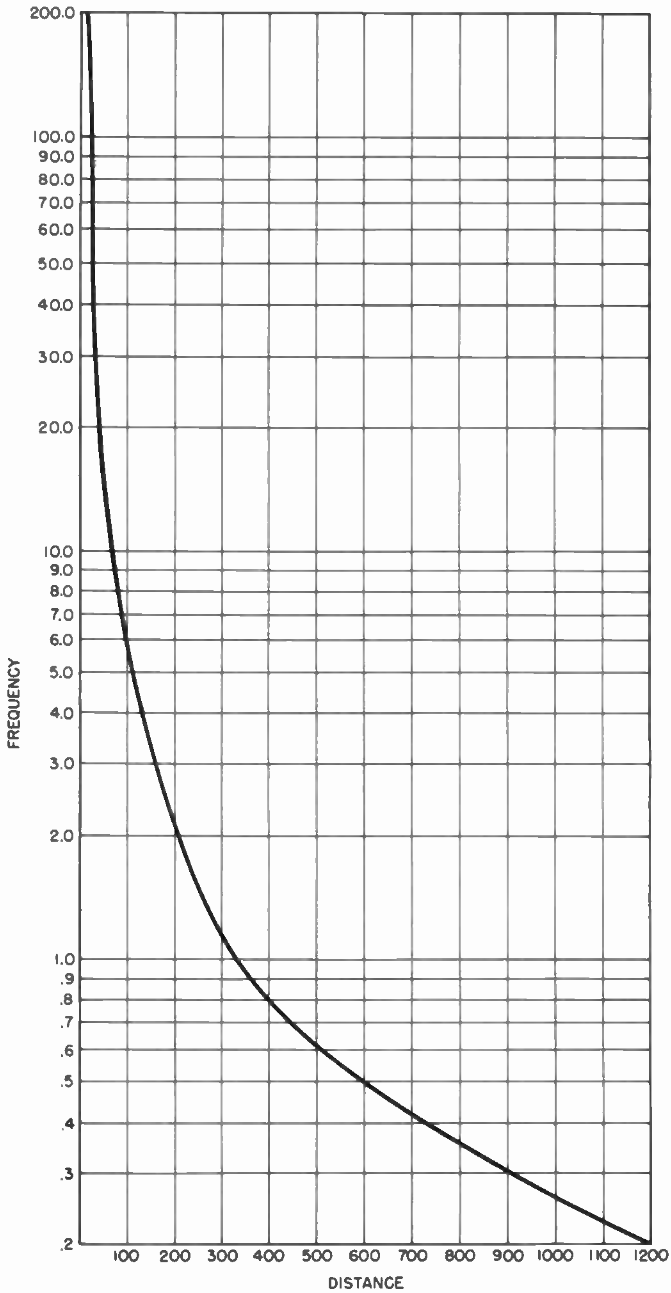

Fig. 2-4. Variation of frequency with distance.

value of field intensity (signal strength), we have plotted frequency in kilocycles versus distance in miles. As the frequency decreases, ground-wave coverage may extend to considerable distances; also, as the higher frequencies are approached, the ground wave falls off very rapidly. At frequencies above 30 mc/sec, ground-wave coverage is so poor that it is practically nonexistent.

The preceding holds true only for vertically polarized waves. The horizontally polarized component of a radio wave is very rapidly attenuated by the earth, regardless of the type of terrain.

The *direct* or *space wave* is the component of the wave that travels directly from the transmitting antenna without touching either the ground or the ionosphere. Direct-wave propagation is also known as "line-of-sight" transmission. From Fig. 2-5 we can see that only Receiver 1 is within the line of sight, whereas Receiver 2 is below the horizon and incapable of receiving the direct wave. Note, on the other hand, how the ground-wave component of the wave travels around the curvature of the earth to Receiver 2.

THE SKY WAVE

By far the most important of the three radio-wave components mentioned previously is the *sky wave*. Without it, long-distance radio communication would be exceedingly difficult, cumbersome, and expensive.

In discussing the ground and space waves, we have limited ourselves principally to the radio waves which left the antenna either parallel to the ground, or at small angles to it. Hereafter we will consider almost exclusively that portion of the radiated energy which leaves the antenna at higher angles, as shown under the shaded arrow-

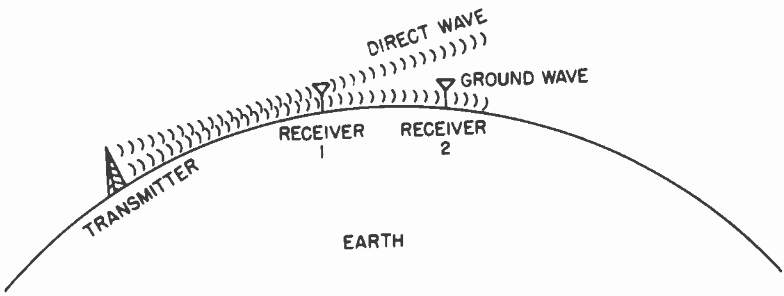

Fig. 2-5. Direct-wave and ground-wave transmission.

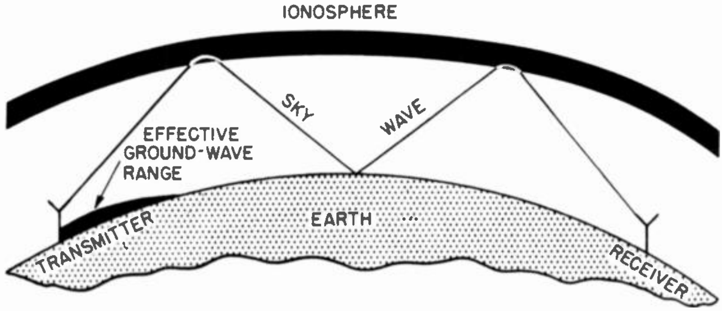

Fig. 2-6. Sky-wave transmission to a distant receiver.

heads of Fig. 2-3(A). These waves, on leaving the antenna, travel upward toward the earth's atmosphere.

If the air surrounding the earth were uniformly homogeneous, the component of the wave traveling into the sky (hence the term *sky wave*) would, in a fraction of a second, be tens of thousands of miles out in space. (In 0.10 second, a radio wave travels 18,600 miles.) Under such conditions, long-distance shortwave radio communication would not be possible.

Fortunately, the blanket of gases surrounding the earth is not homogeneous. Far above the earth, at distances ranging from 40 to well over 200 miles, there is an electrified region consisting of ionized gases and known as the ionosphere, which is capable of returning these radio waves to earth (see Fig. 2-6).

As the radio wave travels into the ionosphere, its direction of motion and velocity begins to change. Slowly, as it penetrates more deeply, it continues to bend back toward the earth until finally it leaves the ionosphere, heading back to earth. The angle at which the wave leaves the ionosphere is the same as the angle at which it entered. By the time the wave is back in "normal" air, it is traveling with its original velocity. On reaching the earth's surface, the wave is reflected and "bounces" back up toward the ionosphere again, like a ping-pong ball. This bounce is known as a reflection, and the angle at which the radio wave is reflected is identical to the angle at which it left the transmitting antenna.

Upon reaching the ionosphere again, the wave is once more bent (this bending process is known as refraction) and is returned to earth a second time. The process by which the transmitted radio wave is refracted by the ionosphere and returned to earth is known as a *hop*. Figure 2-6 shows two such hops.

A fairly large number of hops are possible, and indeed necessary, over very long circuits, for example, from New York to points in the Far East or from San Francisco to points in the Middle East. For all of us interested in radio communications, it is indeed fortunate that multihop transmission is possible.

CHARACTERISTICS OF RADIO WAVES FROM 3 TO 3 MILLION KILOCYCLES

The following shows how radio waves are classified in accordance with Radio Regulations annexed to the International Telecommunications Convention at Atlantic City in 1947. These classifications are currently in effect. In addition, important propagation characteristics for each subdivision are given.

1. Very Low Frequencies (VLF). Frequency range below 30 kc with wavelengths above 10,000 meters (also called Very Long Waves).

2. Low Frequencies (LF). Frequency range from 30 to 300 kc with wavelengths ranging from 10,000 to 1000 meters (Long Waves).

Propagation characteristics of low and very low frequencies are generally similar. Ground-wave coverage is extensive, with possible ranges of the order of thousands of miles. Extensive sky-wave coverage is also possible by propagation from the *D* regions of the ionosphere.

In the European area, the *Long Waves,* as they are known, are used extensively for medium-distance radio broadcasting, and as radio beacons. Very long waves are used extensively in medium- and long-range point-to-point communications, particularly by the military.

3. Medium Frequencies (MF). Frequency range from 300 to 3000 kc/sec, with wavelengths ranging from 1000 to 100 meters. Generally referred to as Medium Waves (MW). During the daylight hours, coverage is limited to the ground-wave range. The daytime medium wave seldom travels over 100 miles. During the evening and nighttime hours, reflection from the lower layers of the ionosphere enables the wave to travel considerably greater distances, with ranges from several hundred up to 1000 miles possible. They are used mostly for medium-wave radio broadcasting (from 550 to 1600 kc/sec generally), as well as maritime and aeronautical, standard frequency, and point-to-point transmission.

4. High Frequencies (HF). Frequency range extending from 3000 to 30,000 kc/sec (3 to 30 mc/sec), with wavelengths from 100 to 10 meters. Generally known as Short Waves (SW). Ground-wave range very limited, and seldom over 30 miles. Under favorable conditions, refraction from the ionosphere enables the wave to travel great distances, making long-distance radio communications possible and practical. Characteristics depend a great deal upon the condition of the ionosphere, which is subject to great variation, depending upon time of day, season of the year, and part of the sunspot cycle. Used for practically every purpose imaginable, including amateur radio communication, international broadcasting, point-to-point communication, etc.

5. Very High Frequency (VHF). Frequency range extending from 30 to 300 mc/sec, with wavelengths from 10 to 1 meter. Occasionally referred to as Very Short Waves (VSW).

6. Ultra High Frequency (UHF). Frequency range goes from 300 to 3000 mc/sec, with wavelengths from 1 meter to 10 centimeters (100 cm equal 1 meter). Also known as Ultra Short Waves.

7. Super High Frequencies (SHF). Frequency range from 3000 mc/sec to 30,000 mc/sec. Wavelengths extend from 10 cm to 1 cm. Known as Super Short Waves.

8. Extremely High Frequencies (EHF). Frequency range 30,000 mc/sec and above. Wavelengths extend from 1 to 0.1 cm. Also called Extremely Short Waves.

Propagation characteristics of VHF, UHF, SHF, and EHF are similar, with practically no ground wave and generally no reflection from the ionosphere except in unusual circumstances. Wave travels either by direct (line-of-sight) path, or through lower atmosphere (the troposphere). Considerable research is being conducted in these ranges, with relatively little known as yet about mechanics of propagation. Used in TV, FM, amateur radio, radar, and relatively short-distance point-to-point communications systems.

Chapter 3

THE SKY WAVE

REFRACTION OF RADIO WAVES

What is it about the ionosphere that gives it the properties of a mirror far above the earth, that enables it to return radio waves to earth, that makes long-distance radio communication possible? Actually the properties of the radio waves themselves have as much to do with their being returned to earth as do the properties of the ionosphere.

Although a complete discussion of the theories involving the motion of an electromagnetic wave in an ionized medium involves advanced mathematics and is extremely complex, a limited discussion of the behavior of the wave in the ionosphere is essential to our understanding of the basic principles involved in long-distance shortwave radio communications.

It will be helpful at this point to review what we have learned thus far about a radio wave and the ionosphere.

1. A radio wave travels through space with a velocity of 300 million meters per second, the speed of light.
2. The radio wave consists of rapidly oscillating electric and magnetic fields which are perpendicular to each other as well as to the direction of motion of the wave.
3. The ionosphere consists of ions and free electrons and is formed by ultraviolet-ray bombardment from the sun.
4. The gases in the ionosphere exhibit the properties of an electrical conductor, whereas ordinary air behaves as an insulator.

With these facts in mind, we can begin our discussion of the behavior of an electromagnetic wave in the ionosphere.

As the radio wave enters the ionosphere, its rapidly alternating electric and magnetic fields interact with the charged particles therein. This interaction exerts an actual force on the ions and electrons, setting them into motion. Since the fields of the wave are changing rapidly, the direction of motion of the ions and electrons on which they act also changes rapidly.

Although the radio wave affects *both* the ions and electrons, only the latter are significant, because the ion is a great deal heavier than the electron. (It consists of a heavy nucleus made up of protons and neutrons, and of planetary electrons.) As a result, the forces exerted

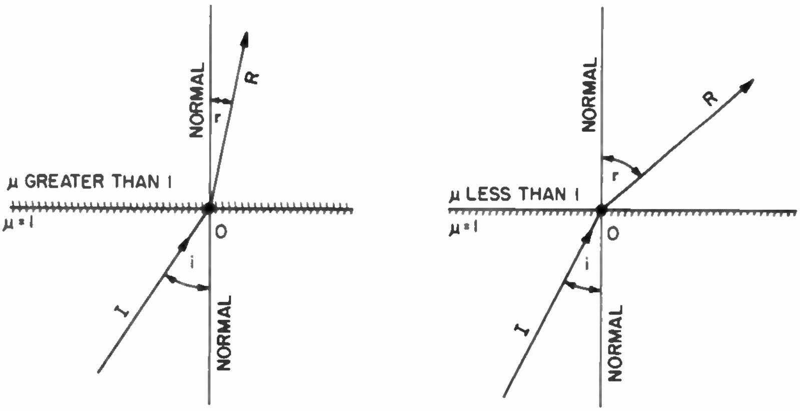

Fig. 3-1. Refraction of a ray of light passing (A) into a medium of greater refractive index, (B) into a medium of lower refractive index.

cause only negligible motion of the ion in comparison to that of the electron. Ionic motion is generally neglected when considering radio waves in the ionosphere.

The electrons which have been set in motion by the oscillating electromagnetic field behave exactly like the electrons oscillating in the transmitting antenna: that is, they themselves radiate electromagnetic waves of the same frequency and wavelength as the original radio wave but out of phase with it.

As a result of this phase shift, the direction of motion of the electromagnetic wave changes. This change in motion depends upon *electron density* (the number of free electrons in a given volume, usually a cubic centimeter). In general, the radio wave will take the path toward the *lowest* electron density. Since the deeper we go into the ionized region, the greater is the concentration of free electrons, the radio wave will tend to be bent back toward earth. This concept can be very well illustrated by drawing an optical analogy.

When a ray of light goes from one medium into another (air to water, or air to glass, for example), it bends. The amount and direction of bending depends upon a property of the medium called the "refractive index," designated by the Greek letter mu (μ).

Figure 3-1 (A) shows what happens when a ray of light passes from a medium of lower refractive index into a medium of higher refractive index. The shading represents the surface of separation between the two media, and a line drawn perpendicular to the two surfaces at the point where the light ray strikes them is called the *normal*. As the ray of light marked *I* passes into a medium of *greater* refractive index, it bends toward the normal. Consequently, the *angle of incidence*, designated *i*, between the incident ray *I* and the normal, is larger than the angle of refraction, designated *r*, between the emergent ray *R* and the normal.

SNELL'S LAW

The relationship between the sines of the angles of incidence and refraction and the refractive indexes of the media through which the ray of light passes is known as Snell's law and is written:

$$\mu_i \sin i = \mu_r \sin r. \qquad (3)$$

Suppose the first medium is air. Since the refractive index for air is 1, equation (3) becomes

$$\sin i = \mu_r \sin r. \qquad (4)$$

This equation shows that for a given angle of incidence *i*, a ray of light passing into a medium whose refractive index is greater than 1 must be bent toward the normal, with a resulting angle *r* which is smaller than *i*. Although in the example given $\mu_i = 1$, the relationship holds for any value of μ_i.

Similarly, Fig. 3-1 (B) shows a ray of light passing from a medium of higher refractive index to one of lower refractive index. Since Snell's relationship applies, the ray must be bent *away from the normal*.

Let us make the assumption once again that $\mu_i = 1$; then,

$$\sin i = \mu_r \sin r.$$

For the special case where $\sin i = \mu_r$, the angle r is 90°. This is true, because when $\sin i = \mu_r$, $\sin r = 1$, and the sine of 90° = 1. Physically, the above special case results in the refracted ray traveling parallel to the two media at an angle of 90° to the normal. Any further decrease in μ_r, or an increase in the angle i, will result in the ray being totally reflected, as shown in Fig. 3-2. The incident ray I_1 is

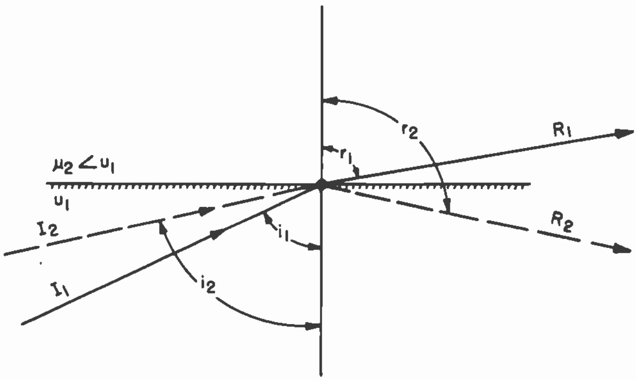

Fig. 3-2. Showing "total reflection" of ray of light I_2R_2.

shown being refracted nearly parallel to the surface of separation, while the ray I_2, shown by dashed lines, has been totally reflected.

If we now imagine the ionosphere to consist of a series of thin shells of increasing electron density, we can apply our optical analogy to the wave motion in the ionosphere.

Figure 3-3 is a pictorial representation of such a series of shells. If we remember that as electron density *increases,* the index of refraction *decreases,* and that, as we go deeper into the ionosphere, electron density *increases,* our picture of the radio wave in the ionosphere can be completed. Let us also assume that where electron density is zero (below the ionosphere), the index of refraction is 1.

We can see from Fig. 3-3 that, at the lower limit of the ionosphere, the ray, or radio wave, is bent *away* from the normal. Since each successive shell represents greater electron density and lower index of refraction, the ray continues to bend away from the normal. As suc-

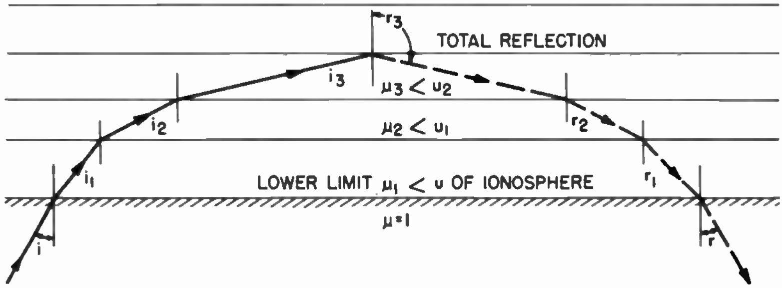

Fig. 3-3. How a ray is refracted by ionospheric "shells" of increasing electron density and decreasing index of refraction. After total reflection, ray enters shells of increasing refractive index, so that ultimately angle at which ray leaves ionosphere is the same as that at which it entered.

cessive shells are reached, the obliqueness of the incident ray increases until the ray is totally reflected, and the ray begins its downward journey. As the ray travels downward, it encounters a decreasing electron density and an increasing index of refraction, which results in a series of successive refractions *toward* the normal. The downward journey of the wave is therefore a mirror image of its travels upward, and it emerges from the ionosphere at exactly the same angle to the normal as it entered.

Figure 3-3 shows that, as the ionospheric shells are made thinner, the path of the ray becomes more and more curved in its journey through the ionosphere. It can also be seen that as the initial angle of incidence is greater, the fewer will be the number of "shells" through which the ray passes, and the greater will be the distance over which the ray travels. In addition, the electron density necessary to reflect the ray back to earth is smaller as the initial angle of incidence is increased. This is so because the ray will not penetrate as deeply as it would, were it sent up vertically or nearly so.

VERTICALLY INCIDENT RADIO WAVES

In the case of a vertically incident radio wave, the electron density which it encounters increases as it penetrates deeper and deeper into the ionosphere. The effect of this increasing electron density is to slow down the signal, and ultimately to bring it to a complete halt. An analogy can be drawn with a ball thrown straight up into the air. It continues to rise, but with decreasing velocity, until it comes to a complete halt and begins to fall back. Its speed, as it is falling, increases continually until it comes back to the ground at its initial velocity.

The radio signal, after it has come to a complete halt in the ionosphere, behaves similarly, and, as it moves back down through the ionosphere, its velocity increases until it comes out of the ionosphere and speeds toward the ground at the velocity of light, where it is received as an echo from the ionosphere.

VARIATION OF REFRACTIVE INDEX WITH FREQUENCY

We have already seen that the refractive index of the ionosphere depends upon electron density and that the greater the electron density a wave encounters, the greater will be its tendency to be bent back toward the earth. If, however, the frequency of the incident wave should be changed, the behavior of the wave in the ionosphere will also change. For example, if the frequency is *raised,* the angle of refraction will *decrease*. This phenomenon is illustrated in Fig. 3-4 for the

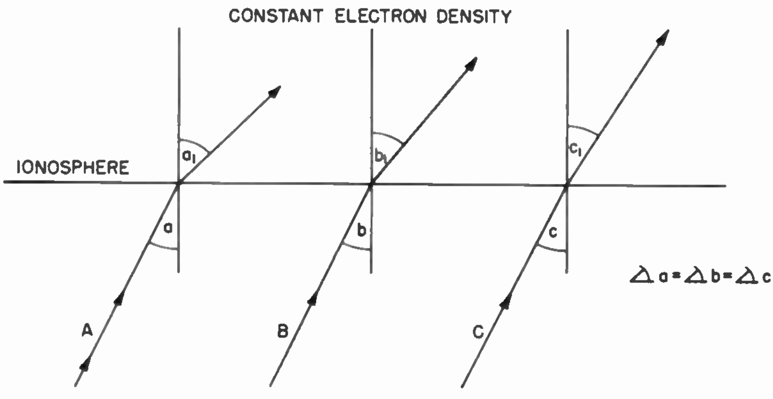

Fig. 3-4. Variation of angle of refraction with increasing frequency but at constant electron density. Frequency C is greater than B, which is greater than A.

three different frequencies, *A* being the lowest and *C* the highest, but all striking the ionosphere with the same angle of incidence. It can be seen from Fig. 3-4 that, with constant electron density, the wave bends less and less as the frequency is increased. This is the equivalent of saying that with *increasing* frequency, the refractive index *increases.*

Thus, the higher the frequency, the deeper the wave will penetrate into the ionosphere, and the deeper it will go toward the point of maximum electron density, which generally occurs toward the center of the ionospheric layer in which the wave is traveling. At this point, if the frequency is sufficiently high to overcome the bending effects of maximum electron density, the wave will continue traveling outward, to be lost in outer space. This is so because, once the wave has passed through the point of maximum electron density, it is traveling into a medium with decreasing electron density and increasing refractive index, and its bending, instead of being away from the normal, will now be toward it.

Chapter 4

MEASURING THE IONOSPHERE

PULSES AND ECHOES — THE IONOSONDE

The ability of the ionosphere to return a radio signal to earth provides us with our most important tool for probing the ionosphere to determine its many properties.

A number of ways have been developed for measuring ionospheric characteristics. The best and most straightforward way of making ionospheric measurements, however, is a method developed over 30 years ago by Breit and Tuve; the instrument which makes these measurements is called an *ionosonde.*

This method consists of sending a succession of short, sharp bursts of radio energy vertically upward. These 'pulses' are sent out at regular intervals (usually from 1/30th to 1/100th of a second); each pulse lasts for from 30 to 100 *millionths* of a second (30 to 100 microseconds).

Since radio waves travel with the velocity of light at the enormous speed of 300,000 kilometers per second, there is ample time for each pulse to make its round trip to the ionosphere and back before the next pulse is sent off. For example, for a layer height of 300 km, a radio wave takes 1/1000th of a second to travel from the earth to the layer, and another 1/1000th of a second to return to earth. Thus in 1/500th of a second, the journey is completed.

A receiver located in the vicinity of the transmitter stands by to pick up the echoes which are returned to earth. The output of the receiver is connected to a cathode-ray oscilloscope, whose time base is synchronized with the pulse repetition frequency of the transmitter. Thus, each time the transmitter sends out a pulse, a trace on the oscilloscope is begun. As a result, a stationary echo pattern is obtained on the oscilloscope. One typical pattern is shown in Fig. 4-1.

In Fig. 4-1, *G* is the ground pulse which traveled direct from transmitter to receiver, *R* is the echo returned from the ionosphere, and *R′* is the echo which was returned a second time. Since the time it

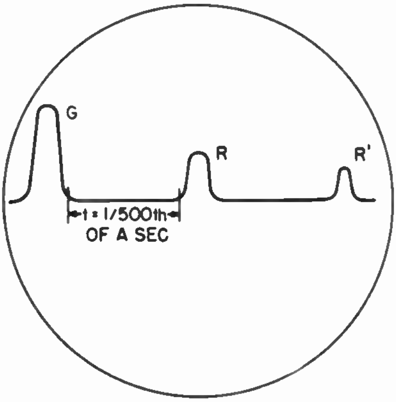

Fig. 4-1. Oscillogram of ground pulse G, echo *R*, and second echo *R′* of original pulse.

takes for each complete trace is known, the time it took for the radio wave to make the journey to the ionosphere and back can be determined by measuring the distance from the ground pulse *G* to the leading edge of the echo *R*.

VIRTUAL-HEIGHT MEASUREMENT

Since radio waves travel 300,000 kilometers in 1 second and since we know how long it took the radio wave to travel to the ionosphere and back, we can determine the total effective distance that the wave traveled. For example, if the time between *G* and *R* in Fig. 4-1 has been determined as 1/500th of a second, then the total effective distance that the wave traveled is 300,000 km/sec multiplied by 1/500 = 600 km. This is the distance of the *round trip*. Half of this gives the one-way distance of 300 km.

The height of 300 km is known as the *virtual* height of the ionosphere and is usually designated by h'. The difference between the virtual height and the actual height of the ionosphere is sometimes significantly large. The reasons for this are shown pictorially in Fig. 4-2 and explained as follows.

The velocity of light times the delay time from *G* to *R* in Fig. 4-1 yields the distance that the pulse would cover if it really traveled at the speed of light. But the signal velocity of a vertically incident radio wave *decreases* as it penetrates deeper and deeper into the ionosphere, and finally comes to a *complete halt* before it starts up again in a reversed direction, finally attaining the velocity of light again as it emerges from the ionosphere. The radio wave, while in the ionosphere, did not travel as fast as we assumed. Consequently, the wave did not go as far as our calculations indicated. Our height calculation was *virtual* and not *actual*.

The virtual height as measured by the pulse method is always greater than the actual height of the ionosphere. The quantity *R* is much

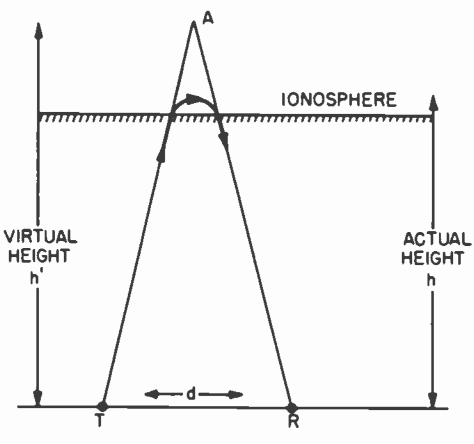

Fig. 4-2. Difference between actual and virtual path of a vertically incident radio wave. Distance between transmitter and receiver is exaggerated.

easier to determine than the actual height; to determine the latter, we would have to know a great deal about free-electron distribution in the region in which the wave must travel.

Actually, the measurement techniques we have discussed thus far refer only to *fixed-frequency* records. That is, height records were made with transmitter and receiver tuned to one frequency. Such records are also referred to as *h'-t* records. It is also possible to vary the frequency of the pulses (from 1 to 20 mc/sec, for example) and thus obtain records of virtual height *vs* frequency. Records thus obtained are known as *multifrequency, sweep-frequency,* or simply *h'-f* records. They will be discussed in detail later.

Modern ionosonde equipment is fully automatic. Tuning, tracking, and photographing of data all take place at regular predetermined intervals.

CRITICAL FREQUENCIES

The refractive index in the ionosphere depends upon the frequency of the incident wave, as well as on electron density in the layer; as the frequency varies, the penetration into the layer varies. As the frequency of a radio wave is increased, it penetrates deeper and deeper into the layer until finally it reaches the center of the layer where electron density is at a maximum.

If, at the maximum electron-density level, the radio-wave frequency is further increased, the electron density in the layer will be insufficient to return the wave to earth, and, consequently, the wave will go through the layer and escape. The frequency immediately below this value—that is, the *highest* frequency that a layer will reflect—is known as the *critical frequency.*

Critical frequency is perhaps the single most important piece of information that we can obtain concerning the ionosphere. Critical frequency and maximum electron density are related by the equation

$$N = 1.24 \times 10^{-2} \times f^2,$$

where N is the maximum number of free electrons per cubic centimeter and f is the ordinary-wave critical frequency in megacycles per second. In addition to telling us the maximum electron density within a particular layer, we can determine what frequencies can best be used in long-distance shortwave communications as well as those shortwave frequencies which cannot or should not be used over such long-distance circuits. Practical application of critical-frequency data to efficient long-distance radio communication will be discussed in more detail further on in this book.

WORLD-WIDE CRITICAL-FREQUENCY DATA

At the present time the Central Radio Propagation Laboratory (CRPL) of the National Bureau of Standards (NBS) receives and analyzes ionospheric data from approximately 120 ionospheric sounding stations throughout the world. From the $h'f$ data that these stations supply, the critical frequencies for each ionospheric layer, for each

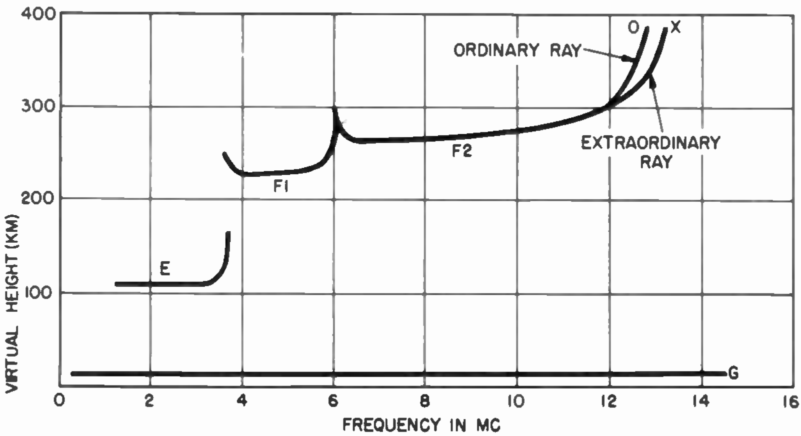

Fig. 4-3. Winter daytime ionogram (h′-f curve)—virtual height vs frequency.

hour of the day, and for each of these locations is determined. A wealth of ionospheric information thus becomes available.

h′-f CURVES

Several minor ionosonde adjustments can be made to give us an instantaneous picture of ionospheric conditions over an entire range of frequencies. This can be accomplished first by making the time-base sweep vertical instead of horizontal. Since the speed of propagation of a radio wave in free space is known, the time base can be calibrated to read virtual height directly, instead of time. The echoes then appear as bright "blips" on the screen.

As the transmitter tunes over a predetermined frequency range of, say 1–20 mc/sec, each succeeding blip will be displaced slightly in a horizontal direction, toward the right. By using a fast sweep (around 15 seconds) and a long persistence screen, the complete *h′-f* curve appears. The screen itself can be marked so that height markers appear as horizontal lines, and frequency markers as vertical lines. The data, as they appear on the scope, can then either be plotted or photographed directly. A plot of a typical winter daytime ionogram appears in Fig. 4-3.

As the sounding begins, we get no echo from the ionosphere because our frequencies, being too low, are absorbed in the lower regions of the *D* layer. At these frequencies the only record on our trace is the direct wave that travels from transmitter to receiver. This is shown at *G*. In the vicinity of 1.2 mc/sec, we get our first echo from a height of approximately 100 km. This continues until we reach approximately 3.5 mc/sec, when the *E* trace suddenly breaks in an upward direction and peters out. At about the same frequency, we get a trace of typical F_1-layer height. Starting at approximately 250 km, the trace then moves *downward* as frequency is further increased, instead of upward as we would expect.

The apparent increase in height of the *E* layer before penetration and the decrease in F_1-layer height in the vicinity of 3.5 mc/sec is an interesting phenomenon. As we approach the *E*-layer critical frequency, the wave is slowed more and more. At the critical frequency, the wave has experienced maximum retardation because it has traveled into a region of maximum electron density. As a result, the time taken for the wave to make a round trip is a maximum, and the virtual height of the layer is also a maximum. We must remember that we are measuring virtual height, not actual height and that h' depends only on the *time* necessary for the round trip. Although virtual height is always greater than actual height, the difference is *greatest* at the critical frequency, when retardation is at a maximum.

Similarly, the cusp in the F_1 trace is due to the fact that just *above* the *E*-layer critical frequency, the wave is still considerably slowed in its passage through the regions of maximum electron density in the *E* layer. After being slowed down, it then travels to the higher F_1 layer, is reflected, returned through the *E* layer again and is further slowed down thereby, and finally returns to the receiver. The additional time taken by the wave in its travels through the *E* layer is shown on the trace as an *increase* in virtual height.

As the frequency is increased to approximately 4.0 mc/sec, the retarding influence of the *E* layer comes to an end, and the F_1 height shown on the trace drops to a value closer to the actual height of the F_1 layer.

F_1-layer reflection continues as we continue to increase our frequency. Then, in the vicinity of 6.0 mc/sec, we again observe the retardation effect with an apparent sharp increase in F_1-layer height followed by a sharp decrease in F_2-layer height. Here, there is no break in the trace as there was between the *E* and F_1 at 3.5 mc/sec, because the distance between the F_1 and F_2 layers is relatively small. Once we have passed the retardation effects of the F_1 layer, we get a more accurate picture of F_2-layer height.

As we continue to increase our frequency, F_2-layer reflection continues with a gradual increase in F_2-layer virtual height as a result of deeper penetration into the layer. Then suddenly, in the vicinity of 12 mc/sec, a very unusual thing takes place—the trace begins to break up. A further increase in the frequency causes a complete split in the trace. The separate traces after this unusual split are labeled *O* and *X* on Fig. 4-3. The ray on the left, labeled *O*, is called the ordinary ray, and the one on the right, the extraordinary ray. The ordinary ray penetrates the F_2 layer first and is followed a fraction of a megacycle later by the extraordinary ray. Thereafter, we get no more return echoes, indicating that the last of the ionospheric layers has been penetrated.

Figure 4-3 shows us at a glance the *E*-, F_1-, and F_2-layer critical frequencies: *E* layer—3.6 mc/sec; F_1 layer—6.0 mc/sec; F_2 layer (ordinary)—12.8 mc/sec; F_2 layer (extraordinary)—13.2 mc/sec. A single trace has given us virtual layer heights, critical frequencies, and a wealth of other information. All of this will be discussed again later. First, however, we must come back to the peculiar split in F_2-layer echoes and a discussion of the ordinary and extraordinary rays.

THE ORDINARY AND EXTRAORDINARY RAY

In optics, certain crystals have the property of double refraction, with a single incident beam of light being split into two parts within the crystal. Although some of the properties of the incident ray have been altered, the emergent beams are parallel and travel in their origi-

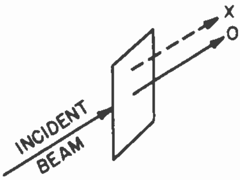

Fig. 4-4. Optical splitting. Ordinary ray O and extraordinary ray X are shown emerging.

nal direction. This is shown in Fig. 4-4. The chief difference in the emerging rays is that they are polarized differently, with the electric field of the undeviated beam oriented horizontally and the electric field of the deviated beam (shown broken) oriented vertically.

Similarly, when a radio wave enters the ionosphere, the interaction of its own changing electric and magnetic fields with those induced in the free electrons in the ionosphere, and the action of the earth's magnetic field, combine to change some of the properties of the radio wave. As a result, the wave splits. Each component is differently polarized and travels at slightly different velocities. The net result is that the critical frequency of the ordinary ray (usually denoted f^o) is a fraction of a megacycle *lower* than the extraordinary-ray (f^x) critical frequency. It would appear at first that f^x would be more important than f^o. We shall see later, when dealing with long-distance shortwave radio communication, that this is not the case.

The reader may wonder at this point why this splitting appears to occur only at the higher frequencies. This is not actually so. Splitting into ordinary and extraordinary components occurs on all frequencies; however, in being reflected from the lower layers on the lower frequencies, the time delay between the ordinary and extraordinary components is not great enough to show up on the trace, because the difference in penetration of the layer is not significantly large at the lower ionospheric levels.

OTHER CURVES

Figure 4-3 showed a typical winter daytime ionogram. Figures 4-5, 4-6, and 4-7 display typical summer night, winter night and summer day ionograms, respectively. A comparison of Fig. 4-5 and 4-6, for summer and winter nights, indicates a number of similarities. For example, at the lower frequencies, we notice some evidence of an *E* layer. However, it is extremely weak and for our purposes can be neglected. *F*-layer heights are similar, with only a single *F* layer as opposed to both F_1 and F_2 layers which exist during the day.

We can see that critical frequencies are about the only significant difference between the two ionograms. During the summer, the f^o value is almost 8 mc, as opposed to 4 mc during the winter. This occurs because, during the long winter nights, recombination takes place for a considerably longer time. As a result, electron density drops to considerably lower values than during summer nights, when darkness, and consequently de-ionization, is shorter lived.

The summer day curve in Fig. 4-7 appears, at first glance, to be considerably more complicated than it really is. As before, the *E* layer can be found at its regular height of about 110 km above the ground. Because, during the summer months, the sun's rays fall upon the ionosphere for longer periods of time, the effective thickness of the layers of the ionosphere is greater during the summer than during the winter. Consequently, deeper penetration of each of the layers is possible during the summer day than at any other time of year.

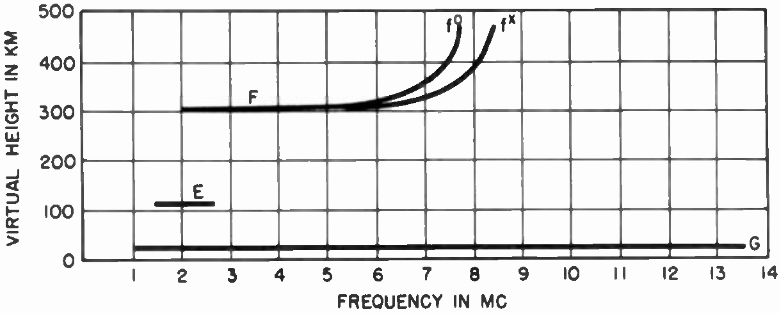

Fig. 4-5. Normal summer night.

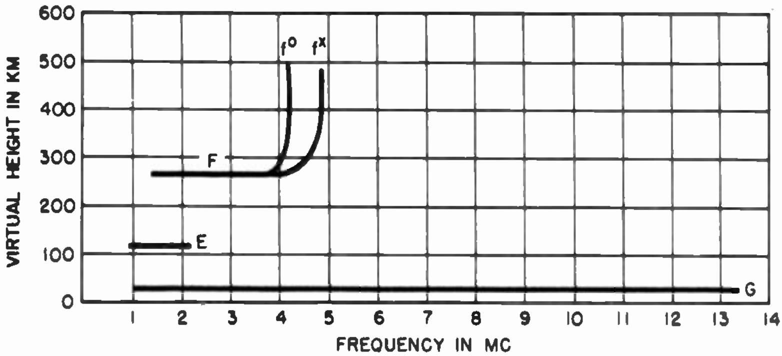

Fig. 4-6. Normal winter night.

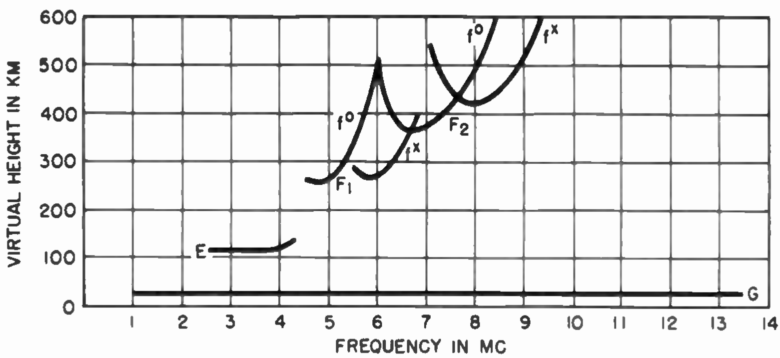

Fig. 4-7. Normal summer day.

We have already seen that the ordinary and extraordinary rays have different charactertistics. These differences, together with the increased thickness of the ionospheric *F* layers, enable both the ordinary and the extraordinary traces to show up on the ionogram. These are clearly labeled in Fig. 4-7.

The increase in the number of daylight hours during summer would lead us to conclude that summertime F_2-layer critical frequencies are higher than winter day critical frequencies. Comparison of Figs. 4-3 and 4-7 shows that this is *not* the case. This is only one of the anomalies in F_2-layer behavior. It, along with others, will be discussed later in this book.

Chapter 5

IONOSPHERIC VARIATIONS: THE SUNSPOT CYCLE

Now we will discuss in more detail the analysis of ionospheric data received from over 120 ionospheric sounding stations throughout the world by the Central Radio Propagation Laboratory of the National Bureau of Standards. From the data that each station submits, a monthly average critical frequency for each ionospheric layer for each hour of the day can be obtained for that station. In addition, average hourly virtual-height readings for each layer can also be obtained. Graphs can then be plotted.

Obviously the analysis of 120 such charts, gathered from all corners of the world, can be an extremely complex task, particularly when we realize that when it is spring in one hemisphere, it is fall in the other; when it is daylight in one part of the world, it is night in another. It is best, then, to study these charts as they have been plotted for a single location and determine whether the information we gather from them can then be applied equally in any part of the world.

Figures 5-1 through 5-4 show average diurnal (daily) variations in critical frequency and virtual layer height as measured in the vicinity of Washington, D.C., during June, 1955, June, 1958, December, 1954, and December, 1957.

Careful study of these charts indicates three major variations in ionospheric behavior. These are:

1. *A diurnal variation,* occurring every day, with nighttime and daytime characteristics of the ionosphere varying significantly.
2. *A seasonal variation,* with significant differences between summer and winter conditions being apparent.

3. *A cyclical variation.* In addition to the regular daily and seasonal changes in ionospheric behavior, a long-term pattern of change is observable. This change, which occurs over a period of approximately 11 years, is caused by changes in the sun which take the same length of time. Diurnal and seasonal changes, on the other hand, result from changes in the earth's position with respect to the sun.

These three major changes in the ionosphere will be understood most clearly if related to Figs. 5-1 through 5-4.

DIURNAL VARIATIONS

The E layer. This layer exhibits the most consistent daily variations, the critical frequency varying with the zenith angle (the angle of the

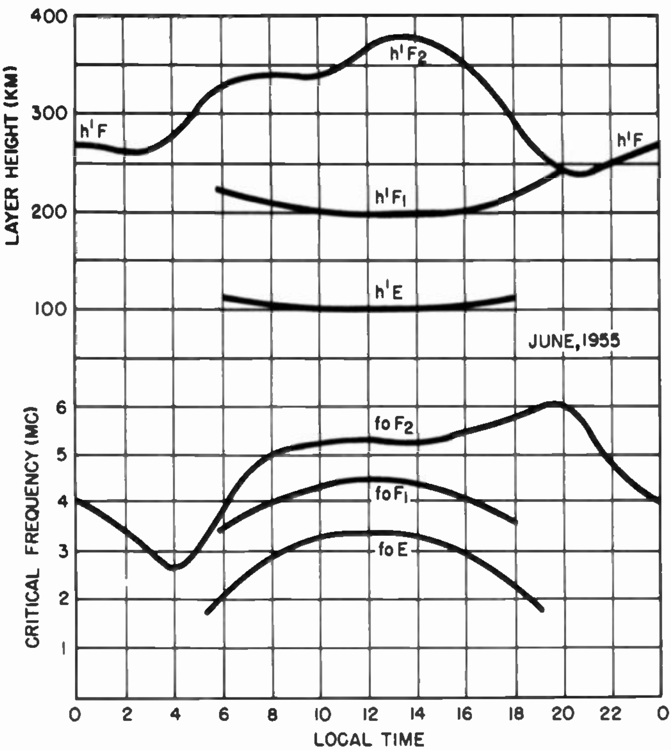

Fig. 5-1. Diurnal variation in layer heights and critical frequencies at Washington, D.C. during June—minimum sunspot activity.

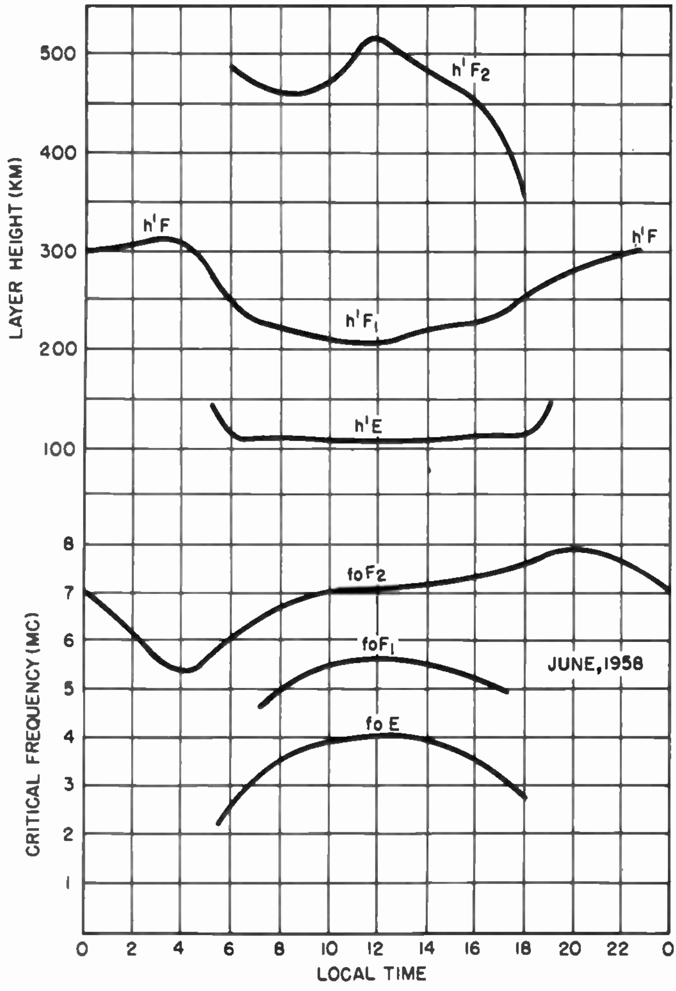

Fig. 5-2. Diurnal variations in layer heights and critical frequencies at Washington, D.C. during June—sunspot maximum.

sun in the sky). Around dawn, the critical frequency for the layer rises from a near-zero value toward a maximum at noon, decreasing steadily thereafter until nightfall, when the critical frequency drops again to near zero. Although there are some traces of the *E* layer at night, they are of no significance to communications and are not shown in Figs. 5-1–5-4.

Layer height is practically a constant, ranging from 100 to 110 km. Because the critical frequency of the *E* layer follows the angle of the sun so closely, we would ordinarily expect the layer to disappear entirely after sunset and during the hours of darkness. Actually this does not happen. It appears that during the hours immediately preceding sunrise and following sunset, *E*-layer ionization continues to some extent as a result of sunlight scattering from the higher layers. It has also been suggested that the presence of an *E* layer, however weak, throughout the hours of darkness may be explained on the basis of ionization caused by meteors which are constantly arriving in the earth's atmosphere.

The F_1 layer. Behavior in this layer is very similar in many respects to that of the *E* layer, with the maximum critical frequency being observed around noon local time. Precise observation of layer characteristics is sometimes complicated by the fact that the height of the F_1 and F_2 layers is often almost identical, with the result that characteristics of the two layers are hardly distinguishable.

During the nighttime hours, the F_1 and F_2 layers combine to form a single layer, often called either the *F* layer or the F_2 layer. The height of this nighttime *F* region is often greater than the F_1 and not as great as the F_2.

At around dawn the *F* region generally splits, although a glance at Fig. 5-4 shows that this need not always be the case. In this instance, no F_1-layer observations were made during any hour of the day.

The F_2 layer—anomalous characteristics. The diurnal and seasonal behavior of the F_2 layer, though similar in some respects to the *E* and F_1 layers, is radically different in others. Because the F_2 layer is the most important layer in long-distance shortwave radio communications, and because the anomalies (irregularities) in the behavior of this layer play a significant role in utilizing the ionosphere for long-range communications, these anomalies must now be treated in considerable detail.

We first note from Figs. 5-1 and 5-2 that the maximum value of critical frequency during the summer does *not* occur around noon, as it does with the *E* and F_1 layers. Instead the value continues to rise quite late in the day. In Fig. 5-1, the critical frequency actually *falls* at 1400 hours before resuming its climb. We note also from Figs. 5-1 and 5-2 that, although the F_2-layer critical frequency begins to fall after sunset, the noon and midnight values are comparable; in fact, we can see that the values shown in Fig. 5-2 for noon and midnight critical frequencies are *exactly equal.*

By comparing the June curves of Figs. 5-1 and 5-2 with the December curves of Figs. 5-3 and 5-4, we find a paradox of a seasonal nature: although the zenith angle of the sun is considerably greater in summer than in winter, and although the hours of daylight are considerably more in summer than in winter, the summer daytime critical frequencies are *significantly lower* than winter day critical frequencies. Nighttime critical frequencies, on the other hand, are—as we would expect them to be—lower in winter than in summer.

Still another irregularity in F_2 behavior is the apparent lack of symmetry with respect to longitude. For a given latitude, we should expect F_2-layer criticals to be the same for the same hour of the day at any longitude, as are E and F_1 criticals. This, however, is not the case, and there appears to be a variation with respect to the geomagnetic equator. This is indicated further by another striking characteristic of the F_2-layer—noontime critical frequencies are *not* maximum in the vicinity of the geomagnetic equator. Maximum values generally occur about 15–20 degrees away from the equator; there is a trough where maximum criticals would be expected to occur.

Geographic variations in F_2-layer characteristics will be discussed again shortly. First, however, we must return to our diurnal and seasonal irregularities in F_2-layer behavior. These may be summarized as follows:

1. F_2-layer critical frequencies continue to increase after E and F_1 criticals have begun to decrease. This is particularly pronounced during the summer months and indicates that F_2-layer criticals do not vary directly with the sun's zenith angle.
2. There is a daytime seasonal variation in F_2-layer critical frequencies which is exactly opposite to what we would expect, with summer day criticals being *lower* than winter day values *despite* more hours of daylight and higher elevation of the sun in the sky during the summer months. These anomalies are explained as follows:

The degree of ionization (electron density) in any ionospheric layer depends to a considerable extent on the *recombination* rate in the layer. We know, for example, that the ionosphere consists of free electrons and ions which are formed as a result of ultraviolet bombardment from the sun. There is a tendency for these to recombine. That is, for the electron to seek out an ion and form a neutral atom. Generally, the greater the concentration of ions and electrons, the greater the recombination rate.

During the summer months, the F_2 layer expands because of the heating effects of the sun. As a result, the upper regions of the iono-

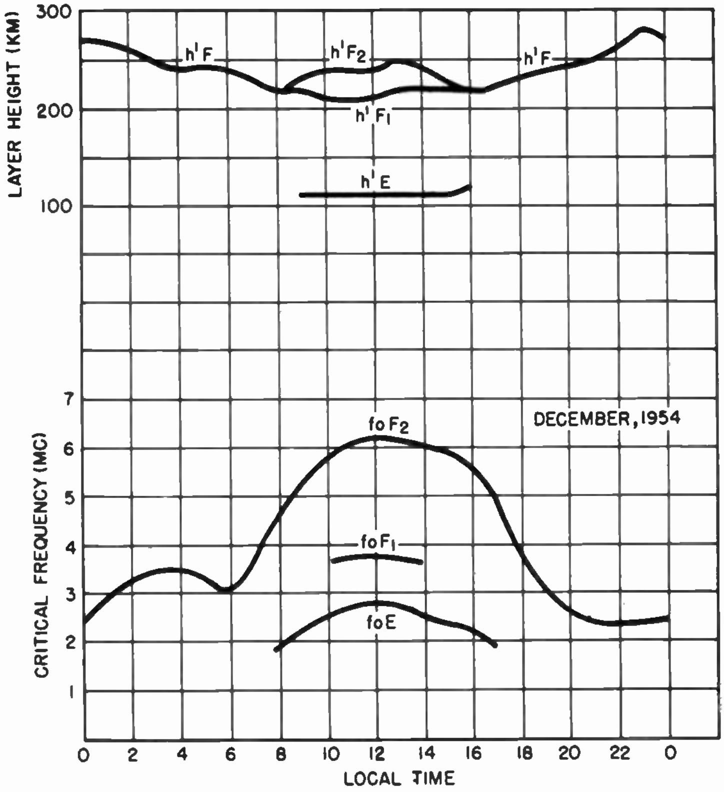

Fig. 5-3. Diurnal variation in critical frequencies and layer heights at Washington, D.C. with time during December—minimum sunspot activity.

sphere are less dense than during other seasons of the year. Because of this decreased density, we have a lower recombination rate. That is, with fewer electrons and ions per cubic centimeter, it takes longer for an electron to "find" an ion with which to recombine.

As long as the rate at which free electrons and ions are formed is greater than the rate at which recombination takes place, the number of free electrons formed, and hence the critical frequency, continues to rise. Thus, during the summer months, critical frequencies increase even past midday. We also know that critical frequency in the ionosphere depends on electron density. The greater the number of free electrons per unit volume, the greater the critical frequency. Since the ionosphere expands in the summer as a result of the sun's heating, electron density, despite longer daylight and higher zenith angle, is less than during the winter months. Therefore summer day critical frequencies are lower than during the winter day.

The expansion due to heating in the F_2 layer during the summer day also causes the drop in critical frequency around midday, again as a

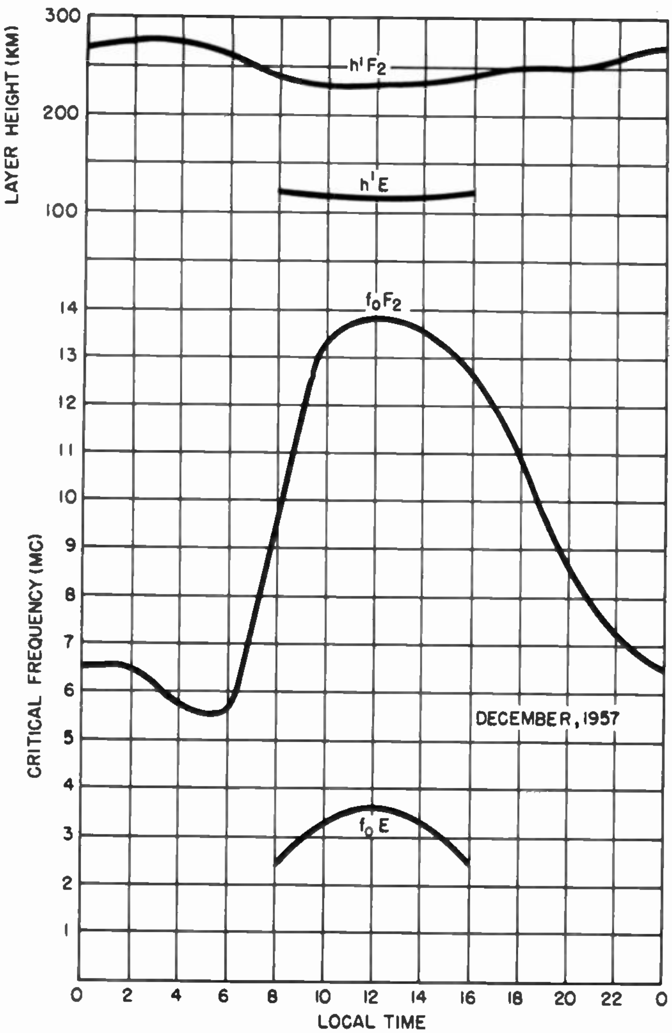

Fig. 5-4. Diurnal variation in layer heights and critical frequencies at Washington, D.C. during December—maximum sunspot activity.

result of a decrease in electron density. After noon, the sun's angle begins to decrease, the ionosphere begins to contract due to cooling, the recombination rate remains low because gas density is still minimal, and critical frequencies again begin to rise.

During the winter night, we see an increase in F_2-layer critical frequency just before dawn (Fig. 5-3, 04 hours local time). This again is an effect of temperature; during the long cold winter night, the ionosphere contracts. Just before dawn it is most dense, since that is the coldest part of the day. Consequently, there is a rise in critical frequencies. At around dawn, the ionosphere is warmed, expands, and the critical frequency drops.

During the daylight hours, the ionosphere remains relatively cool in comparison to summer conditions, and electron density is relatively high. It should be pointed out also that during the winter months, although the northern hemisphere is colder because of the lower zenith angle of the sun, ultraviolet intensity is maximum because the sun is closest to the earth during the winter months by some 3 million miles. It is believed that this increase in ultraviolet intensity is also in part responsible to the very high normal daytime winter critical frequencies.

Winter nighttime critical frequencies for the F_2 layer are *'normal.'* That is, they behave the way we want them to. Because no ionization occurs during the hours of darkness, there is a maximum period during which only recombination takes place. This results in critical frequencies falling to their lowest values.

During the winter, F_2-layer critical frequencies vary from very high values during the day to very low values at night. During the summer, the maximum values of F_2 critical frequencies are below winter values during the day, and above F_2 winter criticals at night.

SEASONAL VARIATIONS

The seasonal characteristics of the *E* and F_1 layers of the ionosphere change with the zenith angle of the sun. These changes are regular and straightforward and are explained by simple theory. Maximum values are reached around noon when the sun's angle in the sky is maximum. Winter nighttime critical frequencies are lower than during the summer; this is also consistent with the theory that ultraviolet radiation is chiefly responsible for the formation of the ionospheric layers. Seasonal variations in the F_2 layer have already been discussed; however, additional factors are responsible for F_2-layer characteristics.

LONG-TERM VARIATIONS—THE SUNSPOT CYCLE

Sunspots are massive whirling cyclonic storms that appear on the surface of the sun as black spots. Although their origin is not understood, we know that they were observed by the ancient Greeks, Romans, and Egyptians. Unfortunately, accurate records of sunspot activity could not be kept before the invention of the telescope, since most sunspots are too small to be observed with the naked eye.

Although sunspots have been observed in fairly regular fashion since the seventeenth century, highly accurate records have only been kept for the last hundred years or so. Since that time the Federal Observatory at Zurich, Switzerland, has acted as a clearing house, gathering and recording sunspot data sent from all over the world.

A uniform method of counting sunspots has been devised. This system takes into account the number of spots on the sun, the number of sunspot groups, and the power of the telescope used. The number thus derived is called the *Wolf* number, after the originator of the system. A study of sunspot numbers showed almost from the beginning that, although daily and even monthly variations were sometimes very large and erratic, a regular long-term pattern definitely existed.

Running averages. In order to obtain a number which would be indicative of the *trend* in sunspot activity, the *smoothed* sunspot number is plotted. This is obtained first by averaging the daily sunspot number over a period of a month. The monthly average number thus obtained is reduced to a *running average*, or smoothed number. Running averages can be taken for any convenient interval, such as 3, 6, or 12 months. The Zurich monthly sunspot numbers for the period July, 1957–August, 1958 were as follows:

July, 1957	194.3	February, 1958	151.6
August	162.6	March	189.4
September	244.3	April	195.0
October	262.9	May	175.2
November	207.3	June	167.9
December	233.9	July	197.7
January, 1958	202.8	August	203.9

Note the wide fluctuation—from a high of 262.9 in October, 1957 to a low of 151.6 in February, 1958, then back up again to over 200 by August, 1958.

To obtain a clearer picture of the *trend*, we can take a 3-month running average. First, add the July, August, and September, 1957

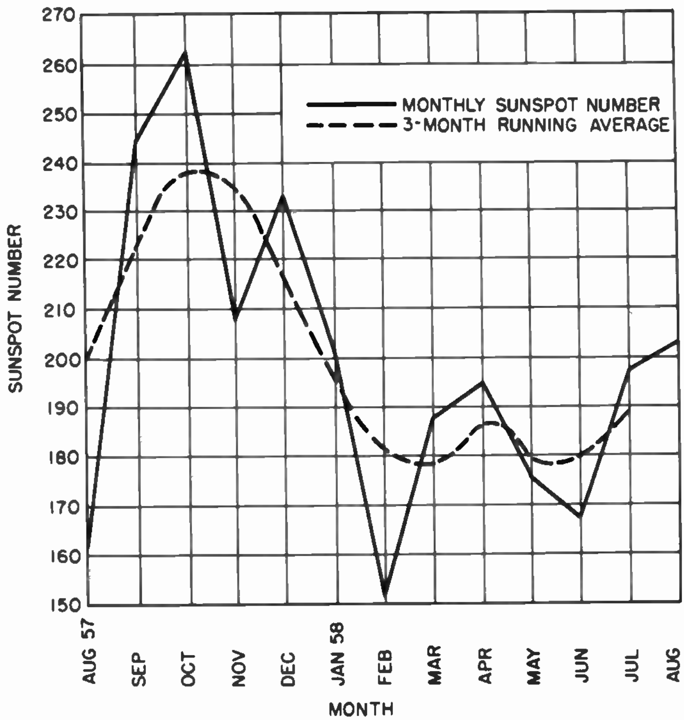

Fig. 5-5. Comparison of monthly average sunspot numbers with 3-month running average sunspot numbers from August, 1957 to July, 1958.

monthly numbers and divide by 3. This gives us 601.2 divided by 3 or 200.4; this number is known as the *running average* centered on August. To obtain the running average centered on September, add the August, September, and October numbers to get 669.8; divide this by 3 and get 223.3. In other words, to obtain the 3-month running average centered on any month, take the number for that month, add it to the number for the month before and the month following, then divide by 3.

Figure 5-5 shows the monthly sunspot numbers plotted against smoothed (3-month running average) sunspot numbers for the period August, 1957–July, 1958. We can easily see that the erratic variations are "smoothed" out, giving us a curve which shows definite trends.

Most sunspot curves are based on longer running averages. These are obtained in the same way. A 13-month smoothed number for July, 1958, for example, would be obtained by adding the monthly number for July, 1958 to the monthly numbers six months before and six months after July, and dividing the total by 13.

Eleven-year cycle. An analysis of running averages of sunspot numbers taken since the middle of the 18th century indicates a long-term periodic variation in the number of sunspots. This variation, meas-

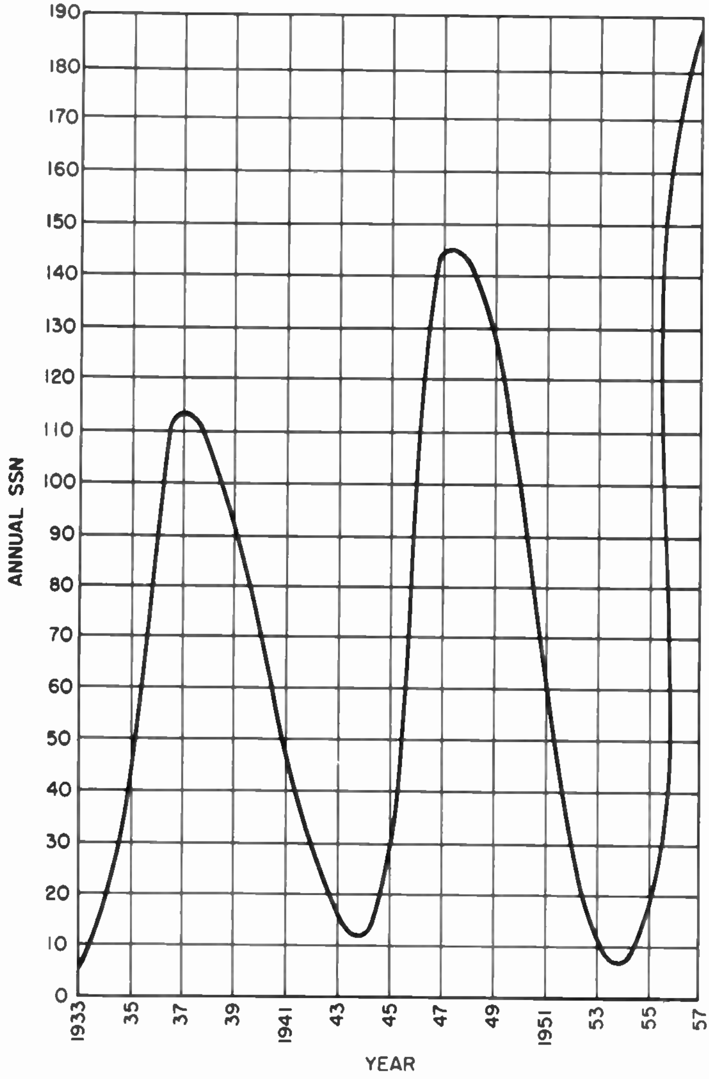

Fig. 5·6. Yearly average of monthly smoothed sunspot numbers, 1933 through 1957.

ured from periods of minimum activity, to maximum, and then back to minimum, has averaged 11.1 years.

Figure 5-6 shows yearly averages of smoothed monthly sunspot numbers from 1933 through 1957. This figure demonstrates that variations in sunspot activity from year to year have been extreme, with minimum years occurring in 1933, 1944, and 1954. Maxima were recorded in 1937, 1947, and 1957. Actually, the maximum of the present sunspot cycle occurred in March, 1958 and was the highest maximum ever observed. Previously the 1947 maximum had been the highest ever recorded.

Variations in ultraviolet intensity. Figure 5-7 shows monthly average values of noon F_2-layer critical frequencies measured at Washington, D.C., from January, 1954 through July, 1958. Yearly average values of smoothed sunspot numbers for each year are shown at the right of each curve. Notice that the yearly increases in sunspot number were closely paralleled by increases in F_2-layer noon critical frequencies. Actually the increase in F_2-layer criticals was accompanied by increases in the critical frequencies of the other layers of the ionosphere, although F_2-layer increases were generally greater than the increases observed in the other layers.

A number of interesting observations can be made by close inspection of Fig. 5-7. First, there is a relatively sharp increase in critical frequencies from September, 1955 to the end of that year, compared to a relatively flat curve the year before.

In 1954, a year of minimum sunspot activity, the monthly smoothed sunspot numbers varied between 6 and 12. In 1955, numbers also started out quite low but suddenly spurted, and by the end of the year the smoothed sunspot number had risen to 81. It would appear from this that the sudden increase in noon critical frequencies followed the trend in the smoothed sunspot numbers. This is further illustrated in 1956, which starts out with critical frequencies and smoothed sunspot numbers running in magnitude at approximately late 1955 levels. After the seasonal dip, there is another sharp rise in critical frequency and sunspot number, which closes out the year at 132. The 1957 curve is symmetrical, with critical frequencies at the beginning and the end of the year of the same order of magnitude. This would indicate that the change in sunspot number during 1957 was not very large. We find, in checking, that the 1957 variation was between 168 and 187.

It would appear, therefore, that a close correlation exists between critical frequency and sunspot number. Although this correlation is universal, it differs according to time of day, season of the year, and

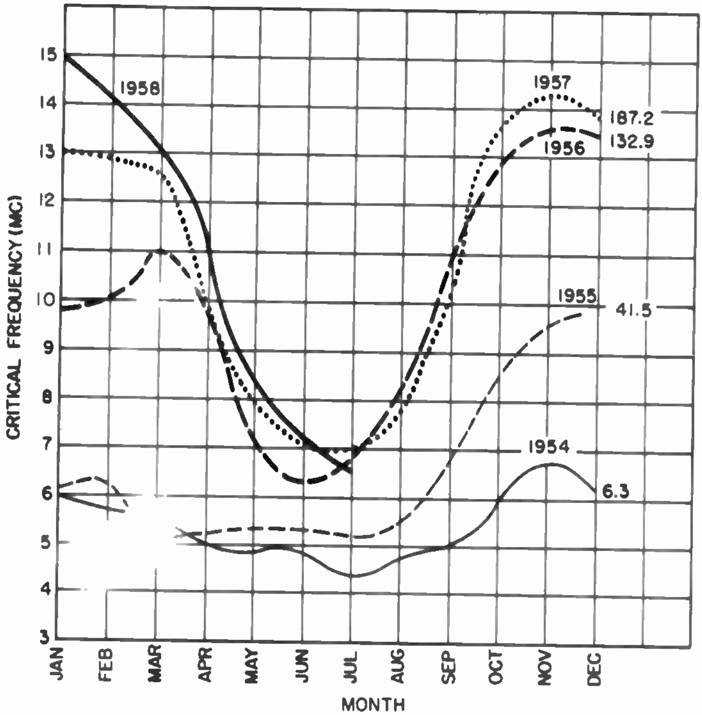

Fig. 5-7. Monthly variation in average noon F_2-layer critical frequency at Washington, D.C., during the period January, 1954 through July, 1958. Yearly average sunspot numbers shown at right for each year.

geographical location. The very good agreement between critical frequencies and sunspot number immediately suggests a possible way of forecasting critical frequencies considerably in advance.

For example, there are known changes in critical frequency which are brought about by daily and seasonal factors. These are clearly understood and can readily be taken into account. If, in addition, we can predict from the latest available data what the sunspot number at some future date will be, this information can be applied to make a prediction of critical frequencies from three to six months in advance. Such predictions are now made with very good accuracy. Since the critical frequency can be used to determine the best frequency to be used for long-distance shortwave radio communication over any circuit, between any two points on the earth's surface, the agreement between sunspot activity and critical frequency gives us a very powerful tool.

Variations with latitude. Variations in the E and F_1 layers of the ionosphere follow the zenith angle of the sun. Thus, during periods when the sun is directly overhead at the equator at noon (during the vernal and autumnal equinoxes), we find that E- and F_1-layer critical frequencies at noon are maximum at the equator and taper off as we move either north or south, being symmetrical with respect to the equator; that is, the values of critical frequency are the same for corresponding values of latitude, on either side of the equator.

When the sun is directly overhead at some point other than the equator, E and F_1 critical frequencies are maximum at that point and decrease as we move either north or south.

The diurnal variation in the E- and F_1-layer critical frequencies has already been discussed. For any given latitude, the daily variations in the E and F_1 layer will be identical. Identical maxima and minima will occur at corresponding local times at any location on the same latitude.

Variations in F_2-layer critical frequency are not solely dependent upon the sun's elevation or the intensity of solar radiation. It appears

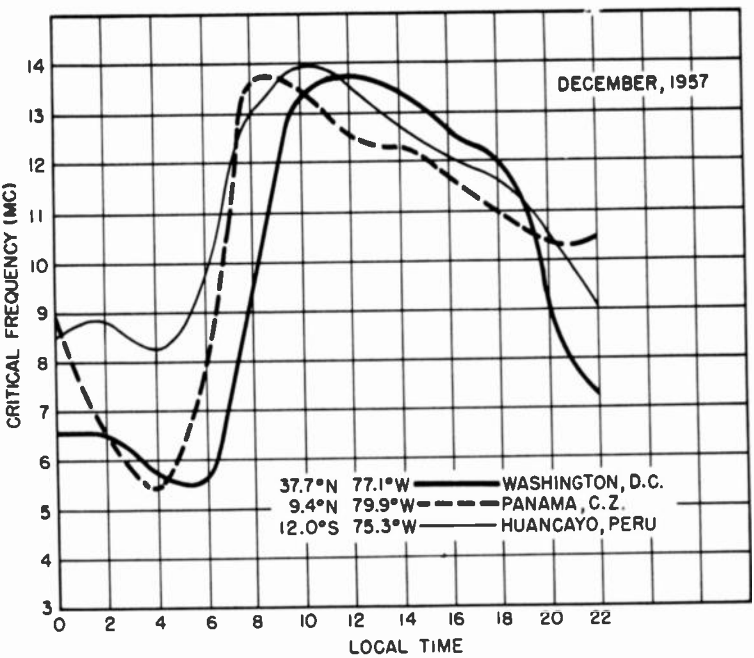

Fig. 5-8. Hourly variations in F_2-layer critical frequencies during December, 1957 at 3 locations of different latitude but similar longitude.

that the earth's magnetic field has an effect on the distribution of ions and electrons throughout the upper regions of the ionosphere. F_2-layer characteristics do not depend only on the zenith angle of the sun, but also on the position with respect to the earth's geomagnetic equator.

Figure 5-8 shows F_2-layer critical frequencies measured at three different locations of similar longitude but different latitude during December, 1957. The northern hemisphere curve for Washington, D.C. shows the wintertime diurnal variations. Nighttime critical frequencies are relatively low, while daytime criticals rise to rather high values. The Panama Station, though located further south and near the equator, still displays winter characteristics, but daytime criticals are lower than in Washington, D.C. This is attributed to the heating effect of the ionosphere due to its proximity to the equator. The third location is located in the southern hemisphere and exhibits some summer characteristics in the relatively high nighttime value of critical frequencies. Daytime values however are relatively high, perhaps because the sun, in December, is closest to the earth and ultraviolet radiation has maximum intensity. Therefore, daytime southern hemisphere critical frequencies in the wintertime are higher than northern hemisphere critical frequencies during the corresponding summer period.

Figure 5-9 gives critical frequency data for the same three stations during June, 1958. Here again the Washington, D.C. curve is typical.

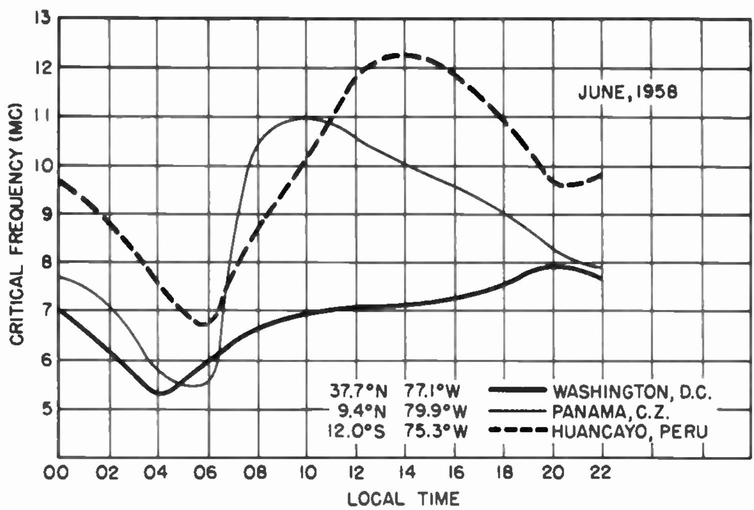

Fig. 5-9. Hourly variations in F_2-layer critical frequencies during June, 1958 at 3 locations of different latitude but similar longitude.

It shows a plateau effect, gradually rising critical frequencies, and a late afternoon peak. The Panama curve shows critical frequencies generally typical of regions near the equator. Note that critical frequencies for both day and night are relatively high. The sharp drop after midnight to a low value around 06 hours local time is characteristic of tropical locations, where after sunset the upper regions of the *F* layer cool rapidly and contract. This causes an increase in critical frequency for a short time, after which recombination takes place relatively rapidly, causing a sharp drop in critical frequencies until dawn. The critical frequency curve for Huancayo in the southern hemisphere is a typical winter curve, with relatively low nighttime criticals and high daytime criticals, compared with the Washington values. Because the sun is furthest away from the earth during June, the winter (June) daytime critical frequencies in the southern hemisphere are not as high as winter (December) daytime critical frequencies in the northern hemisphere.

Variations with longitude. *E*- and F_1-layer variations are fixed and behave as if the earth rotated under them; for any longitude therefore, on the same latitude, the values of *E*- and F_1-layer critical frequencies are the same at corresponding local times. This is not the case for the F_2 layer, which changes characteristics as the earth rotates. Figure 5-10 shows monthly average values of F_2-layer critical frequency at two locations on the same latitude but different longitudes for the month

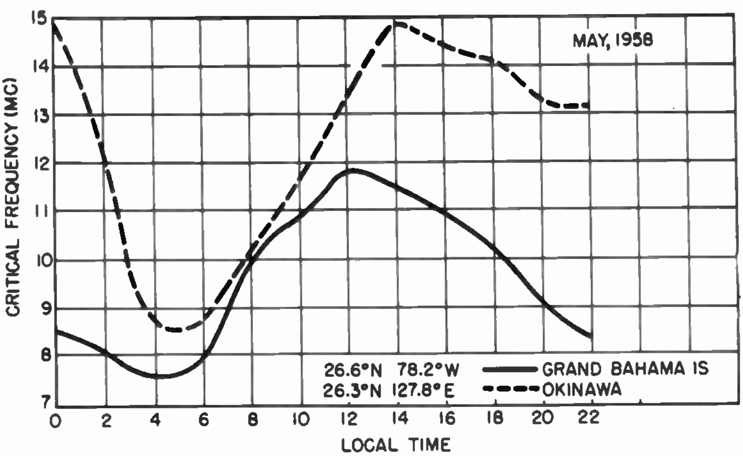

Fig. 5-10. Hourly variations in F_2-layer critical frequencies during May, 1958 at locations of the same latitude but different longitude.

TABLE 1. NORMAL IONOSPHERIC VARIATIONS

	E Layer	F_1 Layer	F_2 Layer
Diurnal	Critical frequency follows zenith angle of sun. Height constant at about 110 km and practically disappears during night hours.	Similar to E layer. Height fairly constant. Maximum critical frequency occurs around noon, as in E.	Height and density increase during the daylight hours. Critical frequency generally continues to increase after sun's zenith angle has reached maximum. In addition there is a complex variation with latitude, longitude, and with respect to the geomagnetic equator.
Seasonal	Both layers vary solely in accordance with sun's zenith angle. During the summer, with high zenith angle, critical frequencies are considerably higher and occur for longer periods than during shorter winter days, when sun's zenith angle is considerably lower.		Daytime summer values much lower than winter day, but summer night critical frequencies are higher than winter night criticals. F_2-layer height subject to considerable variation, with summer heights much greater than at other times, and lower during the winter day than at night. Geographic and geomagnetic variations same as diurnal.
Cyclical	Electron density, and consequently critical frequencies of all layers, both day and night, summer and winter, increase with increasing sunspot activity, and vice versa. Good correlation between critical frequencies and sunspot numbers enables predictions of critical frequencies three to six months in advance.		

of May, 1958. Although the general shape of the curves is similar, critical frequency values in the east longitude sector are considerably higher than in the west longitude sector.

Practical applications. Since critical-frequency values determine the frequency requirements on a given circuit, we learned how critical frequencies were measured and how they varied. A summary of these normal variations in critical frequency is given in Table 5-1. We shall now discuss some of the *abnormal* variations in ionospheric characteristics, since they also are important in long-distance communication.

Chapter 6

IONOSPHERIC VARIATIONS: ABNORMAL PHENOMENA

We have thus far discussed the normal ionospheric phenomena—those regular changes in the ionosphere which could be predicted in advance, provided certain information is given. These normal variations included diurnal, seasonal, as well as cyclical changes in layer heights and in critical frequencies.

In addition, there are abnormal variations which cannot be predicted, and which are generally detrimental to radio propagation conditions and long-distance shortwave radio communication. Strangely enough, although few people seriously question the relationship between solar activity and the normal ionospheric variations which we have discussed, there is actually only one event on the sun's surface, which we can associate directly with an ionospheric phenomenon—the *solar flare*. Its terrestrial effect is the most striking of ionospheric abnormalities: the *Sudden Ionospheric Disturbance* (SID). It is also known as the *Short-Wave Fadeout* (SWF) or the *Dellinger Fadeout*.

SOLAR FLARES AND THE SID

Solar flares almost always occur in a sunspot group vicinity. Although the occurrence of a solar flare is a random event and cannot be predicted at present, there are many more flares during sunspot maximum than at any other time in the sunspot cycle, because there are more sunspot groups on the sun at this time. A solar flare occurs as a sudden bright flash in or near a sunspot. There is a burst of radiation, and a fairly large area near or within the group brightens considerably, giving the appearance of a "white-hot" area. The flare, believed to be a cataclysmic eruption of some kind, emits simultaneously an enormous burst of radiant energy of many wavelengths, and huge quantities of subatomic particles called corpuscles.

Simultaneous with the observation of large solar flares, there occurs in the daylight regions of the earth a complete blacking out of all shortwave signals being propagated by the ionosphere.

Among the forms of energy traveling from the flare with the speed of light are intense bursts of x-ray and ultraviolet radiation. It appears that this radiation causes abnormally great ionization in the lower reaches of the *E* layer, as well as a region right below it, referred to as the *D* layer; these appear to be the areas that absorb shortwave signals.

When the flare is first observed, the lower shortwave frequencies start to go out. During an intense SID, all frequencies in the shortwave range may black out within one minute, ending temporarily all long-distance shortwave radio communication in the world's daylight regions.

Although the duration and intensity of SID's differ considerably, most of these pass within an hour. It has been observed that most flares reach maximum intensity within several minutes after they are first observed, then fade out rapidly. The effects of the flare, however, may be felt for considerably longer.

The indication that an SID is coming to an end usually is the return of the higher bands, first. Generally, communications men quickly schedule the highest useful frequencies for propagation available to them when an SID is observed, because these are the last to go, and the first to return.

IONOSPHERIC STORMS

Figure 6-1 is a photo of the sun taken on July 1, 1957. This was the first day of the recently concluded International Geophysical Year. It started literally with a bang.

The sunspot, shown with an arrow, is believed to have caused one of the severest ionospheric storms of recent years. The storm, which started June 30, continued for about three days.

Throughout its passage across the sun, this sunspot was highly active and the source of a great many flares. On June 28, while it was near

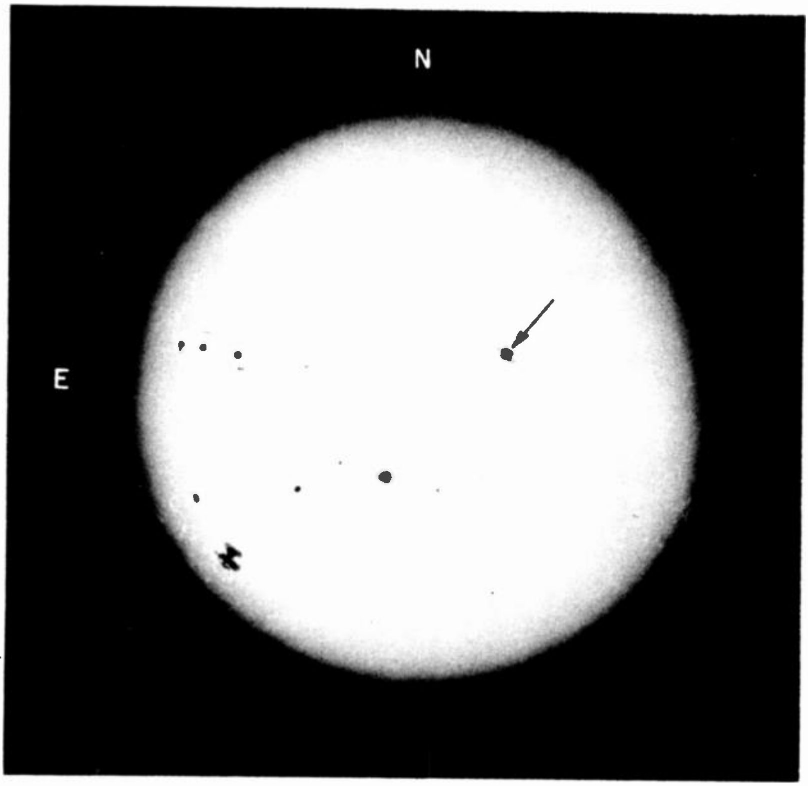

Fig. 6-1. Photograph of the sun taken July 1, 1957, showing sunspot (arrow) believed to have caused severe ionospheric storm of June 30—July 3. *Official U. S. Navy Photograph.*

the center of the sun, an enormous flare and SID were reported as originating from this spot. This flare probably sent countless billions of subatomic particles winging toward the earth at a velocity of about 500 miles per second. On arrival near the earth's magnetic field, these particles set off great currents around the earth, in turn causing magnetic storms and aurora, as well as sudden storms in the ionosphere.

The ionospheric storm is generally characterized by significant deviations from normal values of critical frequency, large increases in absorption, abnormal extremes of fading, heavy noise levels, as well as abnormal variations of layer height and ion density in the regular layers of the ionosphere.

Figures 6-2 and 6-3 are actual ionograms made within two hours of each other at Narsarssuak, Greenland, on September 30, 1958. Fig-like an enormous sudden silent explosion, the bands begin to break up. The sky is filled with green, pink, purple, and sometimes red ribbons and draperies, dancing, shimmering, pulsating violently, wildly. The atmosphere seems to be on fire. The aurora ranks among the most breathtaking and spectacular of all nature's pageantry.

The aurora is only one aspect of a much more general phenomenon —the magnetic storm. Tremendous jets of electrified particles are shot from the sun during certain types of disturbances in the sun's atmosphere. These electrified particles (corpuscles) speed toward the earth at velocities as high as several thousand miles per second. On approaching the earth, the jets are caught in the earth's magnetic field—the

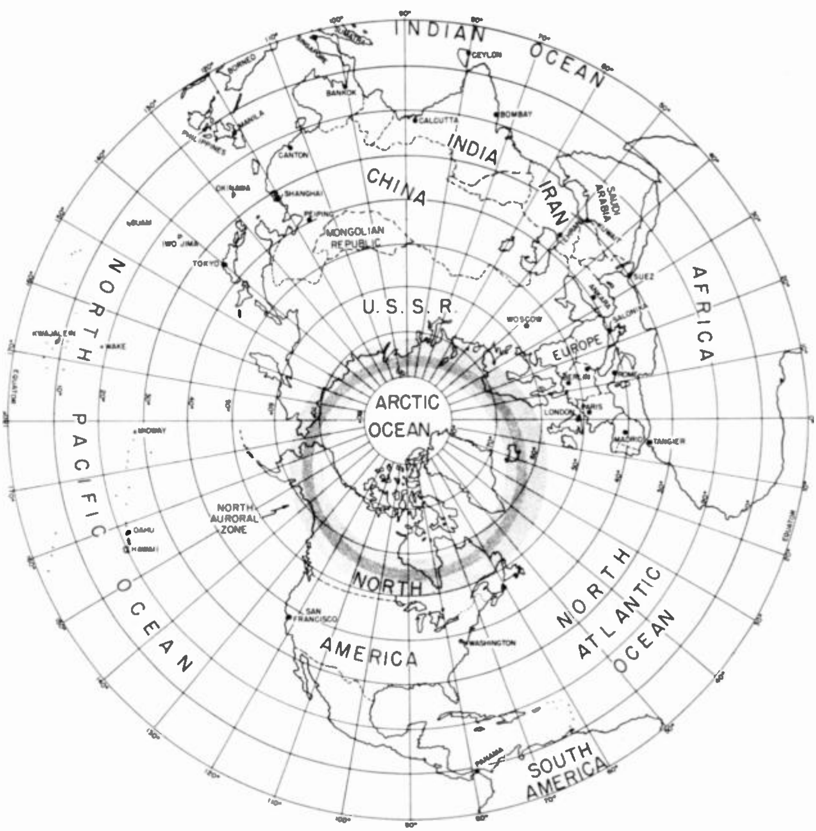

Fig. 6-4. Northern Auroral Zone. Drawing shows average number of overhead auroras observed at various locations in the Western Hemisphere.

invisible, nebulous envelope which surrounds the earth and which extends thousands of miles into space.

The magnetic field of the earth draws most of these particles toward the north and south polar regions. There, the onrushing particles speeding into the earth's upper atmosphere collide with atoms of gases present there. These collisions energize the atoms, and they give off light. The accumulated effect of countless billions of atoms giving off light simultaneously results in what we call the aurora, or "northern lights."

AURORAL ZONES

Observations made during the past century have enabled us to define with some accuracy the areas of the world where auroras occur most frequently. These zones are outlined in Fig. 6-4. The heavy black ring represents an area centered roughly about 23 degrees from the magnetic north pole (which does not coincide with the geographic north pole). Auroral displays occur approximately 250 nights a year in this area. South of this zone, they occur less frequently. Auroral displays occur between ten and forty nights a year in the northern and central United States, whereas several years may pass before a single display can be seen in the southern United States.

The most frequently measured height of the aurora is of the order of 60 or 70 miles, placing it in the vicinity of the *E* region of the ionosphere.

EFFECTS ON THE IONOSPHERE

The absorption (loss of power) experienced by radio waves in their passage through zones of auroral activity is high—even when the ionosphere is normal. Under disturbed conditions, excessive ionization, believed to occur in the auroral zone, results in excessive absorption of any shortwave signal that passes through or near the region. As a result of this, the auroral zone acts as a shield, preventing radio signals from passing through it. For this reason, radio communications across the poles is extremely unreliable and generally not feasible.

Shortwave radio signals passing to the south of the auroral zones are not affected by auroral absorption. The auroral zones are not fixed, and during periods of severe magnetic disturbance, they move southward and expand. Consequently, signals passing through these ex-

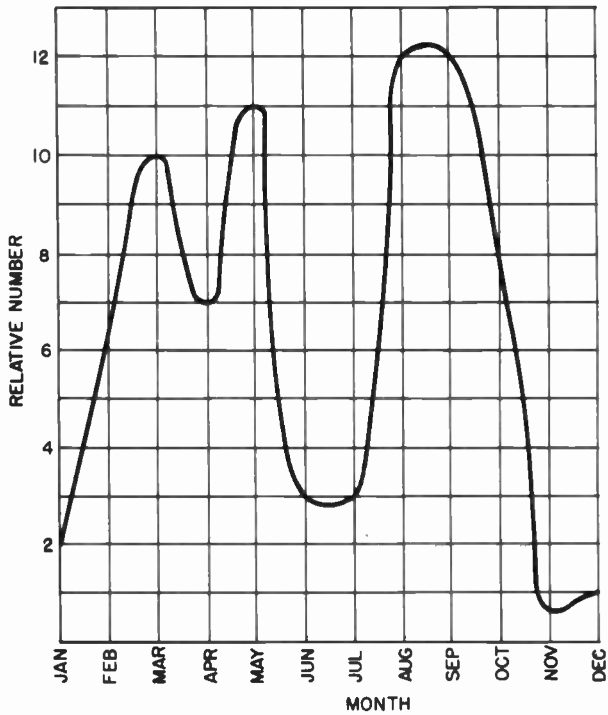

Fig. 6-5. Relative number of overhead auroral displays observed monthly in Central New York State.

panded zones of auroral activity become severely disrupted. During particularly violent disturbances, all forms of radio communications circuits are disrupted, with teletype machines printing garble instead of intelligible messages; transatlantic cables, and long land lines are out and sometimes even the shorter land lines are affected.

AURORA, SUNSPOTS, AND DISTURBANCES

There is an association between big auroral displays and the sunspot cycle, as well as big auroras and ionospheric disturbances. In general most auroras are seen during years of maximum sunspot activity, with the greatest number of auroras observable during the years immediately following sunspot maximum.

The month-to-month variation in auroral displays seen overhead in central New York State is shown in Fig. 6-5. This chart indicates an apparent general peaking during the equinoxial months, with minimum auroral activity being observed during the late fall and early winter months.

An analysis of data collected by the National Bureau of Standards from early 1946 indicates that on 80% of the days on which a large aurora was observed overhead in central New York State or further south, the ionosphere over the North Atlantic was significantly disturbed. However there are a great many days on which the ionosphere is significantly disturbed when no visible auroral display has been reported in the lower latitudes.

27-DAY RECURRENCE TENDENCY OF IONOSPHERIC STORMS

The sun is in a constant state of turbulence. Tremendous explosions, spewing white-hot gases hundreds of thousands of miles into space, are constantly occurring. These formations are called solar prominences. Although most of the material expelled from prominences appears to fall back onto the surface of the sun, there is increasing evidence to indicate that much of the matter escapes into outer space from such active regions. These regions are referred to as *M* regions and appear to emit particles over long periods of time.

What we have, then, are two types of solar disturbance which result in the emission of particles: one of these is the solar flare; the other, the solar *M* region. Disturbances caused by the former are generally very severe, commence suddenly, continue for several days and then end. *M*-region associated disturbances, however, have a tendency to recur at 27-day intervals. Twenty-seven days is also the average period of rotation of the sun.

Figure 6-6 shows the earth being showered with a particle blast such as is emitted either from a flare or from an *M* region. *M*-region storms are not as severe as the flare-associated sudden commencements. In addition to their tendency to recur at 27-day intervals, they generally persist longer (up to 5 days) than sudden commencements. In general, this type of storm recurs most frequently during years of minimum sunspot activity and will probably be most prevalent from 1961 to 1965.

LATITUDE VARIATION

The latitude of sunspots varies, depending upon the period of the sunspot cycle. At the beginning of a new cycle, sunspots occur in relatively high latitudes of approximately 40°. As the cycle progresses to maximum and toward minimum again, the latitude of the spots continues to decrease. During the final years of a cycle, most spots occur in latitudes under 10°.

The beginning of a new cycle is heralded by the appearance, once again, of high-latitude sunspots. As sunspots approach the sun's equator toward the latter part of a cycle, the particles ejected are more nearly in line with the earth. It is believed, therefore, that peak occurrences

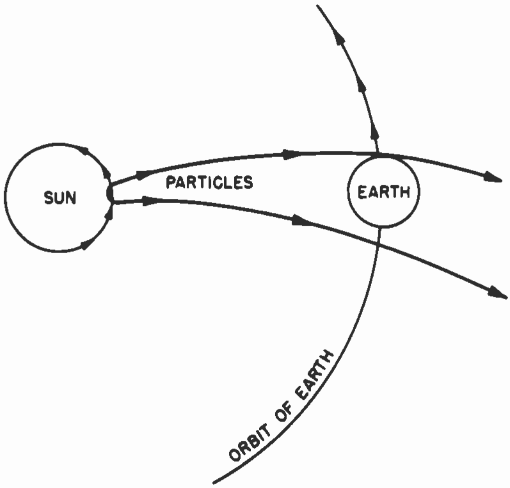

Fig. 6-6. Earth encountering particle blast emitted from active solar region.

of aurora and the great magnetic storms, as well as the 27-day recurring storms later on, are associated with the position of spots on the sun; their effects are felt most when they occur in the lower latitudes.

For a similar reason, auroral displays, as well as magnetic and ionospheric storms, occur most frequently around equinoxial periods. During the spring and fall, the earth passes through the equatorial plane of the sun. As a result, solar eruptions at these times are most likely to occur in the direction of the earth, and their effects are most likely to be felt during these seasons.

ABSORPTION, FADING, AND NOISE

Absorption. Absorption can be referred to as ionospheric friction. Propagation can not take place without the loss of energy. If it were not for absorption, a radio signal would continue indefinitely in a journey around the world, passing back and forth between the earth and the ionosphere.

A radio wave entering the ionosphere imparts energy to the free electrons in the ionosphere. The electrons are set into motion, oscillate, and, in turn, radiate energy at the same frequency as the incident wave. Theoretically, if the oscillating electrons do not collide with ions or molecules in the ionosphere, no energy will be lost. In actual practice, however, this is not the case; electrons do collide with other ions and molecules, and since these are so much more massive than electrons, there is a wave energy loss. This loss is called absorption and will, in general, depend on molecular density in the region, as well as on the wave frequency. If the frequency is large compared with the number of collisions per second, the electrons will make a number of oscillations between collisions.

Since molecular density increases the closer we get to earth, most absorption takes place in the lower regions of the ionosphere, primarily in the lower *E* and *D* regions.

There is another type of ionospheric absorption: we have seen that as a radio wave approaches a region of maximum ion density in the ionosphere, it slows down and changes direction. Since the wave spends more time in a given region when it is slowed down, the chances of collision with heavier ions and molecules increases, and so does absorption. This kind of absorption is known as *deviative* absorption, because it occurs while the wave is changing direction or deviating from its original path.

Absorption which occurs in the *D* and lower *E* regions is called *nondeviative,* since the wave does not deviate from its course.

Absorption varies with time of day, season of the year, and with the sunspot cycle. During the daylight hours, absorption is maximum, peaking around noon and depending generally on the zenith angle of the sun. Absorption is a minimum at night, since ion production during this time is at a minimum. Seasonally, absorption is greatest during the summer daytime, here again due to day length and zenith angle of the sun. There is evidence to indicate that absorption increases with sunspot number, irrespective of time of day or season of the year.

At any given time, absorption *decreases* as the frequency is *increased.* For vertical incidence soundings, for example, absorption is *least* near the critical frequency and increases as we lower the frequency.

Since most absorption takes place in the *D* and *E* regions, it stands to reason that the longer the distance the radio wave travels in these regions, the greater will be the absorption. Thus, a radio wave sent *obliquely* into the ionosphere will be more absorbed than one entering the ionosphere in a perpendicular direction (see Fig. 6-7).

In addition to the normal variations in absorption, there are certain significant abnormal variations. X-rays from flares, as well as corpuscular radiation from the sun, cause abnormal absorption in the *D* and lower *E* regions of the ionosphere. During severe SID's and ionospheric storms, absorption in the *D* layer becomes so great that penetration to the other layers is not possible. Under such circumstances, no communication is possible until sufficient recombination in these layers takes place so that radio waves may pass through to the reflecting layers of the ionosphere.

Relatively little is known about auroral absorption, but it is believed that the same agency which causes visible aurora is also responsible for

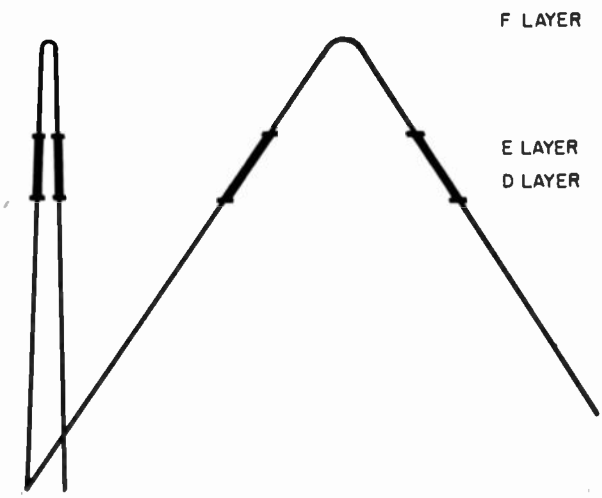

Fig. 6-7. Relative distance traveled in *D* and *E* absorption regions by obliquely and vertically incident radio waves.

the absorption. Several years will pass before the wealth of data taken in northern latitudes during the recent International Geophysical Year will be analyzed. Then, we hope to know considerably more about auroral absorption.

Fading. The downcoming sky-wave signal is rarely constant, but it changes in a more or less random manner with changes in the ionosphere. The signal strength of a downcoming wave changes constantly, sometimes rapidly, sometimes slowly, causing variations in amplitude, distortion, and sometimes, because of its depth or rapidity, impossible listening conditions.

The most general kind of fading is called *interference fading,* and results from radio waves arriving at the antenna out of phase. A radio wave is actually composed of an infinite number of individual rays. Since these rays often travel over slightly different paths through the ionosphere, they may arrive at the receiving antenna from slightly different directions and somewhat out of phase. As a result, some of these rays will reinforce each other, while others, arriving completely out of phase, will cancel each other entirely. As a result, the signal strength of the downcoming wave may fluctuate considerably from instant to instant.

Another type of fading is called *polarization fading.* The direction of polarization of a wave is defined as the direction of the wave's electric component with respect to the earth. Since polarization of a radio wave can vary in a very complex manner, depending on wave frequency, magnitude and direction of the earth's magnetic field, ion density, and polarization of the original wave, the polarization of the downcoming radio wave is often changing very rapidly and in a completely random manner.

These continuous changes in polarization affect the radio wave in the same manner as phase differences do in interference fading. Consequently, a fading component due to polarization differences is introduced.

When the frequency being used is very close to the Maximum Usable Frequency, that is, the highest frequency that can be used over a path, *selective fading* occurs. Under such conditions, a frequency difference of only a few hundred cycles may mean the difference between a satisfactorily received signal or none at all. Since most broadcast transmissions require a bandwidth of the order of 10 kc, it is conceivable that, under certain conditions, the upper or lower range of the carrier frequency may be cut off, resulting in severe distortion. This effect becomes particularly pronounced in the transmission of music, although voice transmissions are very adversely affected also.

Selective fading occurs most often during transition periods, that is, at times when the change from day to night (or vice versa) conditions in the ionosphere is taking place, and the Maximum Usable Frequency is changing rapidly. In general, such rapid changes take place at dawn or dusk over a path.

A peculiar type of fading generally associated with propagation through the auroral zone is usually referred to as "flutter." It consists of an audio component of approximately 100 to 2000 cycles per second superimposed on the carrier signal. During disturbed conditions, when the auroral zone begins to move southward, flutter fading may be observed on circuits passing near or through this zone. At first, this fading component is not severe enough to render transmission useless, but it can get bad enough to render signals unintelligible.

Noise. The energy coming out of a radio receiver can be divided into two broad categories: the wanted and the unwanted signal. The wanted signal is the intelligence which is being transmitted and which we are interested in receiving. Any other signal is unwanted and is classified broadly as "noise."

Noise can be broken into two categories: man-made, and that which is produced naturally. Man-made noise consists of interfering signals caused by electrical apparatus (diathermy machines, auto ignition, motors). Actually, the radio receiver itself generates some noise, depending upon its inherent characteristics. Since man-made noise is generally a geographic phenomenon, it will be discussed only in passing. In general, man-made noise is much more severe in urban and metropolitan areas than in rural and suburban locations.

Noise which is produced by natural phenomena is either terrestrial (atmospheric) or extraterrestrial in origin.

Atmospheric Noise. Measurements of *atmospheric noise* have been made for a number of years over a great many areas of the world. These measurements have shown that atmospheric noise varies widely from place to place, and in a diurnal and seasonal manner. Little is known of noise variations within the 11-year sunspot cycle.

Although all sources of atmospheric noise are not completely understood, the major portion of atmospheric noise is produced by thunderstorms and by precipitation. All of us are familiar with the cracking and crashing produced in a receiver when a thunderstorm is nearby. Thunderstorms occur much more frequently in the tropics than in temperate zones. In all areas, thunderstorms are most frequent during the late afternoon and evening hours.

Since atmospheric noise is propagated both via ground and sky waves, the noise level at any given location depends upon local as well as distant conditions. It is estimated that there are approximately 2000 thunderstorms in progress at any given moment throughout the world. As we go further away from the tropics, the noise produced by storms decreases, and is a minimum in polar regions.

Atmospheric noise is highest in the low- and very-low-frequency bands, and decreases proportionately as frequency is increased. Since noise propagated via the ionosphere follows the same laws as other radio waves, we find that diurnal variations in noise levels behave as we would expect: During the daylight hours the ionosphere supports the higher frequencies more effectively, and the noise levels in these ranges are higher than at night. During the nighttime hours, noise in the lower bands (up to 10 mc) is higher than during the day.

Extraterrestrial Noise. At frequencies above 15 mc and on into the VHF and UHF bands, the primary sources of noise are extraterrestrial in origin and come primarily from the sun within our solar system and from the Milky Way in our galaxy (the star system to which the sun belongs).

Solar noise is generally associated with active regions on the sun, and occurs principally in the VHF and UHF ranges.

Cosmic noise occurs in a random manner and appears as an aggregate of a large number of individual disturbances which occur at random and have random phase relationships.

SPORADIC-*E*

From time to time there occur in the *E* region of the ionosphere relatively small areas of exceedingly high ionization density. Because their occurrence is not predictable and because they occur in the vicinity of the *E* layer, these areas are usually referred to as *sporadic-E clouds,* or patches. They are capable of reflecting radio waves of much higher frequency than the normally ionized layers of the ionosphere.

Although it could be argued validly that a discussion of sporadic-*E* activity rightly belongs in a chapter on abnormal ionospheric phenomena, we have chosen to include our discussion of sporadic-*E* activity in our chapter on the radio amateur, since sporadic-*E* is so closely connected with amateur activity, from its discovery to its frequent and effective utilization in long-distance communication.

Chapter 7

CIRCUIT ANALYSIS: SKY-WAVE PROPAGATION

A fairly wide range of shortwave frequencies, when transmitted vertically, will be returned to earth by the ionosphere. The highest frequency so returned by each of the layers of the ionosphere is called the critical frequency for that layer.

Although the critical frequency is invaluable in scientific work, it is of little value in long-distance communications, since it is returned to earth near the transmitter. To enable it to cover the great distances required in radio communications, the radio wave must leave the transmitting antenna at an angle such that the wave will strike the ionosphere obliquely.

For a given path, the value of the best frequency to be used depends upon a number of things, among which are critical frequency, layer height, and distance between transmitter and receiver.

THE SECANT LAW

There is a direct relationship between an obliquely incident frequency which will be reflected from a given layer height and the critical frequency at the same layer height. This relationship is written

$$f = f_0 \text{ secant } \theta ,$$

where f is the obliquely incident frequency, f_0 is the critical frequency at the same layer height, and θ (theta) is the angle of incidence. See

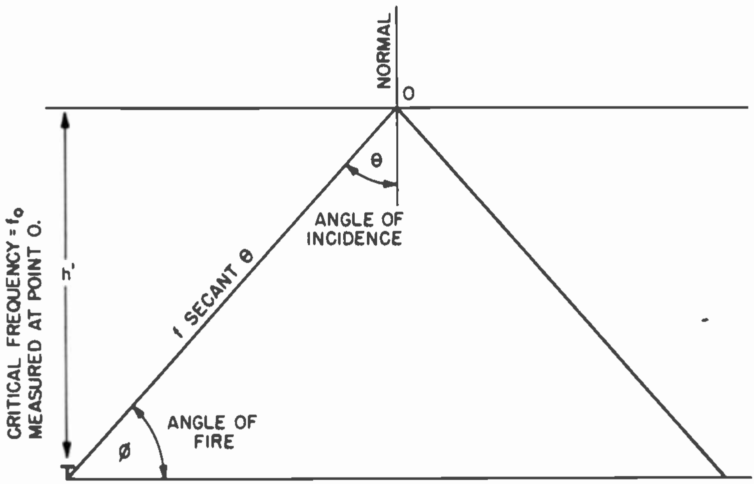

Fig. 7-1. Secant law for flat earth and flat ionosphere.

Fig. 7-1. This relationship, called the Secant Law, permits us to calculate the oblique incidence critical frequency for any angle of incidence, provided the vertical incidence critical frequency for the same layer height is given. The Secant Law applies only in the theoretical case of a flat earth and ionosphere. To allow for curvature both for the earth and the ionosphere, the law must be modified. Since these modifications are quite complex, and beyond the scope of this book, they are only mentioned to remind the reader that they must be allowed for in the final calculations.

MUF

The critical frequency for any given distance, that is, the *highest* frequency that can be used over a particular transmission path, is called the *Maximum Usable Frequency* (MUF). Frequencies above the MUF will not be heard at the receiving location for which they are intended.

Although there is actually a range of frequencies which may be used in transmitting to a particular location, the MUF represents the frequency at which absorption is a minimum and signal strength maximum. Although it is generally desirable to work somewhat below the MUF, the use of frequencies far below the MUF may result in excessive absorption and noise, and therefore in an unintelligible signal.

MUF FACTORS

There is a relationship between critical frequency, MUF, and angle of incidence of the radio wave with the ionosphere. The MUF at any distance is determined by multiplying the critical frequency at zero distance by a factor related primarily to the secant of the angle of incidence. This factor is called an *MUF factor*. Its value is unity at vertical incidence and can reach a maximum of around 5 for large angles of incidence.

Figure 7-2 shows a typical MUF-factor curve for the ordinary ray for the F_2 layer. At distances below approximately 1000 km, the value

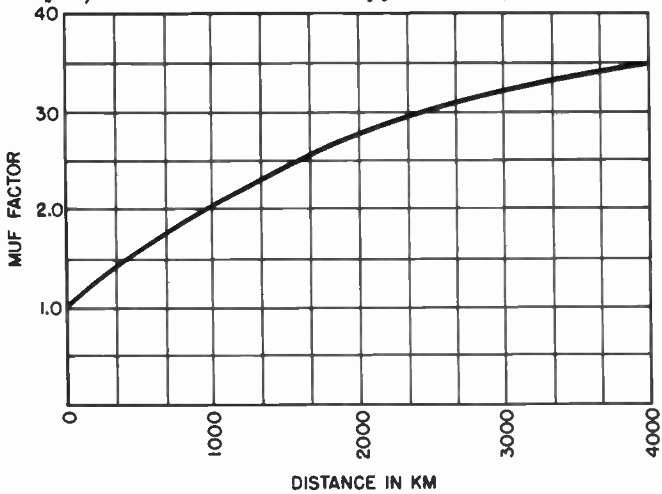

Fig. 7-2. Typical MUF-factor curve for F_2 layer, ordinary ray.

determined from the MUF-factor curve must be increased somewhat (generally of the order of 0.5 mc or thereabouts), in order to correct for the extraordinary ray. Above these distances, the difference between ordinary- and extraordinary-ray critical frequencies becomes insignificant.

The MUF factor is a function of layer height. Consequently, it will vary for a given layer in accordance with the height variations within that layer.

From the geometry of the path, we may determine what the elevation angle (angle of fire) of the transmitted radio wave must be for various distances and for various layer heights. One such curve is shown in Fig. 7-3 for one-hop distances up to approximately 2800 km (1600 miles).

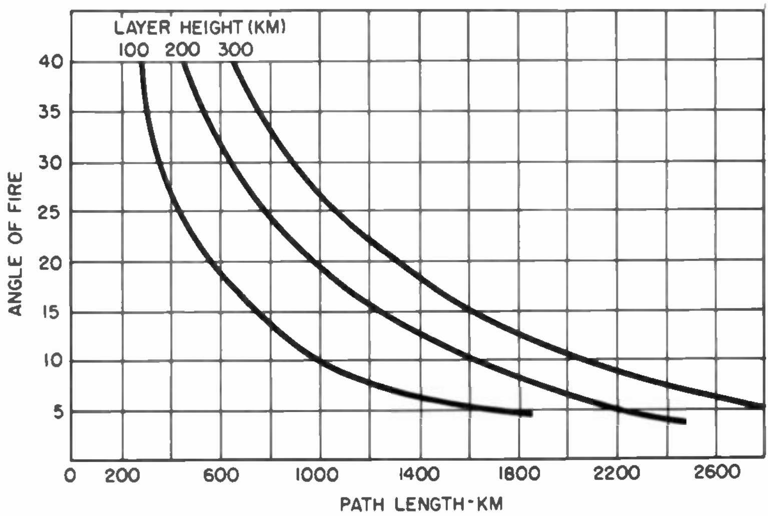

Fig. 7-3. Vertical angle of antenna vs path length for different layer heights.

Angles of fire are important in circuit planning, since a knowledge of the optimum angle of fire in relation to ionosphere layer height enables us to design optimum antennas for use on specific circuits.

SKY-WAVE MODES

Figure 7-4 illustrates several of the possible paths that a radio wave, entering the ionosphere and being refracted by one of its layers, may take. At certain of the higher angles of fire, the frequency may be too high. Thus, penetrating the layer of the ionosphere, the radio wave may be lost in outer space. As we lower the angle of fire, we approach the *critical angle*. When the sine of the angle of incidence equals the index of refraction of the ionosphere, the angle of refraction becomes 90°. The radio wave travels parallel to the ionosphere at an angle of 90° to the normal, instead of penetrating the ionosphere, going to outer space, or being refracted back to earth. The angle of incidence at which this occurs is called the critical angle. The critical angle is also defined as the highest radiation angle (angle of fire) for a particular frequency that barely returns the wave to earth. If the angle in the first case is lowered by a small amount, the second case occurs. Therefore both definitions hold. At the critical angle the distance covered by the wave is maximum. As the angle of fire is lowered beyond the critical angle, the distance at which the wave is returned to earth decreases until the point of minimum distance for the particular frequency is reached. This minimum distance is called the *skip distance*. Figure 7-4 shows that the skip distance is the distance from the transmitter where there is no

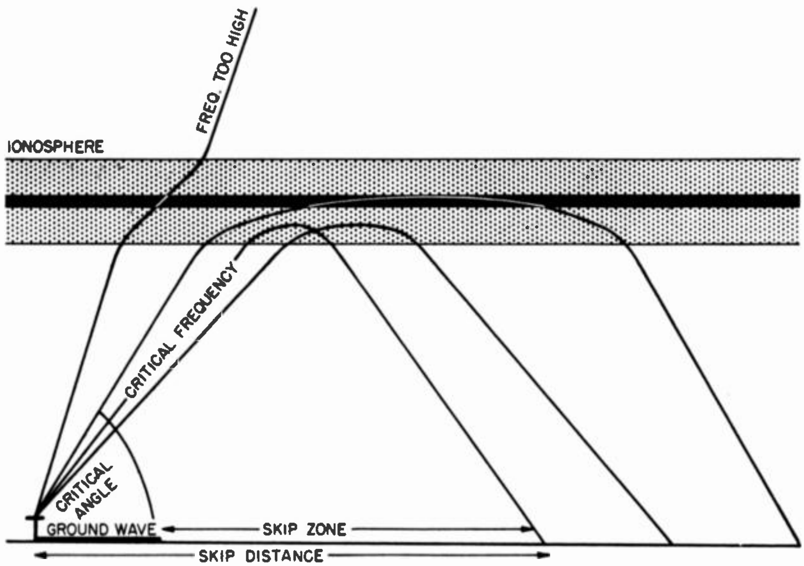

Fig. 7-4. Differing sky-wave paths.

sky-wave signal coming down for that particular frequency. This radiation angle is called the *skip angle*.

If the angle of fire is further decreased, the distance from the transmitter at which the radio wave is returned to earth *increases* (see Fig. 7-4).

The critical angle and the skip angle are very similar in value. As the skip angle is lowered, the ionosphere simply begins to act primarily as a refracting medium for the incident radio waves.

Figure 7-4 shows an area between the outer limits of ground-wave coverage and the skip distance where *no signal whatsoever* is heard. This area is called the *skip zone*.

At certain frequencies near the value of the vertical-incidence critical frequency, the skip distance occurs within the outer limit of the ground-wave coverage area. In such cases, it is possible for the ground and sky waves to reinforce or cancel each other in a random manner. This causes severe interference fading and can make reception in such an area totally unintelligible. In cases where the sky wave and ground wave deliver approximately the same signal strength to an area, intelligibility is usually very bad owing to this fading effect. The area so affected is generally called the *fading ring.*

MULTIHOP PROPAGATION

The behavior of a radio wave in the ionosphere depends on the radiation angle, the height of the reflecting layer, its ion density, and the frequency of the waves. A radio wave which has been refracted by the ionosphere returns to the earth either to be received at a receiving antenna or to be reflected again by the earth. Although a radio wave which has been returned to earth in this manner loses energy, a significant part of the wave is usually reflected and travels back again to the ionosphere. This method of travel, whereby a radio wave is propagated from the earth to the ionosphere and back to earth again, is called a "hop." Such hops enable long-distance radio communication to take place, as shown in Fig. 7-5. The possibility of radio communication via many such hops is very significant, since, without it, really long-distance shortwave radio communication could not take place.

Because of the earth's curvature and the limited height of the ionospheric layers, the maximum distance that a radio wave can travel in one hop, via the highest F_2 layer, with the smallest possible radiation angle, is of the order of 2400 miles (4000 km). For the other layers, the E and F_1, this maximum distance is smaller, of the order of 1400

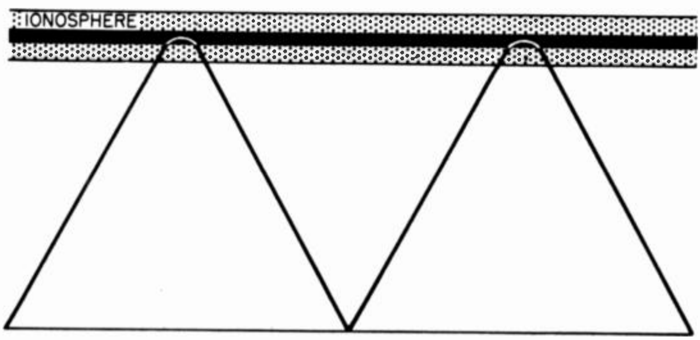

Fig. 7-5. Multihop propogotion.

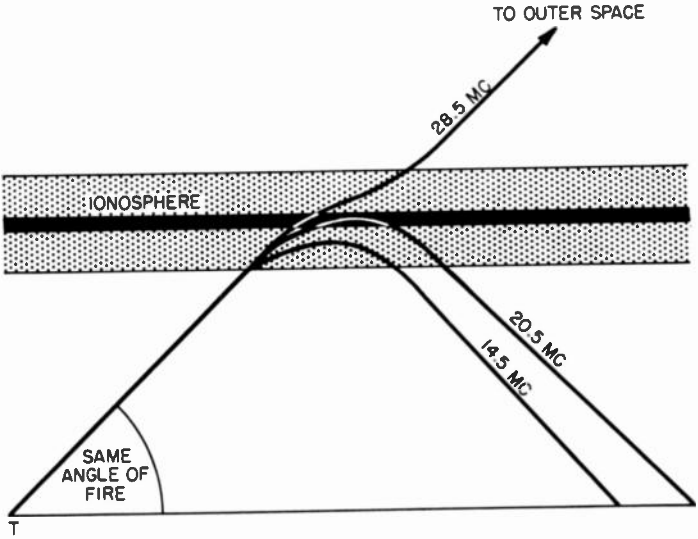

Fig. 7-6. Variation in distance with frequency at same angle of fire.

miles for the *E* layer and 1700 miles for the F_1 layer. Thus, without multihop propagation, radio communication via short waves beyond these distances is generally not possible.

VARIATIONS WITH FREQUENCY

For a given ion density and angle of fire, if frequency is increased, refraction decreases, as shown in Fig. 7-6, for frequencies of 28.5, 20.5, and 14.5 mc. In the case of the highest frequency, ion density is not sufficient to refract the wave, and it is lost in outer space. The 20.5-mc frequency signal is returned to earth. Because its frequency was relatively high, penetration of the ionospheric layer was relatively great, refraction was less than for the 14.5-mc wave, and it was therefore returned to earth at a greater distance from the transmitter. We thus conclude that, on any given day or night, the higher the frequency, the greater will be the skip distance until penetration takes place.

PREPARATION OF CIRCUIT ANALYSIS CURVES

With a fixed angle of fire for a particular ionosphere layer of given ion density, a frequency exists higher than any other that will be returned to earth at a given distance. The particular frequency has been defined as the MUF for that distance. In general, a Maximum Usable Frequency exists over any great circle path. As the distance between transmitter and receiver increases over a great circle path, the MUF for that path increases up to a distance of approximately 2400 miles. Beyond that distance, which is the maximum "one-hop" distance, the MUF for the path may decrease.

Between any two points on the surface of the earth, a plane can be drawn which passes through these points and the center of the earth. The line through which this plane cuts the surface of the earth is defined as the *great circle path* between the two points. The great circle path is generally the shortest distance between given points on the earth's surface and is the path a radio wave most often follows in traveling from one of the points to the other. The portion of the ionosphere which controls propagation lies directly over the great circle path.

Since the ionosphere lying over the great circle determines the mode of propagation, a method for determining the MUF over that path suggests itself: we must first determine the critical frequency at the *midpoint* of the path at a particular layer height. Knowing the path length will enable us to determine what the MUF factor will be.

Suppose that our F_2 layer critical frequency at the midpoint of the path is measured to be 6.2 mc and that our path length is 3000 km. From Fig. 7-2 we find that the MUF factor has a value of 3.5; multiplying the critical frequency by 3.5 gives us the F_2-layer MUF for the path at the particular hour at which the critical-frequency measurement was made, that is 21.7 mc.

In most instances, it is desirable to choose a frequency as close to the MUF as possible, because at frequencies above the MUF, the wave penetrates the ionosphere and does not return to earth, whereas at frequencies below the MUF, the absorption increases rather rapidly during the daylight hours, while at night the noise becomes greater as we lower the frequency.

Fortunately, the diurnal, seasonal, and cyclical variations in critical frequency enable us to predict months in advance the values of critical frequency at any hour, in any part of the world. Consequently, the MUF over any circuit can be predicted. The use of MUF factors to determine path MUF can become rather complicated, since variations in layer height must be interpolated to obtain the appropriate MUF factors. These variations are sometimes very complex and difficult to predict.

The National Bureau of Standards has developed a method of predicting MUF's over any path, irrespective of path length. This method entails the use of world contour maps; we will describe it fully in the next chapter.

LONG-PATH MUF CALCULATIONS

The limiting distance for one-hop propagation is of the order of 4000 km (2400 miles). Under such conditions, only the critical frequency at the midpoint of the path is required for determining the MUF for the path. This single "control-point" method does not apply to circuits which extend beyond one-hop limiting distances.

Ionosphere engineers believed that in multihop propagation, the condition of the ionosphere at every reflection point was equally important to determine whether propagation over the entire path was possible. It has been determined experimentally, however, that propagation failure occurs only in cases where the ionosphere at "control points" lying at a distance of approximately 2000 km (1200 miles) from either terminal of the circuit could not support the frequency, but that in cases where these control points were able to support the frequency, communication was possible regardless of ionosphere characteristics between control points. The reason appears to lie in the complex behavior of a radio wave when encountering scatter sources in the ionosphere.

Figure 7-7 shows a multihop propagation path as presented heretofore. The radio wave is traveling along a ray path, but if this were actually the case, there would be a skip zone for each hop over the entire length of the path. We know, however, that this is not the case, because actually the only skip zone occurs between the transmitter and the area where the radio wave first returns to earth. After that, coverage is continuous.

The simple ray explanation is not satisfactory. A detailed explanation of what occurs introduces concepts beyond the level of this book. A

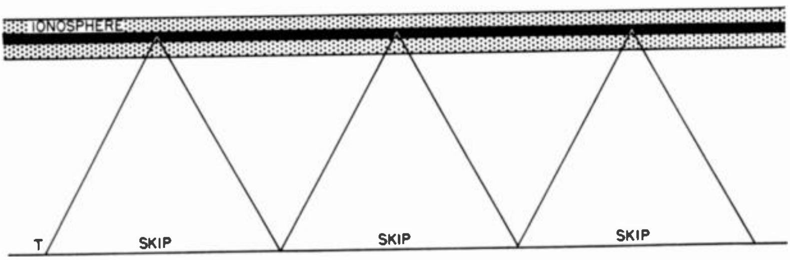

Fig. 7-7. Ray picture of multihop propagation path.

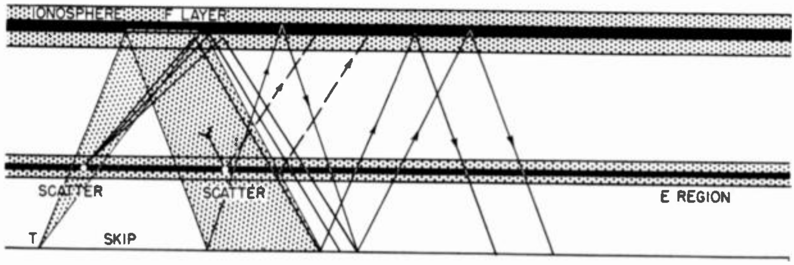

Fig. 7-8. Propagation modes for multihop path showing long and short scatter and regular ionosphere refraction.

simplified representation, however, is shown in Fig. 7-8. In addition to the regular refraction by the ionosphere, a scattering of radio energy occurs as the radio wave passes through the different ionospheric levels. Scattering of this nature occurs both on the way up and on the way down. The former is called *short scatter*; the latter *long scatter*. Also the radio wave, in leaving the transmitting antenna, does not actually travel along a ray path, but in a beam composed of a great many rays. This beam is shown only several degrees wide in the figure, but in actual practice the beam width can be any angle up to 180°. Therefore, the energy returned to the earth, both from regular refraction of all the individual rays that make up the beam and from short and long scatter, makes coverage continuous after the first hop.

OPTIMUM WORKING FREQUENCY

There are normal day-to-day variations in the ion density of the ionosphere. Since predictions of the MUF are made several months in advance, they must of necessity be calculated on the basis of *average* conditions expected to occur during any month. Because these predictions cannot therefore take into account the day-to-day deviations in MUF, the best working frequency at any time is found at a level somewhat below the predicted MUF. This ensures that on days when the actual MUF is below the predicted MUF, communication still takes place. For the F_2 layer, the best working frequency, or Optimum Working Frequency (OWF), is chosen at a value of 85% of the MUF. This value is also referred to as the FOT.

Working at a frequency as close as possible to the OWF will, in general, assure effective communication over a circuit on every normal day of the month. In the case of radio amateurs, to whom the use of a particular band rather than assignment at the OWF may be of prime interest, it should be noted that the MUF value during a month can vary considerably.

For example, on approximately one-third of the days of the month, the MUF will exceed the average MUF by a value of from 5 to 15%. On approximately 15% of the days of the month, the MUF will be as high as 30 or 35% above the predicted MUF. Thus, if at a given hour the predicted average MUF over a given path is 22 mc, then on approximately 10 days of the month the ionosphere supports a frequency of the order of 25 mc over the same path, while on 5 days of the month, a frequency of the order of 29 mc is satisfactory over the path at that particular hour.

LOWEST USEFUL HIGH FREQUENCY

The communications man finds of great value a set of curves which shows the monthly predicted MUF over the particular circuit which interests him. Methods involved in preparation of such curves will be given later in great detail. Figure 7-9 shows such a curve for a circuit between Tangier, North Africa, and Munich, Germany, for December, 1958. Inspection of such a curve enables us to determine the monthly average MUF at any given time of day. When a monthly MUF curve is drawn, the definition of MUF changes slightly, referring to the highest useful frequency over the circuit on 50% of the days of the month, since we are, in this case, obtaining the *average* MUF over the circuit.

Figure 7-9 also shows a second curve, labeled LUF (Lowest Useful High Frequency). This curve represents the lowest useful high frequency that can be used over the circuit during the hours indicated.

Earlier we discussed absorption and noise and indicated that it is actually the ratio of the delivered signal to the unwanted noise that is of prime importance in long-distance shortwave radio communications. The LUF is a measure of these factors and represents the frequency at which the strength of the signal just overrides the noise level in the area.

Calculation of the LUF is fairly complicated and depends upon transmitter power, antenna gain, noise levels in the receiving area, and absorption.

The rule laid down about working as close to the OWF as possible still applies, but there are instances where, for one reason or another, it is not possible to do so, and the use of a lower frequency is necessary.

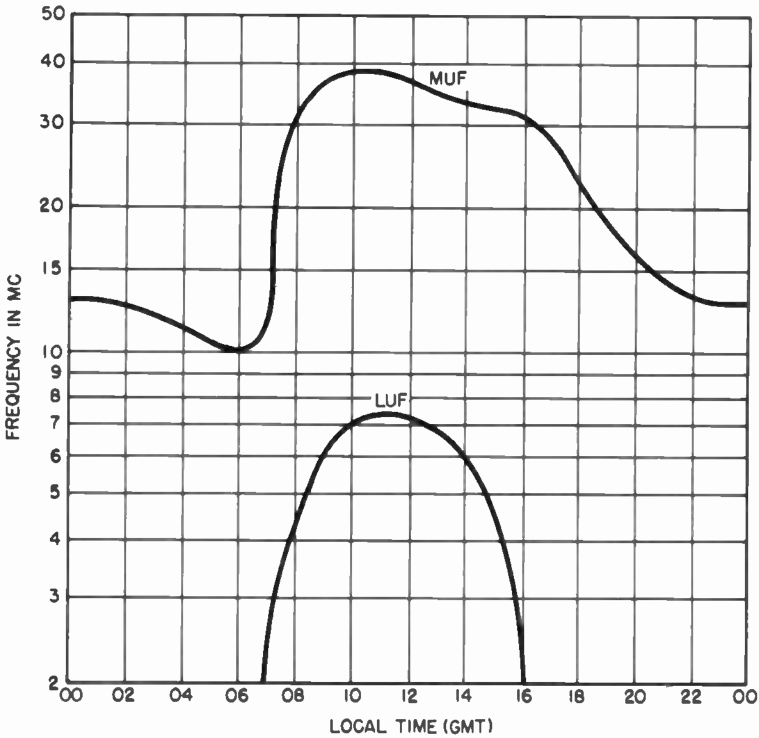

Fig. 7-9. MUF/LUF curve on the Tangier/Warsaw path for December, 1958. ERP: 1000 kw.

For a given radiated power, the LUF curve is the guide which shows us how low we can go. Frequencies below the LUF do not propagate. During certain times of day over some circuits, the LUF is greater than the MUF. In such cases, propagation at the radiated power for which the LUF was calculated is impossible over the path.

REQUIRED FIELD INTENSITY

To assure satisfactory reception in a given area at a particular time, the strength of the incoming signal must be sufficient to override noise levels (natural or man-made) in the receiving area. The signal which barely enables delivery of a satisfactory signal over the noise level in an area is defined as the minimum required signal strength, or minimum required field intensity. We can see here that the LUF can also be defined as the lowest frequency which is capable of delivering a signal which just overcomes the noise levels in the area.

DELIVERED FIELD INTENSITY

The strength of the signal *delivered* to the receiving antenna will, among other things, be a function of transmitter power, antenna gain, absorption on the particular frequency in use, and distance attenuation. The radio wave becomes weaker the further it travels; this is due to its "fanning out" with distance, as well as to energy losses incurred while contacting the earth during hops. (See Fig. 7-8.)

Practical communications are possible when the strength of the signal delivered is equal to or exceeds the minimum required field strength for satisfactory reception. LUF is also that frequency at which the delivered field strength equals the minimum required field strength.

ANGLES OF FIRE

For single-hop transmission, the angle of fire can be calculated geometrically, or obtained with curves similar to the one shown in Fig. 7-3. However, since critical frequencies, layer heights, and ion density fluctuate from hour to hour and from day to day, it is not possible to arrive at a single optimum angle of fire for intermediate distance propagation. The distance from the transmitter at which the radio wave returns to earth depends on frequency, layer height, and ion density. Since these factors are subject to considerable variation, best practical results can be obtained with an antenna that radiates most of its energy in a radiation pattern which is sufficiently wide to cover all possible variations in layer height, ion density, and critical frequency, as well as distance between transmitter and receiver, or reception area, in cases where communication will be from a point to an area rather than from point to point.

In choosing the range of elevation angles for intermediate range reception, the effect of the lower layers must also be taken into account. For example, during the summer, the *E*-layer frequently shields the upper layers, and the frequency which controls propagation over the path is *E*-layer propagated. This occurs most when, around noon, F_2 ionization is relatively low, while *E*-layer ionization is at a maximum. Propagation in these cases occurs off the *E* layer; as a result, to cover the same distance, the elevation angle must be somewhat lower than when the radio wave is propagated off the other layers.

The problems involved in multiple-hop communications are considerably more complex. Because of scatter, the radio waves become considerably diffused by the ionosphere and arrive from various directions. Experiments have shown, though, that there is a tendency for most of the energy to arrive from one general direction; this direction appears to depend on the least number of hops possible over the path, taking into account the average height of the ionosphere over the entire path. Calculation of departure angles under these conditions can become fairly cumbersome. As a general rule, the antenna used for long-distance multihop propagation should be designed so as to radiate maximum energy at as small an angle as practicable. Our experience has shown that optimum reception at great distances is obtained when the radiated energy is concentrated in a range of vertical angles of about 10°, with maximum radiation occurring at about 7°.

Chapter 8

CIRCUIT ANALYSIS: INSTRUCTIONS FOR PREPARING MUF CURVES

The propagation of shortwave radio signals over long distances depends primarily on the ionosphere as a medium of transportation. The characteristics of the ionospheric layers which reflect these radio signals are constantly changing. To maintain regular and reliable radio communication, whether amateur or professional, it is essential that the nature and order of these changes be thoroughly known.

In addition, if the radio operations are to be planned ahead of time, as is generally the case, ionospheric variations must in some way be anticipated, to make predictions of usable frequencies at some future date between any two places at any hour.

The prediction methods and techniques currently in use are presented to the reader with step-by-step methods to determine three months in advance the MUF and OWF between any two points on the earth's surface at any hour of the day or night.

Predictions for obtaining MUF's and OWF's on two circuits will be discussed. These are from New York to Berlin, and from Washington, D.C., to Baton Rouge, La. The procedures illustrated will apply to any circuit.

NEW YORK TO BERLIN

Figure 8-1 is a map of the world. We will need this map, a straightedge, a pencil, a few work sheets, and some transparent paper.

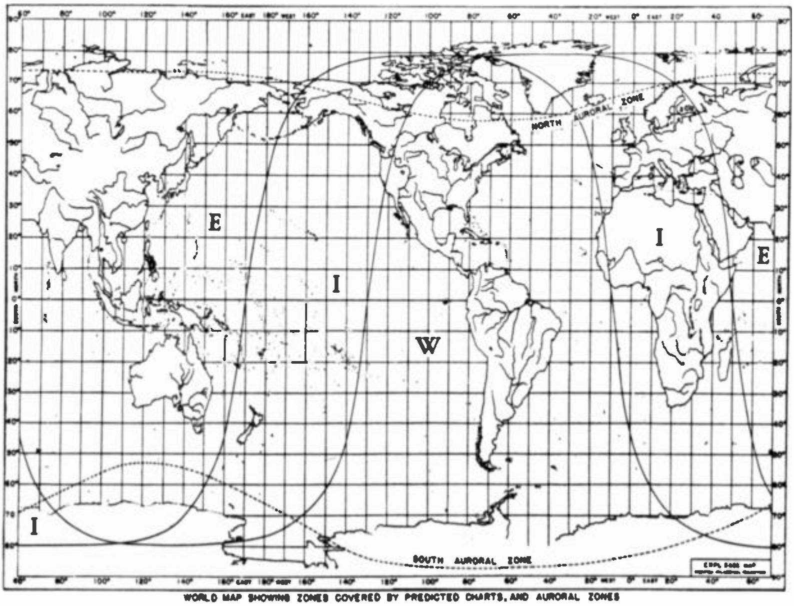

Fig. 8-1. World map showing zones covered by prediction charts, and auroral zones.

1. Place a sheet of transparent paper over Fig. 8-1. For reference, draw in the equator (0° latitude line), the Greenwich Meridian (0° longitude line), and place dots at the positions of our two stations:

New York 40.8°N, 74.0°W
Berlin 56.6°N, 13.2°E

2. Take the sheet of transparent paper on which we have marked our reference lines and points and place it on the great circle chart (Fig. 8-2), keeping the equators of the transparent paper (called an overlay or transparency) and Fig. 8-2 coincident. Keeping the equators coincident, slide the overlay back and forth until both stations lie along the same great circle (shown as solid contours on Fig. 8-2) or equidistant from adjacent great circles. A pencil line joining the two station locations runs parallel to adjacent great circles. The shaded area on Fig. 8-2 illustrates the above steps.

3. Referring again to Fig. 8-2, note that in addition to the solid line great circles, there are dot-dash lines numbered from 1 to 19. The distance between each pair of these lines represents a distance of 1000 km. Thus, the distance between dot-dash curves *6* and *12* is 6000 km. Simi-

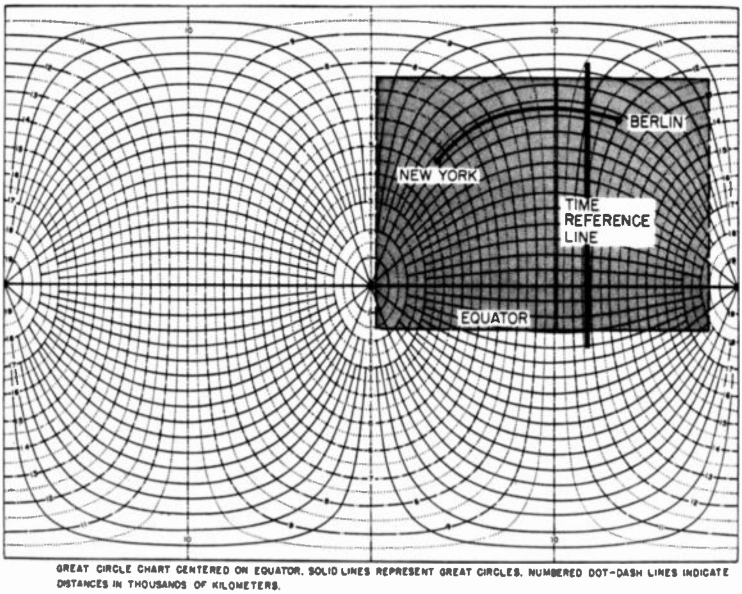

Fig. 8-2. Great circle chart centered on equator, solid lines represent great circles. Numbered dot-dash lines indicate distances in thousands of kilometers.

larly, the distance between pairs of dotted lines on Fig. 8-2 (not numbered) is also 1000 km, and the distance between adjacent dot-dash and dotted lines is 500 km.

4. The next step in the preparation of our overlay is to determine the distance between stations. Looking at the shaded sector of Fig. 8-2, we note that the New York terminal of our circuit falls exactly on a dotted line between dot-dash lines numbered *5* and *6*. Counting the 500-km steps, we find that the distance between New York and Berlin is approximately 6400 km.

Path length determines the course we are to take in determining the circuit MUF. If the path length is *less* than 4000 km, place a small marker at the midpoint of your path on the overlay. If the path length is *greater* than 4000 km, put markers 1000 and 2000 km from each station. At one end, the 1000- and 2000-km markers are labeled *A'* and *A*, respectively, and *B'* and *B*, respectively, at the other end.

Actually what we have in the overlay is a picture of the circuit projected onto a flat surface. One more step in necessary before we are ready to start in the actual determination of circuit MUF's.

5. Once again, place the overlay on Fig. 8-1. Make sure that the equatorial and Greenwich reference lines on the overlay and the world map coincide. The world map of Fig. 8-1 is divided into separate zones, *E*, *W*, and two *I* zones. Show on the overlay the zone in which each of our control points—*A′*, *A*, *B′* and *B*—lies. Both New York control points lie in the *W* zone and both control points on the Berlin end of the circuit lie in the *I* zone. The completed overlay is now ready; Fig. 8-3 shows the portion in which we are interested.

Before we actually proceed and use the contour charts, however, a few words about their preparation are appropriate. The Central Radio Propagation Laboratory (CRPL) of the National Bureau of Standards receives and analyzes ionospheric data from approximately 120 stations located throughout the world. These stations make regular soundings throughout the 24 hours of each day. From the data collected, *h′-f* curves are plotted. These observations result in a wealth of information

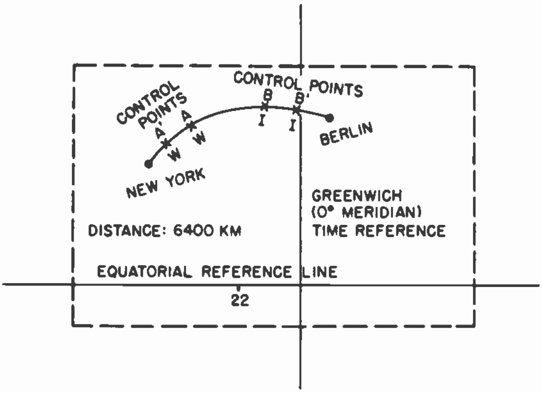

Fig. 8-3. Overlay section showing reference lines and control points.

which gives an overall picture of ionospheric conditions as they exist at any time at a given location. The data can then be plotted on maps similar in appearance to weather maps.

From the data that each station submits, a monthly average critical frequency for each hour of the day is obtained for that station. If the data that every station submits are then plotted, we obtain a chart showing the average world-wide critical frequencies on an hourly basis.

The next step is to join with a line all points of equal critical frequency. A typical chart thus plotted is shown in Fig. 8-4. This chart shows these data for the *W* zone for December, 1958.

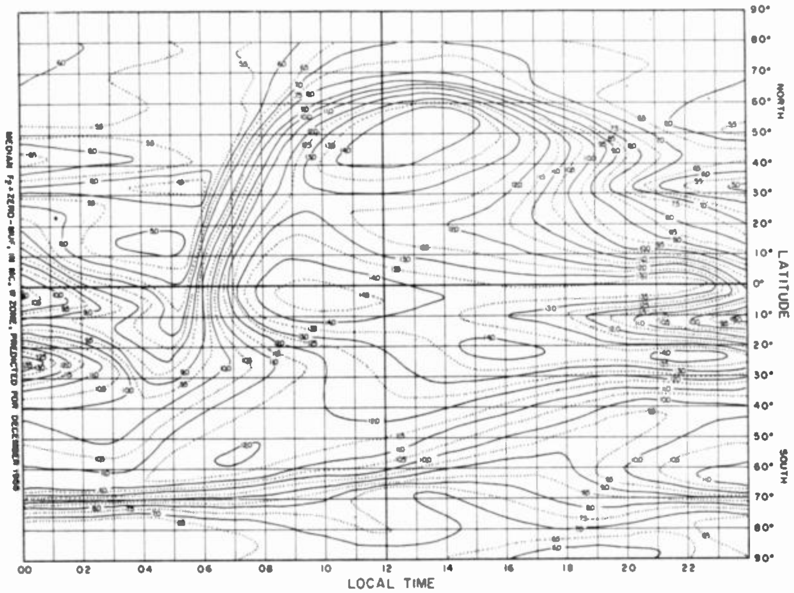

Fig. 8-4. Median F_2-zero MUF, in mc, W Zone, predicted for December, 1958

One major modification must be made in the critical frequency data submitted by the world-wide network of sounding stations. Ionospheric characteristics are dependent not only upon geographical coordinates (position with respect to the north and south poles), but also upon geomagnetic coordinates (position with respect to the north and south magnetic poles). Consequently, the data received from a station of given geographic latitude in one part of the world may not necessarily be similar to those received from a station of the same geographic latitude but in a different part of the world. To compensate for these differences, the world is broken into "zones" of similar geomagnetic and ionospheric characteristics. They are designated *E* (east), *W* (west), and *I* (intermediate).

All data received from stations within a particular zone are used in preparation of charts for that particular zone. Figure 8-5 shows contours for the *I* zone (Afro-European sector). Frequency information given on this chart is applicable only to conditions within this area.

The reader may very well ask how observed data, collected at many stations and analyzed and plotted *after* it has been observed, can be of value in predicting future conditions. Essentially, the normal ionospheric

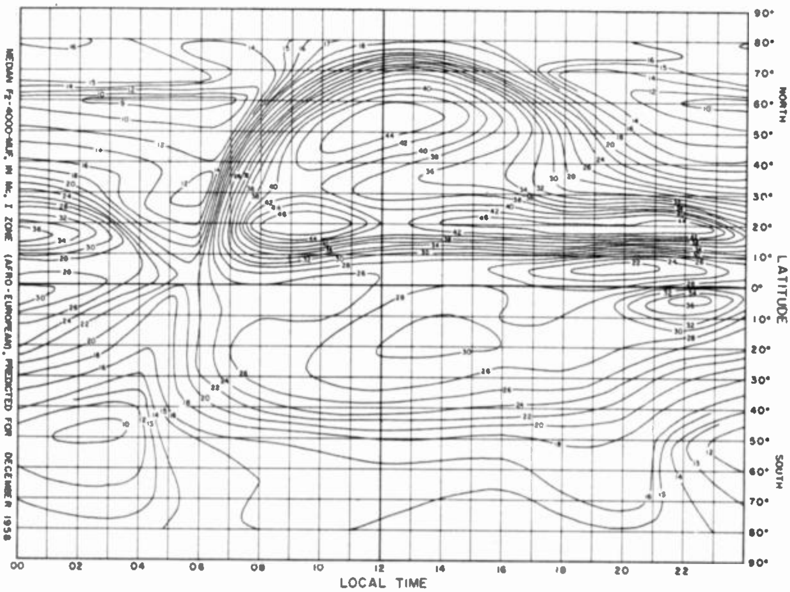

Fig. 8-5. Median F_2-4000 MUF, in mc, I Zone (Afro-European), predicted for December, 1958.

variations that take place are diurnal (daily changes brought about by length of day), seasonal, and cyclical. Generally, the daily and seasonal changes are constant and easily predictable. The cyclical changes brought about by changing sunspot activity are most important in forecasting ionospheric conditions. Fortunately, there is a very good relationship between running averages of sunspot numbers and critical frequencies. Since running averages of sunspot numbers can be forecast with reasonable accuracy, at least over a relatively short period of time (3 to 6 months), critical-frequency data can also be predicted with a good degree of accuracy. The critical-frequency contour charts of Fig. 8-4 can be converted to MUF contour charts (Fig. 8-6) for any distance (in this case, 4000 km) by multiplying the critical frequency by the MUF factor for the appropriate distance and layer height.

Now we are ready to begin MUF calculations:

6. Place the overlay on Fig. 8-6, with the equators coinciding. Note that Fig. 8-6 is valid only in the *W* zone. Since only our New York control point is in this zone, the information we gather will only be applicable to that end of the circuit. It is suggested at this point that

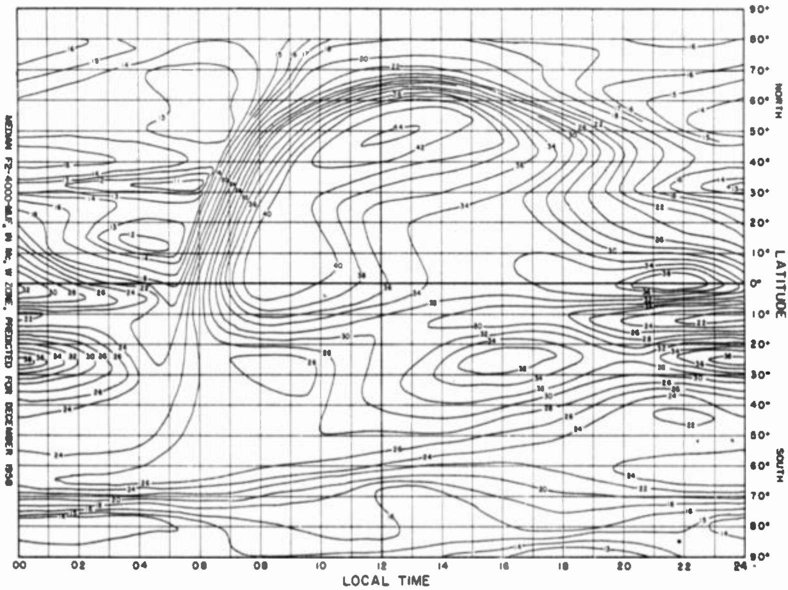

Fig. 8-6. Median F_2-4000 MUF, in mc, W Zone, predicted for December, 1958.

the reader trace Fig. 8-3 on a sheet of transparent paper and work along as procedures are explained.

7. Keep the equatorial line of the overlay over the equatorial line of the F_2-4000 chart and slide the transparency horizontally until the Greenwich Meridian coincides with 00 on the local time scale.

We have chosen our time reference through the 0° meridian. All data will be in terms of Greenwich Meridian Time (GMT). This terminology is desirable because most communications men prefer to work with a single time base.

Twelve hours GMT, for example, is 7 A.M. EST, 4 A.M. PST, and 1 P.M. CET. Use of GMT thus avoids the possibility of confusion. GMT is also at times referred to as Greenwich Civil Time (GCT), Universal Time (UT), or simply Greenwich Time.

8. Note that with the Greenwich Meridian at 00 hours, our *A* control point falls off the chart. The next step is to slide the time reference line to 02 hours. The *A* control point still falls off the chart. Keeping the equatorial lines of overlay and chart coincident, slide the time reference to 04 hours. Here, our *A* control point falls at 13.8 mc. This is the F_2-4000 MUF for the *A* end control point. At 06 hours, our reading is again 13.8 mc and at 08 hours, 13.0 mc.

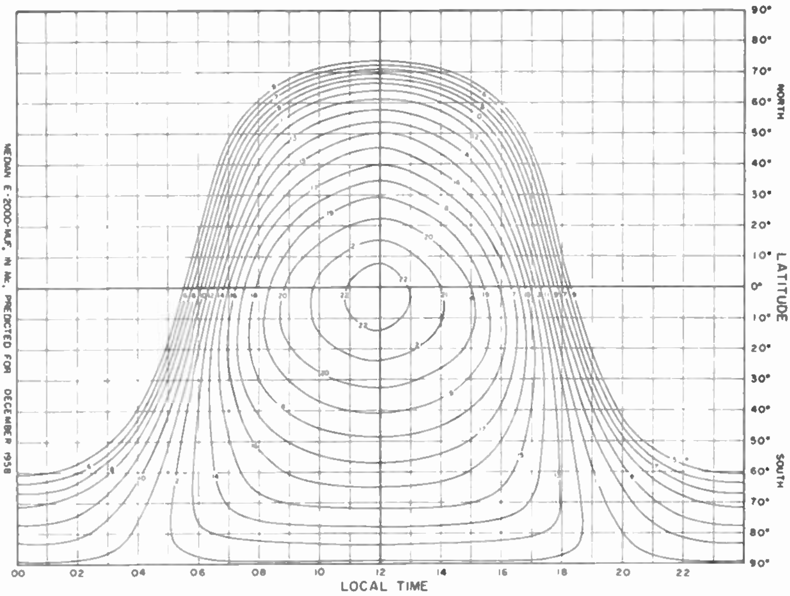

Fig. 8-7. Median E-2000 MUF, in mc, predicted for December, 1958.

9. Repeat this operation on the time scale at 2-hour intervals right across the chart; record only values for the *A* control point.

10. Note at 24 hours that the reading is 18.0 mc; this reading on the 24-hour time scale is the equivalent of 00 hours, the reference at which we started. Note that all values along the 24-hour line are the same as those along the 00 line, because the distance from 00 to 24 hours on our time scale is the equivalent of 360° of longitude. We get a reading at 02 hours by making our time reference coincide with an imagined 26 hours (the same as 02 hours) on our time scale. Keep the time reference line at 24 hours, and put a small mark on the equatorial line of the transparency over the equivalent of the 22-hour time line on Fig. 8-6. This is shown on Fig. 8-3. Then slide the transparency over until the mark just made coincides with the 24-hour time line on Fig. 8-6. Our *A* control point reading is 14.0 mc. Moving our time reference over to 26 hours is the equivalent of 02 hours.

11. We now have a complete set of *W*-zone readings for our *A* control point. Our *B* control point falls in the *I* zone. Figure 8-5 is the F_2-layer MUF chart for the *I* zone; repeating steps 7 through 10, obtain another set of readings for the *B* control point of the overlay for this zone.

12. The next step is to repeat steps 7 through 10 for the *E*-layer

2000 MUF, shown in Fig. 8-7, using control points *A′* and *B′*. This is done because *E*-layer characteristics do not vary significantly with longitude, hence one chart is satisfactory for all zones.

The data obtained at the completion of step 12 are shown in Table 8-1 in columns a, b, d, and e.

TABLE 8-1. MUF and OWF Calculations, New York / Berlin Circuit, December, 1958. Distance 6400 km

	A END				*B* END				PATH	
·	a	b	c	c′	d	e	f	f′	g	h
TIME (GMT)	F_2-4000 MUF	*E*-2000 MUF	MUF	OWF	F_2-4000 MUF	*E*-2000 MUF	MUF	OWF	MUF	OWF
00	18.2		18.2	15.5	10.0		10.0	8.5	10.0	8.5
02	14.0		14.0	11.9	9.4		9.4	8.0	9.4	8.0
04	13.8		13.8	11.7	9.0		9.0	7.7	9.0	7.7
06	13.8		13.8	11.7	9.0		9.0	7.7	9.0	7.7
08	13.0		13.0	11.0	9.0	5.8	9.0	7.7	9.0	7.7
10	13.0		13.0	11.0	25.0	11.8	25.0	21.2	13.0	11.0
12	25.0	9.6	25.0	21.2	40.5	13.0	40.5	34.4	25.0	21.2
14	40.0	14.2	40.0	34.0	44.0	12.0	44.0	37.4	40.0	34.0
16	43.5	15.9	43.5	37.0	40.0	6.2	40.0	34.0	40.0	34.0
18	42.5	14.9	42.5	36.1	29.0		29.0	24.6	29.0	24.6
20	36.0	11.3	36.0	30.6	16.0		16.0	13.6	16.0	13.6
22	26.0		26.0	22.1	11.9		11.9	10.1	11.9	10.1
00	18.2		18.2	15.5	10.0		10.0	8.5	10.0	8.5

13. The highest frequency that will propagate from New York is the highest frequency that will be propagated considering MUF values at *A* and *A′*. Similarly, the highest frequency that will propagate from Berlin is the higher of the two values obtained at points *B* and *B′*. The *higher* of the values at *A* and *A′*, and *B* and *B′* are entered in columns c and f respectively, as shown in Table 8-1.

14. The MUF for the path is obtained by taking the *lower* of the two frequencies entered in columns c and f. These are shown in column g. The highest frequency that can be propagated from New York to Berlin is the same as the highest frequency that will propagate from Berlin to New York. This principle is known as "reciprocity."

The MUF for the New York/Berlin path, therefore, regardless of which of these terminals is transmitting, is shown in column g.

The above procedures have outlined in some detail the steps necessary to obtain the MUF for a path over 4000 km long.

The following steps describe methods used for obtaining the Optimum Working Frequency (OWF) on paths greater than 4000 km. No new data will be required. Take 85% of the F_2-4000 MUF in columns

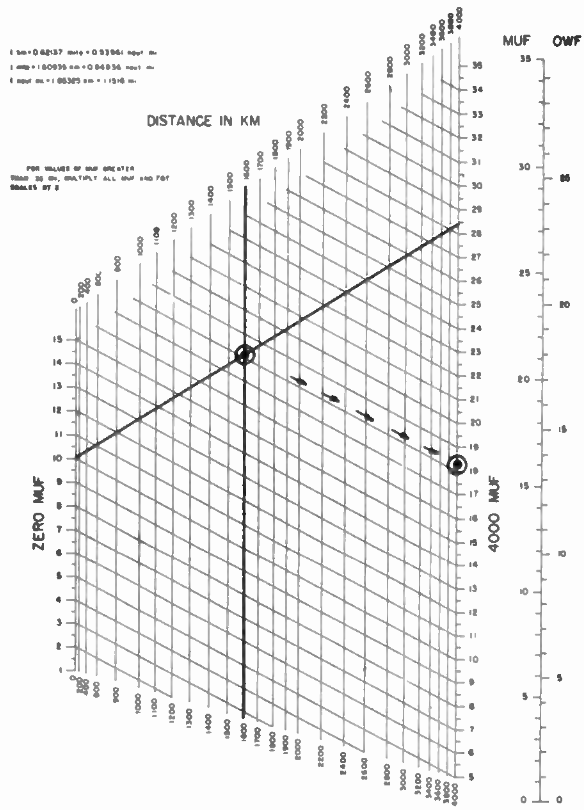

Fig. 8-8. Nomogram for transforming F_2-zero MUF and F_2-4000 MUF to maximum usable frequencies at intermediate transmission distances; conversion scale for obtaining optimum working frequency (OWF).

a and d. To do this, multiply by 0.85; use a slide rule, or use the conversion scale at the right of Fig. 8-8. The MUF on the left can be converted directly to OWF on the right of this scale. Thus, for example, an MUF of 20 mc yields an OWF of 17 mc. An MUF of 23.5 mc gives an OWF of 20 mc.

The remaining steps are *identical* to those taken in determining the path MUF, namely:

a. Compare the *A*-end OWF with the *E*-2000 MUF, column b. The higher of the two is the New York-end OWF, and is shown in column c′.
b. Compare the *B*-end OWF with the *E*-2000 MUF, column f.

The higher of the two is the Berlin-end OWF, and is shown in column f′.

c. The *lower* of the two values thus obtained for each hour is the path OWF. The laws of reciprocity discussed above hold here also. These values are shown in column h.

The foregoing has been a description of methods used in calculating MUF's and OWF's on circuits greater than 4000 km in length. Because procedures differ somewhat when circuit length is less than 4000 km, we shall discuss them in the next example.

WASHINGTON TO BATON ROUGE

Let us choose a circuit between Washington, D.C. (39.0°N, 77.5°W), and Baton Rouge, La. (30.47°N, 91.18°W) and proceed as follows:

1. Prepare an overlay, as described in steps 1 through 5 in the foregoing, again using Figs. 8-1 and 8-2. Be sure to put a small marker at the midpoint (a point equidistant from either end) of your path and

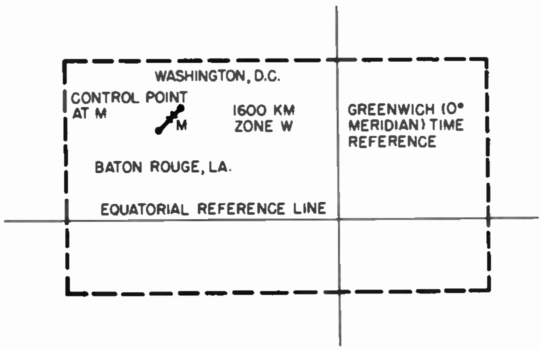

Fig. 8-9. Washington, D.C./Baton Rouge, La. overlay, showing reference lines and control points.

indicate the zone in which the midpoint lies, as outlined previously. The overlay is shown in Fig. 8-9.

2. Since the midpoint falls in zone *W*, we shall use Figs. 8-4 and 8-6, which are *W*-zone contour charts, as well as Fig. 8-7, which applies to any zone.

3. To start, place the overlay over Fig. 8-4, which is the F_2-zero MUF chart for the *W* zone. Keep the equatorial line of the overlay

over the equatorial line of the F_2-zero chart, and slide the overlay horizontally until the Greenwich Meridian coincides with 00 on the local time scale at the bottom of the chart.

Our control point *M* falls off the chart, and the time reference line must again be moved before we get our first reading. This occurs when our time reference line is at 06 hours, with a reading of 5.3; at 08 hours the reading is 5.1.

Repeat the operation at 2-hour intervals, right across the chart. In order to fill in the readings for 02 and 04 hours, make the time reference coincide with imaginary time references at 26 and 28 hours. The readings obtained are 7.2 and 5.7 for 02 and 04 hours, respectively.

4. Step 3 is then repeated for the F_2-4000 MUF chart (Fig. 8-6) and the *E*-2000 MUF chart (Fig. 8-7). The data so obtained are entered on a form. Use a form similar to the one shown in Table 8-2. The information gathered thus far is shown under columns a, b, and c in this table.

The F_2-zero MUF chart shows the predicted critical frequency for any hour at any point in the zone for which it is valid for the particular month for which it was issued.

The F_2-4000 MUF contour gives similar data except instead of being valid at zero distance (definition of critical frequency), it is valid for a distance of 4000 km.

Since our path length falls somewhere between zero and 4000 km, it will be necessary to adjust the MUF values obtained to the proper distance. This is done by using the *nomogram* of Fig. 8-8. Similarly, the *E*-2000 values for MUF must be adjusted to equivalent MUF values for other transmission distances. The nomogram used for making these adjustments is shown in Fig. 8-10. A nomogram is generally defined as a chart having three or more scales which can be used instead of mathematical formulas. It is, in other words, a shortcut in solving otherwise lengthy and complicated problems. Use of nomograms is usually very simple, requiring only a straight-edge.

To adjust the F_2-zero and F_2-4000 values of columns a and b, Table 8-2, proceed as follows:

5. For each hour for which we have readings, we use a straight-edge on Fig. 8-8, joining the F_2-zero MUF value on the left-hand side of the nomogram, with the F_2-4000 value on the right.

For example, from Table 8-2, we note that at 00 hours, the F_2-zero value is 10.0, the F_2-4000 is 28.5. These are joined, as shown on Fig. 8-8. We note different lines running vertically through Fig. 8-8 for different distance values. Since our path length is 1600 km, the point where the

1600-km line meets our straight-edge is the adjusted MUF value which we seek. This value is 18.3 mc.

The operation is repeated for each of our hourly values; the information is then recorded in column d of Table 8-2. Note that the F_2-4000 MUF scale on the right of Fig. 8-8 only runs up to 35 mc and that our values from 14 through 20 hours, column b, go above 35 mc. Therefore, in this case we divide our F_2-zero and F_2-4000 readings by 2, find

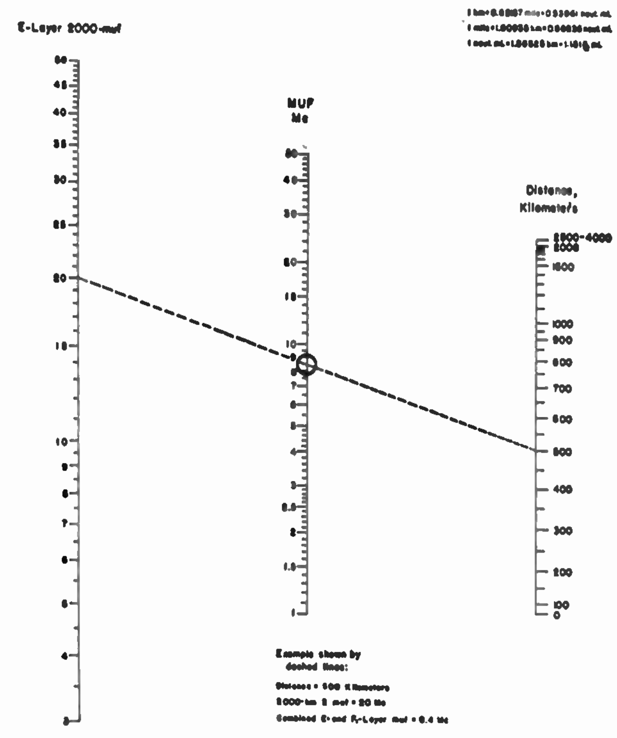

Fig. 8-10. Nomogram for transforming *E*-layer-2000 MUF to maximum usable frequencies and optimum working frequencies due to combined effect of *E* layer and F_1 layer at other transmission distances.

our adjusted MUF from the nomogram, then multiply by 2. For example, at 16 hours we see from Table 8-2 that the F_2-zero and F_2-4000 values are 13.4 and 41.0 mc, respectively. Divide these by 2, and we get 6.7 and 20.5 mc. Using the nomogram for 1600-km distance, we get 12.7 mc. Doubling this, we get 25.4 mc and enter this in column d as our F_2 MUF adjusted.

6. Our next step is adjustment of our E-2000 MUF. This is done by use of the nomogram of Fig. 8-10. In this operation, the E-2000 MUF value on the left is joined by a straight-edge to the path length on the right; the adjusted E-F_2 MUF is then read off the center scale. An example of this is shown by dashed lines on Fig. 8-10.

Adjusted values of our column c E-2000 MUF are shown in column e. As we have mentioned elsewhere, E-MUF values occur only during the daylight hours. This accounts for the fact that we have readings only from 14–22 GMT in columns c and e.

TABLE 8-2. MUF and OWF Calculations, Washington/Baton Rouge Circuit December, 1958. Distance 1600 km

	a	b	c	d	e	f	g	h
Time (GMT)	F_2-zero MUF	F_2-4000 MUF	E-2000 MUF	F_2 MUF	E MUF	Path MUF	F_2 OWF	Path OWF
00	10.0	28.5		18.3		18.3	15.6	15.6
02	7.2	20.8		13.2		13.2	11.2	11.2
04	5.7	15.5		10.0		10.2	8.5	8.5
06	5.3	14.2		9.2		9.2	7.8	7.8
08	5.1	13.0		8.6		8.6	7.3	7.3
10	4.7	12.0		7.9		7.9	6.7	6.7
12	5.5	13.0		8.8		8.8	7.5	7.5
14	11.6	37.0	14.3	22.6	13.4	22.6	19.2	19.2
16	13.4	41.0	17.0	25.4	16.0	25.4	21.6	21.6
18	13.5	39.0	17.9	24.6	16.9	24.6	20.9	20.9
20	12.9	37.0	15.9	23.6	14.9	23.6	20.1	20.1
22	12.2	35.0	10.6	22.1	9.9	22.1	18.8	18.8
00	10.0	28.5		18.3		18.3	15.6	15.6

7. The MUF for the Washington/Baton Rouge path is now obtained by taking the *higher* of the two adjusted MUF values (columns d and e, Table 8-2) and entering in column f.

8. The OWF for the path is obtained by taking 85% (multiplying by 0.85) of the F_2 MUF, column d (shown in column g), and comparing it with the E MUF, column e. Once again, the *higher* of the two values (columns e and g) is chosen. This path OWF is shown in column h. Again reciprocity holds.

We have now completed our discussion of the procedures involved in obtaining MUF's and OWF's on circuits above and below 4000 km in length.

The data we have calculated are shown plotted in Figs. 8-11 and 8-12 for the New York/Berlin and Washington/Baton Rouge circuits, respectively, the solid-line curve showing MUF, the dashed OWF.

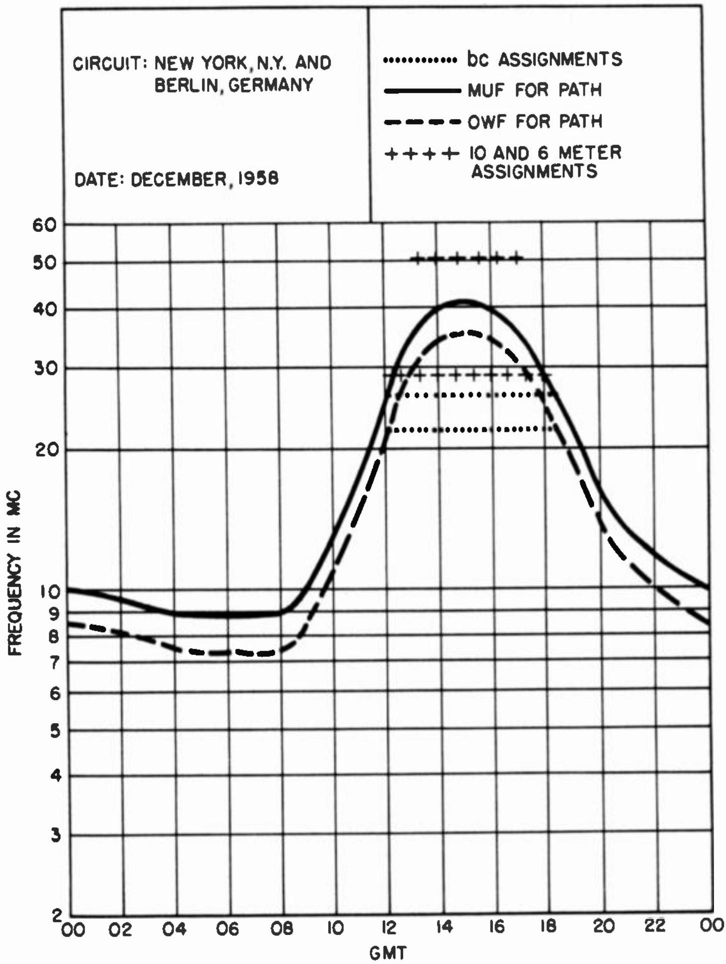

Fig. 8-11. MUF/OWF curve, New York/Berlin.

Choice of the frequencies with which we are to work depends primarily on the type of service in which we are interested. An example will illustrate.

Referring to Fig. 8-11, let us suppose that we are interested in the period 12–18 GMT. Any assignment, regardless of the type of service in which we are interested, should be made as close to the OWF as possible, but not above it. Thus, for example, if we were interested in the shortwave broadcast bands, we could only assign a frequency in either

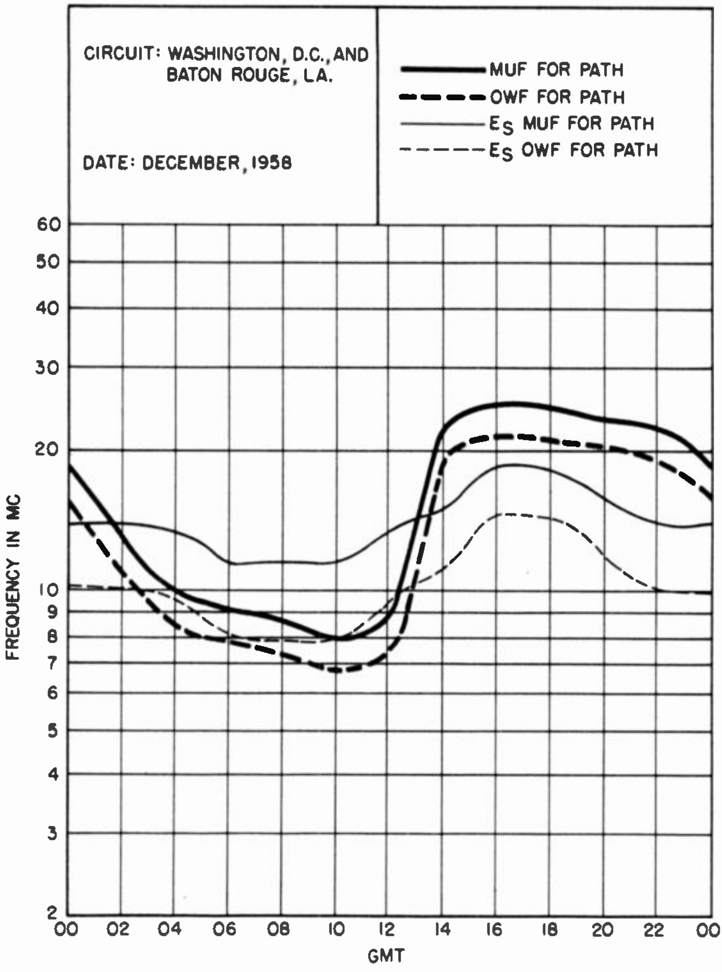

Fig. 8-12. MUF/OWF curve, Washington, D.C./Baton Rouge, La. with E_s MUF and OWF included.

the 21- or 26-megacycle bands as indicated by the horizontal dotted lines on Fig. 8-11. This assignment would be based *solely* on technical factors, because the assignment is made as close to the OWF as possible. For the broadcaster, however, other factors are involved. One of these is the fact that shortwave receivers available commercially seldom tune above the 17-mc band. As a matter of fact, the majority of receivers available generally to the public tune only the lower (6 through

15 mc) bands. That is why the engineering considerations in frequency assignment must be weighed against other, equally important factors.

In addition, the broadcaster or technician operating a communications circuit must think in terms of consistency: he must operate the circuit reliably on most of the days of the month. The radio amateur is not often concerned with such consistency, nor is his band as restricted as that of the broadcaster.

For example, the amateur could start his operations in the 10-meter band, as shown by the crossed horizontal lines on Fig. 8-11. In addition, since the MUF on approximately 5 days of the month is exceeded by as much as 30% or more, he could start out during several peak hours, as shown, by transmitting in the 6-meter band.

Essentially, these are the latest techniques used to determine ionospheric conditions several months in advance. They may be employed by any broadcast technician whether he is interested in amateur or in professional transmission. The agency responsible for the preparation of these data is the Central Radio Propagation Laboratory (CRPL) of the National Bureau of Standards. This agency issues the *CRPL Series D Basic Radio Propagation Predictions* on a monthly basis, three months in advance. Thus, the predictions issued in March, 1959 are for June, 1959 conditions, etc.

Contour charts similar to those shown in the foregoing appear in these predictions to determine the best sky-wave frequencies over any path at any time of day for average conditions for the month of prediction. The predictions are available from the Superintendent of Documents, U. S. Government Printing Office, Washington 25, D.C., for $.10 per single copy, or $1.00 for an annual subscription of 12 copies. Cost for an annual subscription outside of the United States is $1.25.

Anyone seriously interested in shortwave radio, whether from the amateur or professional viewpoint, should make use of these predictions. They permit the application of a practical engineering approach to the assignment of frequencies, and remove all guesswork.

In addition to the calculation of MUF and OWF, the radio amateur is also interested in sporadic-*E* propagation. The remainder of this chapter is devoted to the prediction of this phenomenon.

SPORADIC-*E* PROPAGATION

Sporadic-*E* (E_s) propagation is often possible on frequencies considerably above normal MUF or OWF values. At the present stage of

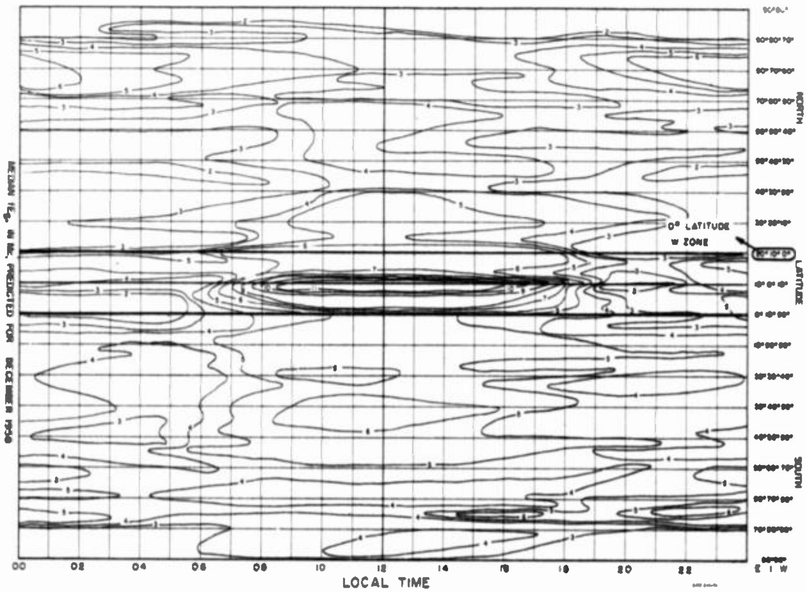

Fig. 8-13. Median fE_s, in mc, predicted for December, 1958.

the art, predictions of sporadic-*E* effects are not highly accurate and should be used primarily as a guide.

Figure 8-13 is a chart showing sporadic-*E* contours for the month of December, 1958 for each of the three zones, *E, I,* and *W*. Since these E_s charts are based on geomagnetic latitude considerations, there are three different geographic latitude scales at the right of Fig. 8-13.

Since multihop E_s transmission is rarely accomplished with any degree of consistency, the procedures for calculation of E_s effects for one-hop transmission only will be considered.

Since we have already prepared an overlay for the Washington to Baton Rouge path, E_s for this circuit will be calculated:

1. Place the overlay over the E_s critical-frequency chart, Fig. 8-13, make sure to use the proper latitude scale. This is shown encircled in Fig. 8-13. The equatorial reference line of the overlay will then correspond to the 0° equatorial line for the *W* zone. Note that if the path midpoint fell in the *I* or *E* zone, the overlay reference line would have been placed on one of the *lower* scales.

2. Proceed to take readings at 2-hour intervals at the midpoint of the path in accordance with procedures already explained.

TABLE 8-3. Data obtained in determining E_s-MUF and E_s-OWF data on the Washington/Baton Rouge Circuit, December, 1958.

	a	b	c	d	e
Time (GMT)	fE_s	fE_s ×5	E_s MUF	E_s-2000 OWF (b-4)	E_s OWF
00	3.0	15.0	14.0	11.0	10.2
02	3.0	15.0	14.0	11.0	10.2
04	2.9	14.5	13.5	10.5	9.7
06	2.5	12.5	11.6	8.5	7.9
08	2.5	12.5	11.6	8.5	7.9
10	2.5	12.5	11.6	8.5	7.9
12	2.9	14.5	13.5	10.5	9.7
14	3.2	16.0	15.0	12.0	11.1
16	4.0	20.0	18.8	16.0	15.0
18	3.9	19.5	18.1	15.5	14.5
20	3.4	17.0	15.9	13.0	12.0
22	3.0	15.0	14.0	11.0	10.2

3. Multiply the critical-frequency values of E_s thus obtained by 5, to obtain the E_s-2000 MUF.

4. Next, the E_s MUF for the particular path under consideration is obtained by use of the nomogram, Fig. 8-10, using procedures outlined in step 6 of the foregoing section.

5. There are methods for incorporating the E_s MUF found in the previous step into the other MUF calculations so that only one MUF value results. My personal preference is to plot E_s data separately, since considerably less is known about the calculation of this than the regular layer MUF.

6. To obtain the E_s OWF for the path, first subtract 4.0 from the E_s-2000 MUF. This yields the E_s-2000 OWF. To find the E_s OWF for the path, use the Fig. 8-10 nomogram. This is the E_s OWF for the path, and is similarly plotted as a separate entity. All data appear in Table 8-3.

In general, the E_s MUF and OWF are only significant when they are higher than the regular layer MUF and OWF values, as shown in Fig. 8-12.

Chapter 9

ACHIEVEMENTS OF THE RADIO AMATEUR

HISTORY

The following is an excerpt from an American Radio Relay League (ARRL) filing made in 1957 with the Federal Communications Commission:

> " . . . The amateur is an experimenter and his contributions to the technique of radio have been manifold. When the amateur was first restricted to the territory above 1500 kilocycles (1913), he astonished the world by devising apparatus and methods to communicate at considerable distances on these frequencies. The discovery of the practical value of short waves and their opening for government and commercial work, in a diversity of services embracing the world, was essentially an amateur accomplishment. The first published explanation of the ionospheric transmission of high frequencies was by an amateur. The first exposition and demonstration of the extended ranges obtained on very high frequencies by virtue of the bending of waves in the lower atmosphere was by amateurs. Amateurs were the first to develop simple and reliable equipment for operation in the VHF region, first to occupy this territory in large numbers, and first to evaluate its fundamental characteristics."

Thus from humble beginnings after Marconi's historic experiment, the radio amateur has made numerous significant discoveries and contributions to the art of radio communication.

The radio amateur has also distinguished himself as a public servant in times of national emergency and disaster. During earthquake, flood, and hurricane emergencies, the equipment of the radio amateur has often been the only means of communication with a disaster area.

The FCC has set aside frequencies in the 10-, 6-, and 2-meter bands for use by amateurs in the event of war or other national disaster. The Radio Amateur Civil Emergency Service, RACES as it is called, is part of a network of highly skilled amateurs with special training in emergency communications techniques.

Amateur radio, being essentially a scientific hobby, has contributed significantly to other fields. Among these are radio astronomy and geophysics. Radio amateurs were instrumental in the recent initial discoveries that the sun was a source of radio noise in the 10-meter band.

During the recent International Geophysical Year (IGY), hundreds of amateurs volunteered to assist in various radio tracking and propagation studies, among these being the MINITRACK installations for tracking the paths of earth satellites and rockets.

With such a record of accomplishments, any book on radio propagation should devote several chapters specifically to the needs, requirements, and interests of the radio amateur.

SOME ACCOMPLISHMENTS

Amateur radio is among the more exciting hobbies. There is almost always the opportunity of doing something phenomenal, even of doing something that no one has ever done before. Beginning with two-way transatlantic communication on 110 meters in 1923, adventure-minded radio amateurs quickly moved into and utilized with uncanny effectiveness the 80-, 40-, 20-, and finally the 5-meter bands.

These precedent-shattering accomplishments, however, were only the beginning. The desire to do the impossible, to effect a fabulous number of DX contacts, to work a record number of countries, continues to goad the amateur on to new and untried fields. Among these have been, in addition to exploitation of the regular *F* layers, accomplishments in sporadic-*E* propagation, VHF tropospheric propagation, auroral propagation, use of meteor trails, and a host of other new techniques. In the following pages, we will discuss some of the more important and exciting new phases of radio propagation, much of which has been pioneered by radio amateurs.

USE OF THE *F* LAYER

One of the reasons for the success of the radio amateur is the nonrestrictive aspects of the hobby. Whereas the professional radio engineer must always "go by the book," very few limitations are placed on the radio amateur.

For example, the short wave engineer is generally required to maintain communications between fixed points on as many days of the month as possible. Consequently, he has little leeway for experimentation; he must work as close to the OWF as he possibly can: maintaining circuit reliability is of prime importance.

The amateur, on the other hand, ignores such restrictions. He can work far above the MUF. His objective is the exploitation of a certain band, the desire to work a colleague in some remote part of the world, or to work a record number of countries in the shortest possible time.

The amateur cannot ignore the characteristics of the regular layers of the ionosphere, particularly the *F* layers. On the contrary, he is very much aware of their existence and behavior. Their significance, however, is not the same.

The amateur has pioneered the discovery and explanation of new phenomena; he has contributed data that have been significant in furthering the understanding of the structure and formation of the ionosphere; he has contributed to the art of shortwave communication, and because of the uninhibited nature of amateur radio, he has experimented on ever-higher frequencies, and has been in the forefront regarding new techniques or new media. Some of these are the following.

SPORADIC-*E* PROPAGATION

Sporadic-*E* clouds, or patches, are areas of exceedingly high ionization, which form within the *E* layer of the ionosphere, and which are capable of reflecting radio waves of considerably higher frequency than any of the normal layers of the ionosphere.

The first record of sporadic-*E* propagation dates back to the mid-thirties, when amateurs working in the 56-mc band reported contacts ranging up to 1200 miles distant. The observations opened the field of VHF propagation wide, for it had previously been believed that long-distance communication at frequencies above 30 mc was impossible.

Sporadic-*E* regions in the ionosphere cover relatively small areas; the ionized region itself is usually rather thin, as ionospheric layers go, and recent measurements indicate that their motion through the ionosphere is swift, ranging up to 300 miles per hour in a westerly direction.

Because the effects of these regions are relatively short-lived and appear to occur in a more or less random fashion (except for specific variations which we shall discuss subsequently), they are called *sporadic*. The *E* comes from the region in the ionosphere in which they occur.

Some sporadic-*E* clouds have been known to reflect frequencies in the 2-meter band, although occurrences of this nature are rather rare. In general, sporadic-*E* propagation is most prevalent in the bands above 10 meters, although 6-meter activity, particularly during the summer months, is not infrequent.

Sporadic-*E* density can be sufficiently great to present a highly efficient reflecting surface to the incident wave. This mirror effect occurs with a minimum of absorption, and results in the reflection back to earth of an extremely strong signal. The phenomenon often occurs on

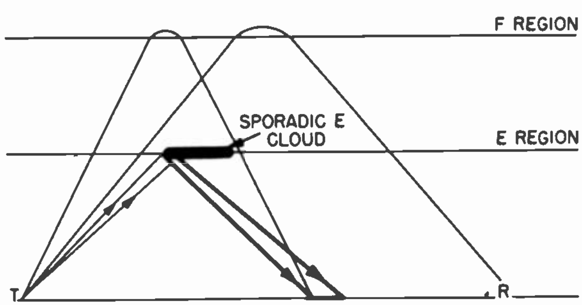

Fig. 9-1. The "mirror effect." In areas shown, signal reflected by sporadic-E cloud is far stronger than signal refracted by normal F-layer propagation.

the relatively higher wavelengths of 15 and 20 meters at times when the regular layers of the ionosphere will support these frequencies also. However, absorption of sporadic-*E* reflected signals is so much lower than on regular *F*-layer reflected signals that the effect at these times is virtually to blot out all other signals in these bands. (See Fig. 9-1).

Propagation by way of sporadic-*E* clouds is, in most cases, limited to distances of 1500 miles or less, because the limited geographical area covered by a patch of sporadic-*E* usually precludes any possibility of multihop propagation. There have been cases, however, where either the simultaneous occurrence of sporadic-*E* patches over widely separated areas, or a combination of sporadic-*E* clouds, and regular F_2-layer reflection made communication over a circuit possible, when communication solely by the regular F_2 layer over the same circuit would have been impossible.

Sporadic-*E* propagation, because its range is generally limited to relatively short one-hop paths, is also called "short-skip," although the use of the latter term does not necessarily mean that propagation is always via a patch of sporadic-*E* ionization.

Although sporadic-*E* propagation has been known for 25 years, a satisfactory scientific explanation for all the effects thus far attributed to sporadic-*E* patches is yet to be found, and there is evidence to indicate that there may actually be more than one kind of sporadic-*E*. For example, sporadic-*E* occurs most frequently in mid-latitude during the daylight hours of the summer months. This would indicate that its occurrence is connected with ultraviolet radiation from the sun, which is of extreme importance in the formation of the ionosphere. On the other hand, sporadic-*E* occurs frequently at night. This might indicate that perhaps some agent other than ultraviolet radiation is the cause.

Figure 9-2 shows the typical variations in sporadic-*E* activity at Washington, D.C., indicating the percentage of the time the sporadic-*E* value exceeded 4.0 mc during a typical year. It can be seen that during

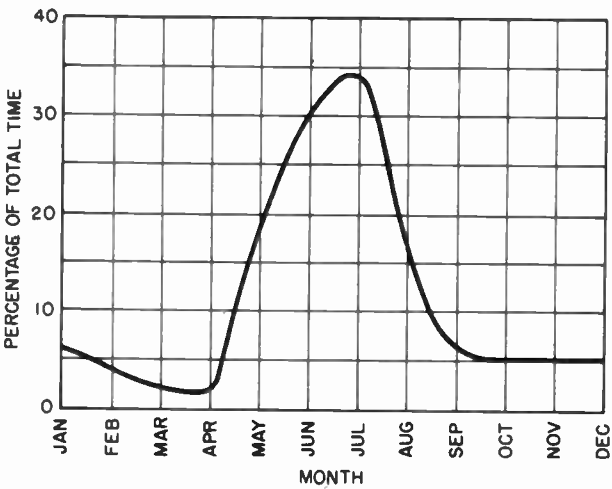

Fig. 9-2. Typical variation in sporadic-*E* at Washington, D.C., showing percentage of the time E_s exceeded 4.0 mc.

May, June, July, and August, activity is at a maximum, while it is at its lowest during February, March, and April.

Figure 9-3 shows typical diurnal variations, with the percentage of the time during each hour that sporadic-*E* exceeds 4.0 mc during a typical year. Note that values of sporadic-*E* are at a minimum during the hours of darkness and reach maximum around midday, with a

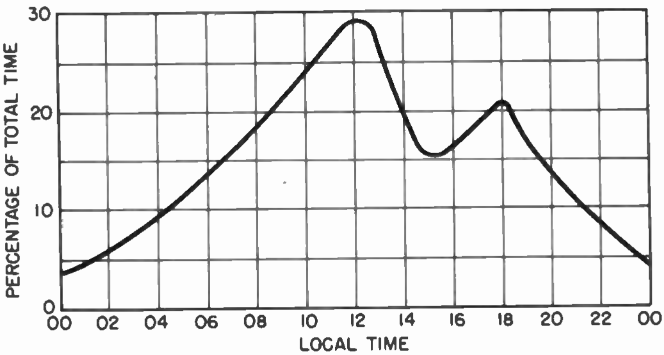

Fig. 9-3. Typical diurnal variation showing percentage of total time E_s exceeded 4.0 mc at Washington, D.C.

secondary peak in the early evening. The curve is significant in that it shows that sporadic-*E* exceeding 4.0 mc occurred during every hour of the day. By applying MUF factors, we find that for a distance of 1200 miles, a sporadic-*E* critical frequency of 4.0 mc yields a sporadic-*E* MUF in excess of 20 mc.

Variations in sporadic-*E* activity have also been observed with geomagnetic latitude. In the auroral zones, for example, sporadic-*E* occurs most frequently and is particularly prevalent during ionospheric storms. To confuse the situation further, there is also peak sporadic-*E* activity in equatorial regions. Some scientists believe that many of the openings attributed to sporadic-*E* occur by means of bending in the earth's lower atmosphere, because of thermal differences there. However, a great many of the openings reported occurred on days when sporadic-*E* activity was recorded at a maximum. This indicates that clouds of high ionization density are the reason for most of these openings.

TROPOSPHERIC AND IONOSPHERIC SCATTER

Tropospheric propagation. In 1932, Marconi made the remarkable prediction that VHF and UHF radio communication at distances considerably beyond the line of sight was a future likelihood. Actually at the time of the prediction, Marconi had already had some success in sending a UHF signal in the 500-mc range, a distance of 165 miles. It was during the years immediately following that exploration of the VHF and UHF ranges really began. Quoting further from the ARRL filing with the FCC we find:

> " . . . Begun in 1934, a comprehensive investigation of the effects of varying weather conditions on the propagation of VHF waves was undertaken by amateurs. This project, carried out on 56 and 112 mc entirely by amateur methods, has been called one of the truly outstanding examples of original research in any scientific field. In this work, airmass boundary bending of VHF waves was discovered, and a theory was formulated to explain it. These basic but then revolutionary ideas laid the ground work for all later progress in the field of tropospheric propagation of VHF signals."

Since the troposphere is the region of the earth's atmosphere that lies below the stratosphere and the ionosphere at a distance of several miles, tropospheric scatter propagation has become fairly important in radio communications during the past several years. During World War II information on tropospheric scatter propagation really became plentiful. This was due, at least in part, to the emergence of radar and the ensuing use of very high radiated powers in the VHF and UHF bands.

With this increased use of the bands above 30 mc, more and more reports of "anomalous propagation" came in; sometimes, they told of extremely strong signals being received for relatively long periods of time over paths that would have been thought impossible for communication because of their distance.

At the present time, no theory satisfactorily explains tropospheric phenomena, although it is generally believed to be connected with turbulence in the troposphere connected with weather fronts which result in the refractive index fluctuating at random.

Although tropospheric scatter has been observed to occur both in VHF and UHF ranges, it has been found that results are generally optimum in the range between 400 to several thousand megacycles. Successful operation of scatter links for communications purposes entails the use of highly directional transmitting and receiving antennas, as well as relatively high effective radiated powers, of the order of many kilowatts.

Tropospherically propagated signals are characterized by two fading components, one rapid, the other slow. In addition, there are variations in the median signal levels on a seasonal basis with the strongest signals being observed during the summer, as well as meteorological variations, with best signal levels being observed when very warm or very dry air is found in the troposphere.

Although the general range of frequencies most successful in tropospheric scatter propagation includes the range from 400 mc upward, it has been found that as the frequency is increased, the efficiency of the circuit decreases. On the other hand, there does not appear to be a deterioration of efficiency with increased distance at the same frequency. Thus, at constant frequency, there is no appreciable difference in efficiency on circuits from one hundred to several hundred miles distant. At present, most scatter links for communications purposes do not run much beyond 500 miles, with most links running considerably below. However, experiments have shown that fairly high reliability can be attained on circuits up to 750 or more miles in length. A great deal more work needs to be done in the field.

During recent years a great many significant advances, particularly by the military, have been made in the field of tropospheric scatter propagation. There are now in operation a number of such links which relay wideband telephone signals up to several hundred miles with amazingly high reliability.

Ionospheric scatter—meteors. The mechanism involved in ionospheric scattering is believed to be quite similar to that which causes tropospheric scattering. In the section on sporadic-*E* propagation, we mentioned the motion of the sporadic-*E* patches as being in a westerly direction at velocities ranging up to 300 miles per hour. The motion of these patches is believed to be due to ionospheric "winds" which blow similar to winds here on the surface of the earth, but with much greater intensity.

These ionospheric winds cause considerable turbulence in the ionosphere, as the result of which there are very rapid fluctuations of refractive index in certain regions of the ionosphere.

It is generally believed that ionospheric scatter occurs because of these random fluctuations of the ionospheric refractive index. The total energy received at the antenna is then made up of all of the different contributions from the many regions which contributed to the scattering of the signal.

There is yet another theory explaining ionospheric scatter. This theory accounts for scatter solely on the basis of ionized meteor trails which are formed continually in the regions of the *E* layer. Two kinds of meteors arrive in the earth's atmosphere. One of these is the regular shower which occurs at regular intervals. The *Perseids,* which occur every August, are an example of the shower variety. In addition, there are those which arrive daily, at random from random directions. It is estimated that hundreds of millions of these arrive in the earth's atmosphere on any given day.

A meteor, because of the very high travel velocity, produces a trail of ionized gases in its track. Therefore radio signals can be reflected from the meteor trail. The heights of these reflected meteor-trail signals have been calculated, and the results indicate their height at around 110 km above the earth in the vicinity of the *E* region. (See Fig. 9-4.)

This proximity to the *E* region of the ionosphere has led some scientists to speculate that sporadic-*E* activity was at least in part attributable to ionization by meteors. This theory does not explain summertime peaks in sporadic-*E* activity.

Both the turbulence and meteoric ionization theories predict that the useful range of frequencies would run approximately from 25 to

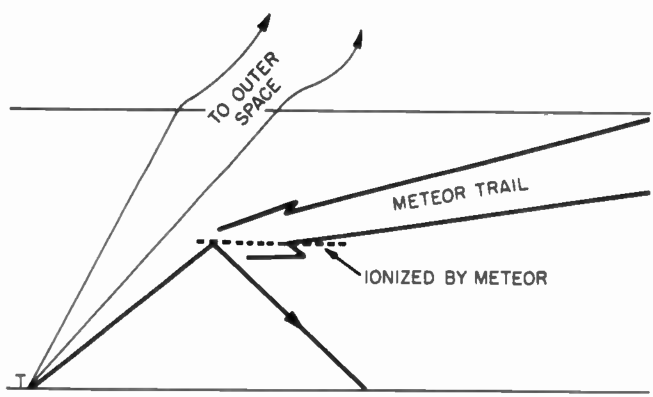

Fig. 9-4. Ionospheric-scatter propagation brought about by ionization in the *E* region by a meteor. The frequency reflected was too high for normal *F*-region refraction.

60 mc, after which the field strength of the signal would drop off rapidly. A great many experiments conducted during recent years have tended to confirm this.

Prior to the discovery of ionospheric-scatter propagation, it was believed that as the frequency used for transmission was raised above the OWF, the delivered signal intensity would drop off, until eventually it would disappear completely. Several notable experiments conducted in the United States recently have shown that this is not the case and that actually the signal reaches a certain minimum value. This minimum level is attributable to ionospheric scatter.

As was the case in tropospheric-scatter propagation, highly directive transmitting and receiving antennas are required to carry on reliable service, with effective radiated powers of the order of hundreds of kilowatts usually being necessary in order to maintain adequate signal-to-noise ratios. Scatter circuits have been used effectively for some time by the military. Highly reliable telegraph circuits have been maintained; the optimum distance for this kind of service lies between 600 and 1200 miles. Another highly important aspect of ionospheric-scatter propagation has been the fact that signal levels are generally maintained or perhaps even enhanced during periods of ionospheric storms.

AURORAL PROPAGATION

During the 1930's, amateurs working in the 5-meter band found that during periods of severely disturbed radio conditions, they could communicate over distances considerably greater than normal by beaming signals in a northerly direction, rather than toward each other.

Further investigation showed that during the nighttime hours this phenomenon could generally be associated with a visible display of aurora borealis. The conclusion was thus drawn that auroral displays also occurred during the daylight hours, even though they could not be seen.

Although little was known in those early days about the aurora, the numerous observations made by radio amateurs throughout the world have helped immeasurably in furthering our knowledge about this interesting phenomenon.

Dr. Carl W. Gartlein of Cornell University, who has long been one of the outstanding auroral researchers, has made considerable use of the data submitted by radio amateurs throughout the United States, Canada, and Alaska. After World War II, auroral propagation was extended into the 2-meter band, where contacts in recent years have occurred at least as frequently as in 6 meters. To date, the highest known frequency to be "bounced off the aurora" is in the vicinity of 230 mc. In general, the 10-meter band represents the highest band that has been effective in auroral propagation. Lower frequencies are absorbed.

The characteristics of aurora-propagated signals vary. On the lower frequencies, the characteristic auroral flutter fade is present, but as the frequency is raised, the note begins to resemble a hiss similar to the sound of steam escaping from a radiator.

Since the fading component will have a frequency ranging from 100 to 2000 cycles, radio telephony is generally rendered unintelligible. Therefore, a slow c-w signal has a much greater chance of success.

The importance to amateurs of auroral propagation has been far-reaching. It has enabled stations up to 800 miles apart, lying in an east-west direction, to communicate by beaming their signals in a northerly direction. Since auroral phenomena are generally associated with severe ionospheric storms during which normal shortwave radio contact is either impossible or very difficult, their importance cannot be minimized.

In general, auroral displays are most common during the spring and fall and occur more frequently during periods of maximum sunspot activity than at other times, with peak activity usually occurring from 2 to 3 years after sunspot maximum. The next period of maximum auroral propagation should therefore occur in 1960 and 1961.

Recent experiments have shown that auroral reflection takes place from a region behind the visible aurora and is best when the incident radio waves are beamed in a direction perpendicular to it. It would therefore seem advisable to keep the vertical radiation angle as low as possible so that the effective reflecting surface of the aurora will be at right angles to the incident wave.

Although several theories explaining auroral propagation have been extended, none of these are wholly satisfactory. It is generally believed that the incident radio signals are scattered from primary and secondary ions resulting from the bombardment of the earth's atmosphere by corpuscles coming from the sun.

LONG vs SHORT PATH

In radio propagation, the shortest distance between two points on the surface of the earth is the path of least absorption. For the most part, the path of least absorption and the shortest distance in miles coincide. The shortest distance in miles between two points on the earth's surface is over a great circle path.

There is, however, *another* great circle path which can join the same two points. This second path—the long way—goes around the "other side" of the earth. Thus, we can go from New York to London via the North Atlantic Ocean, or in the much longer opposite direction via the continental United States, Mexico, the Pacific and Indian Oceans, the Middle East, and Europe.

Absorption depends upon a number of factors; among these are the distance the radio signal must travel, as well as the amount of daylight on the path. A radio signal is attenuated (weakened) with distance—the longer the path length, the weaker it gets. In addition, since during the daylight hours absorption is maximum, the greater the distance the radio wave travels in daylight, the greater is the attenuation of the signal.

It therefore becomes highly unlikely that a New York–London radio signal will take the long path around, first, because the relative distances are so different, being of the order of 3000 miles for the short path *vs* 25,000 miles for the long. Second, irrespective of the time of day, there will be at least as much daylight over the long path as there is over the short, even though the entire length of the short path may be in daylight.

We can now begin to see what conditions are required for a signal to take the long path instead of the short: first, the relative distances via either path must be of the same order—they must be similar; second, the relative amounts of daylight (or darkness) over the path must be of the same order.

These conditions are most likely to be met on antipodal paths (to the "other side" of the earth), during the spring and fall. For example, on circuits from the eastern United States to southeast Asia, the difference between the long and short paths is not significant, and the radio signal is likely to come over the path with the least daylight.

It should be understood clearly at this point that the signal, on leaving the antenna, does not "know" which path has more or less daylight. We have assumed that equal or nearly equal amounts of energy are being radiated in both directions. Under such conditions, the signal traveling the path of most daylight is more likely to be absorbed.

During the spring and fall, the longest periods of darkness occur on antipodal paths, and it is during these months when conditions for long-path propagation are most favorable.

In traveling over long paths, in either direction, a radio signal is very likely to pass through areas of daylight as well as of darkness. Long-path propagation also is a function of frequency. Since 10 meters is principally a daytime band, long-path propagation is not likely; neither is it likely on 80 meters, which is almost exclusively a nighttime band. The band best suited to both daylight and darkness is the 20-meter band. This is actually the band on which most long-path phenomena have been observed.

ONE-WAY SKIP

It frequently happens that stations from a particular area can be heard, but cannot be worked. This effect is especially provoking when transmitter power and antenna characteristics are similar at both ends of the circuit. Under such conditions, the laws of reciprocity should apply. Reciprocity in radio propagation is the condition that a frequency which is satisfactory over a circuit going from point *A* to point *B* should also be satisfactory in going from point *B* to point *A*. The fact of the matter is that reciprocity usually *does* hold true as far as signal strength is concerned.

Suppose, for example, that point *A* is in the northern hemisphere, while point *B* is south of the equator. Signal strength alone does not determine whether a signal will be heard and understood; what determines the intelligibility of a signal is the ratio of the signal strength to

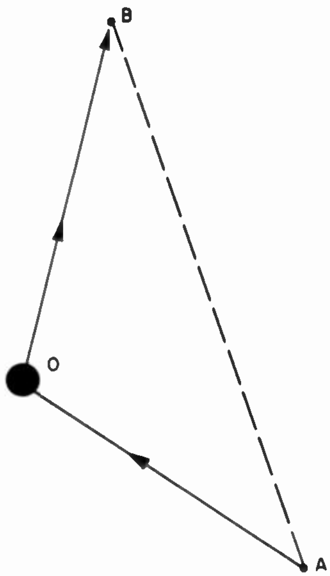

Fig. 9-5. Illustrating "one-way skip" via side scatter. Signal beamed toward O is scattered and received at *B*. Transmitter at *B* is not heard by *A* in the same band because of the disturbed condition of the ionosphere.

the noise level at the receiving site. Since noise levels throughout the world depend on time of day, season of the year, and geographical location, it is possible for a significant difference in noise levels to exist between points *A* and *B*.

If, for example, point *B* lies near the equator where noise levels are naturally higher, then a greater signal strength at point *B* will be required to produce *the same intelligibility* as exists at point *A*. The magnitude of the additional required signal strength varies, but in some equatorial areas the noise levels are as much as 15 db *greater* than throughout many parts of the northern hemisphere.

Thus, in a case where our signal *from* point *B* is coming in, say, 6 db above the threshhold of intelligibility, the *same signal* as received at point *B* will be 9 db *below* the threshhold of intelligibility.

Thus, what appeared to be an inconsistency in the laws of reciprocity was actually due to a difference in noise levels at the two terminals of the circuit, thus accounting for the *one-way skip* phenomenon. During periods of pronounced ionospheric storminess, *one-way skip* conditions may be brought about by scatter propagation. Under extreme conditions, the turbulence may be such as to scatter the signal in a direction that has little or no relationship to the transmission angle. Figure 9-5 represents a top view of a transmitter at *A*, and a receiver at *B*. Note that the signal from *A* strikes the ionosphere at point *O*, and is scattered almost at right angles, being received at *B* from a direction not related to the direction of transmission. The condition of the ionosphere between points *B* and *A* is such that transmission from *B* to *A* on the same frequency is not possible. *One-way skip* by scatter can usually be recognized by the characteristics of the scattered signal. It is weak, with rapid fading.

TELEVISION DX

During periods of maximum sunspot activity, the MUF over many circuits may rise to 50 mc or even higher during the winter months. Because of this, long-distance television reception becomes possible. With the growth of television, reports of such long-distance reception have become rather commonplace. BBC channel 1 has been received in the eastern United States on practically every day during December, 1957 and 1958.

One of the most interesting examples of long-distance television reception occurred in December, 1956 with the setting of a world's record for long-distance reception, when George Palmer of Victoria, Australia, logged in a British television station in London, England—a distance of over 10,000 miles.

Chapter 10

THE AMATEUR BANDS AROUND THE CYCLE

The following is a band-by-band summary of conditions as they are expected to exist during the summer, winter, and equinox periods of sunspot high, medium, and low. Such a summary is a very ambitious undertaking and can only serve as a guide. A complete presentation would have to describe conditions on a great many circuits for many different periods. It would take more space than has been allocated here.

We attempt to present an *overall average* picture for an amateur located somewhere in the northern hemisphere. Frankly, much of it is guesswork.

For example, the last sunspot minimum occurred in April of 1954. Taking the *average* length of a sunspot cycle to be 11.1 years, the next minimum should occur in 1965. But when we consider that sunspot cycles have run from 9 to 14 years, we find that the next low *could* occur anywhere between 1963 and 1971. Obviously, then, showing minimum conditions to occur from 1964–1966 is just an educated guess. Actually, there is no way of knowing how long a sunspot cycle will run. (See Fig. 10-1.)

Discussing band conditions by season also entails considerable guesswork. For example, some maxima have been low ones, with the smoothed sunspot number running only to a high of 70 or thereabouts. Our medium conditions are calculated on a sunspot number of 70. Again we have relied on the average.

This summary of band conditions is therefore intended to indicate qualitative changes in each amateur band from season to season during

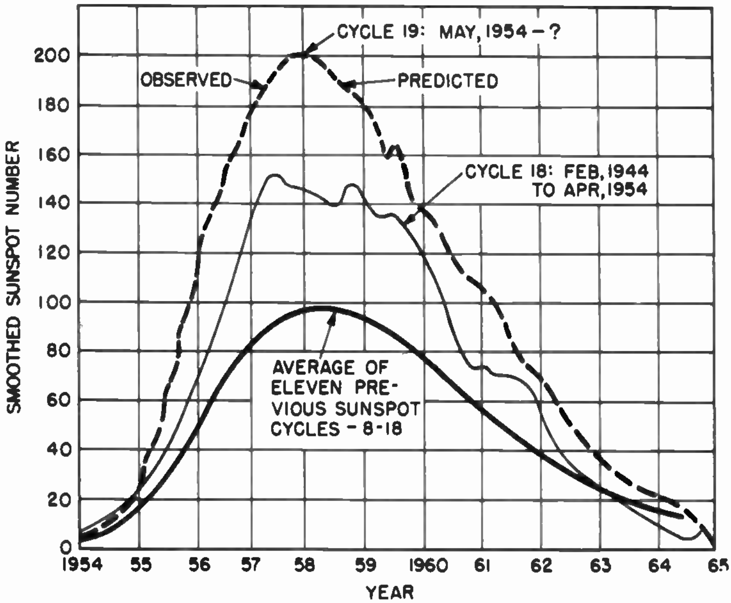

Fig. 10-1. The last complete sunspot cycle and the present sunspot cycle, as well as the average of the past 11 sunspot cycles. Both the previous cycles, as well as the current one, have been unusually high, with cycle 19 being the highest maximum ever observed.

various phases of solar activity. For information on a specific circuit at a specific time during a particular month, for a known degree of sunspot activity, an MUF curve is required.

For each phase of sunspot activity (maximum number 125, medium number 70, and low number 5) we have given band conditions from 6 to 160 meters for summer, winter, and equinox periods. In addition, the years during which this activity is expected to take place are given for each phase of solar activity.

SUNSPOT 125 (Maximum) 1959-60

6 meters. *Summer:* Very little long-distance activity, with the possible exception of an occasional opening between the northern and southern hemisphere. Because of the seasonal increase in sporadic-*E* activity, there should be a few openings ranging from 1000 –1400 miles.

Winter: DX television reception at its best, with BBC Channel 1 (41.5 mc audio, 45 mc video) receivable in the eastern half of the

United States quite frequently. (See Fig. 10-2.) World-wide 6-meter openings are never better for DX in this band. Short-skip meteor-type openings expected to result from Geminids meteor shower in mid-December.

Equinox: Some openings to many parts of the world. Little short-skip activity because of seasonal slackened sporadic-*E* activity.

10 meters. *Summer:* With daytime MUF's at their lowest values, there should be fewer DX openings in this band than during the other seasons. Since sunspot activity is high, however, there should be some success to most areas of the world, particularly during the late afternoon and evening hours, local time.

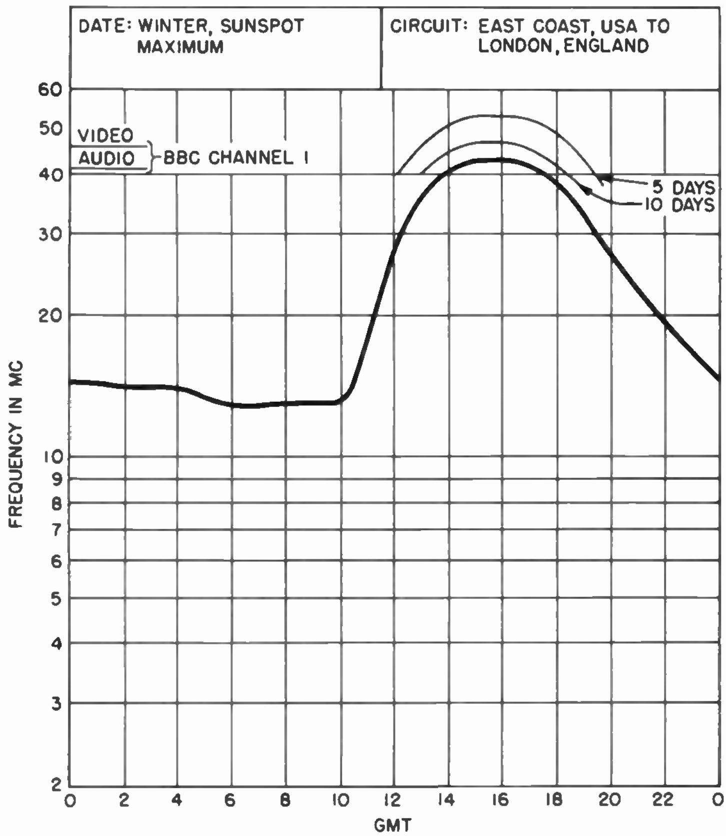

Fig. 10-2. Periods when reception of BBC Channel 1 is most likely in the eastern third of the United States. Reception of both sound and picture are likely on at least 10 days of each month.

Winter: During winter high, this will be the best band to many areas of the world, with excellent DX possibilities almost daily from slightly after sunrise to sunset.

Equinox: Fairly good conditions in this band, particularly in early spring, and late fall. The closer we get to summer, the fewer the openings. Conditions should be optimum during the daylight hours, and in particular from a few hours after sunrise to sunset.

15 meters. *Summer:* This is generally the best all-round band for DX during the summer months. In addition to very good overall conditions in the band during the daylight hours, the band is often open to some areas of the world around the clock. Because of increased seasonal sporadic-*E* activity, many short-skip openings, some up to 2000 miles distant, can be expected.

Winter: Although not nearly as good as during the summer months, conditions should still be excellent during the daylight hours, with peak conditions existing from around noon until sunset. Because of high daytime critical frequencies, short-skip openings from distances of 600 miles outward should occur with regularity.

Equinox: Peak conditions in this band are expected from a few hours before, to a few hours after, sunset. Generally, DX should be excellent from early morning well into the evening, with the possibility of the band remaining open all night on some of the longer north-south circuits.

20 meters. *Summer:* Although daytime conditions on 20 meters are expected to be fair, this will definitely be the best nighttime band for DX to most areas of the world, with good activity expected throughout the hours of darkness. Because absorption increases as the daytime frequency is lowered, there may be some days of the month when daytime openings beyond 1500 or 2000 miles will not be possible.

Winter: Since F_2-layer critical frequencies reach maximum levels in the early afternoon during the winter, and since sunspot activity is at a maximum, short-skip openings during the early afternoon and early evening hours are expected to occur quite frequently. Although the band may be open for DX all day long, it will be at its best at a little after sunrise, and again around sunset.

Equinox: During the evening hours, 20 meters is generally best, with around-the-clock DX possible toward the end of spring, and at the beginning of fall. Early spring and late fall short-skip should also be quite good, but as vernal and autumnal equinox dates are approached, skip should increase.

40 meters. *Summer:* Because of high absorption, daytime DX possibilities are not considered very good. Short-skip daylight openings are expected during the daylight hours at distances ranging from 100 to 1000 miles. In the evening and night hours, DX becomes more likely, but noise levels are still rather high, and the band is only fair for DX.

Winter: During the hours of darkness this is generally a satisfactory band for DX, with daytime activity limited to short-skip openings varying from a few miles to several hundred miles, increasing in the evening and nighttime hours. At night, absorption and noise levels in this band are exceptionally low, and some really booming signal levels can be expected.

Equinox: The 40-meter band is usually the best around-the-clock short-skip band for the spring and fall months. Through the evening and nighttime hours the band should be fairly good for DX, although late spring and early fall noise levels might still be rather high.

80 meters. *Summer:* Conditions in this band are generally unsatisfactory in the summertime. Daytime absorption is so high that contacts beyond 100 miles or thereabouts are unlikely, with even the short-skip contacts subject to high noise and heavy absorption. There is a possibility that some nighttime DX openings can be established, but it is generally unlikely. Expected nighttime limit in this band is 1500 to 2000 miles.

Winter: Heavy daytime absorption in the 80-meter band limits openings to 300 miles and below. During the evening hours, this distance increases and DX openings over all-dark paths should be possible on several nights in the winter period. Conditions over a typical circuit are shown in Fig. 10-3.

Equinox: Daytime openings are again limited to relatively short distances, with DX a virtual impossibility. Skip distance gradually increases as darkness approaches. Although occasional DX contacts over all-dark paths are possible, they are not likely.

160 meters. *Summer:* There is very little hope for openings of any significance in this band throughout the daylight hours, with noise and absorption much too high for success. At night, if one is patient, openings beyond several hundred miles are possible, but not very likely.

Winter: The winter offers the best opportunities for 160-meter devotees. During the daylight hours, critical frequencies are much too high, and absorption, even of vertically incident waves, is usually complete. Therefore, there is not even any skip. At night, however, it is a different story. After sunset, critical frequencies begin to fall rapidly with a resultant increase in 160-meter skip. Although the skip often is

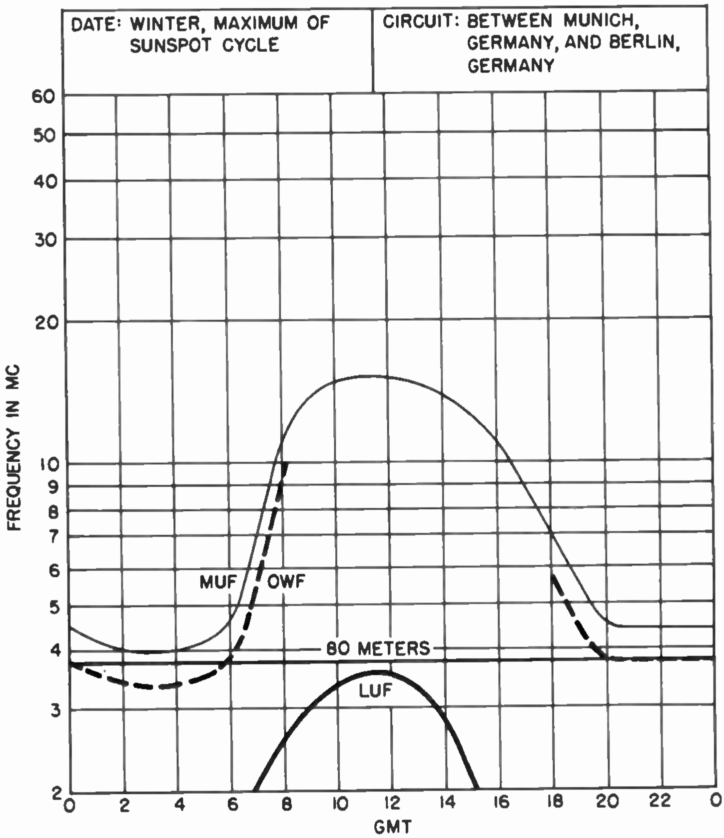

Fig. 10-3. Typical conditions for winter high in the 80-meter band.

limited up to distances of 1000 to 2000 miles, multihop contacts at distances up to several thousand miles are possible.

Equinox: In the evening and nighttime hours, skip distances can extend from 100 to 1500 miles, with some DX openings to considerably beyond this range possible. Propagation via the ionosphere during the daylight hours is again unlikely.

SUNSPOT 70 (Medium) 1961-64

6 meters. *Summer:* No DX activity expected. As during sunspot high, seasonal sporadic-*E* levels should make a few openings possible at distances from 1000 to 1500 miles out. When 10 meters is skipping in at distances below 500 miles, there is a possibility that 6 meters will also be open in the same direction but at greater distances.

Winter: Not much activity. Outside of an occasional sporadic-*E*, meteor, or auroral opening, there will not be much activity in this band.

Equinox: Auroral displays are at a maximum during equinoxial months, and 6-meter propagation off the aurora is about the best hope there is for activity in this band during the period.

10 meters. *Summer:* Conditions on north-south circuits, particularly into the southern hemisphere, should be fairly good, with a fair chance for DX openings during the daylight hours. The summer peak in sporadic-*E* activity should make short-skip openings from 500 to 1500 miles out possible approximately 25% of the days.

Winter: DX openings in the 10-meter band will be fair to good for this period. Restricted to the daylight hours, conditions should be optimum during the early afternoon local time on east-west circuits. There will also be a number of short-skip openings at distances ranging from 1000 to 2000 miles.

Equinox: During the spring and fall, DX openings on east-west circuits are relatively infrequent. North-south openings, on the other hand, are more frequent than in the winter months. This balance makes the overall DX picture fairly good during the daylight hours. In addition, the closer we are to summer, the more frequent will be short-skip sporadic-*E* openings.

15 meters. *Summer:* Increased sporadic-*E* activity should make short-skip openings from 500 to 1500 miles out a fairly regular daytime occurrence. DX conditions should also be fairly good on 15 meters, and particularly good on circuits into the southern hemisphere. Regular F_2-layer propagation should be at its best from around noon to sunset, local time.

Winter: This is expected to be the best daytime band for DX, with contacts to most areas of the world possible on practically every day. Higher daytime critical frequencies should result in regular short-skip openings beyond 700 miles or so.

Equinox: Daytime DX is excellent, with conditions in this band similar to what they are in the winter, except that the band remains open somewhat longer.

20 meters. *Summer:* Just as 15 meters was the best daytime winter band, so 20 meters is the best daytime summer band. It should remain open from sunrise to after sunset to most areas of the world, on practically every day of the period. Short-skip propagation from distances of 200 to 2000 miles should be possible practically every day.

Winter: Band conditions are generally similar to summer, except that they will not be open as long. This is due principally to the fact that the length of the day is considerably less than for other seasons.

Equinox: Although daytime conditions in the 20-meter band are not as good as during the summer months, overall conditions are still fair, with increased DX contacts over north-south circuits during the daylight hours and with the possibility that the band will be open around the clock on some of these circuits on several days. Short-skip propagation similar to summer, but from the *F* region rather than via sporadic-*E*.

40 meters. *Summer:* In general, DX openings will be possible during the evening and nighttime hours. Daytime skip should range up to 700 miles or so, with noise levels during these hours rather high.

Winter: This is expected to be the best all-round nighttime band, both for DX as well as regular short-skip propagation. Daytime activity is expected to be limited to short-skip openings up to approximately 1000 miles distant.

Equinox: During the evening and nighttime hours, generally satisfactory conditions are expected for DX. During the daylight hours, short-skip propagation varies from local contacts to distances up to approximately 100 miles.

80 meters. *Summer:* Because of relatively high F_2 critical frequencies, as well as high absorption levels, daytime openings beyond 250 miles will be rare. During the evening and nighttime hours, conditions will improve, with fair DX expected on some nights to some areas of the world.

Winter: Throughout the daylight hours, because of generally high critical frequencies, DX openings in this band are not expected; short-skip openings will be possible on a 24-hour basis, while during the hours of darkness, because of seasonally lower nighttime critical frequencies, generally satisfactory DX to many areas of the world is expected.

Equinox: Daylight conditions in the 80-meter band are expected to be similar to winter conditions; at night, conditions will improve, with some DX possible, particularly on circuits into the southern hemisphere. Short-skip is expected to vary from approximately 350 miles during the day, to over 2000 miles at night.

160 meters. *Summer:* As during sunspot high, daytime absorption is still too high to enable contacts much beyond 100 or so miles. As darkness approaches, the skip is extended until, in the hours of darkness, openings out to about 2000 miles are possible. Some DX into the southern hemisphere, where winter conditions prevail, can be expected.

Winter: For the daylight hours, the 160-meter band is far below the workable range, even on short-skip. During the late afternoon, critical frequencies begin to fall rapidly; with this fall, an improvement in openings is expected, until chances for DX become fair during the late night hours. Short-skip becomes possible from around sunset to sunrise.

Equinox: As before, the 160-meter band is at its best during the period from sunset to sunrise, when absorption is at minimum. During these periods, skip may vary from 1000 miles to distances considerably beyond, with DX possible on nights when noise levels are below the seasonally normal levels. Very little, if any, daytime skip is expected.

SUNSPOT 5 (Low) 1965-66

6 meters. The low part of the sunspot cycle is indeed a bleak one for 6-meter enthusiasts. Because of relatively low ultraviolet radiation from the sun, normal critical frequencies are also quite low. Consequently, even when abnormally high radiation occurs for this time of the cycle, it is not enough to boost frequencies to levels where the 6-meter band will open. During the spring and fall, when some auroral activity is possible, the band may open for short-skip. In the summer, when sporadic-*E* is at a maximum, there may also be an occasional opening, but it is not likely. In addition, during periods of heavy meteor activity, such as the Perseids of early August, openings are possible. However, in all of the above cases, openings are the exception, and, as we said above, these are bleak years for 6 meters.

10 meters. DX possibilities in this band, too, are rather poor, although overall activity is considerably better than in 6 meters. The best opportunity for DX in the 10-meter band occurs in the late fall, winter, and early spring, and then only on circuits into the southern hemisphere. During the summer months, when sporadic-*E* activity is at a maximum, fairly regular short-skip openings up to 1000 to 1500 miles distant can be hoped for. As with 6 meters, openings for brief periods can be expected for periods of meteor showers, and aurora.

When 10 meters is open at distances of 500 miles or below, there is an excellent chance that 6 meters will be open in the same direction, at about two or three times the distance.

15 meters. *Summer:* DX openings in this band are expected to be fairly good, and fairly regular, particularly on circuits into the southern hemisphere. Because of relatively high sporadic-*E* activity, short-skip activity should be good to excellent at distances from 300 to 1500 miles out.

Winter: Through the daylight hours, DX openings should be generally fair to good, particularly during the period from noon to around sunset. Short-skip should be fairly consistent from around sunrise to sunset, but not much expected at night, when critical frequencies are way down.

Equinox: About the only consistent DX in this band in the spring and fall occurs on circuits to Africa and Latin America from the northern hemisphere. Short-skip openings may be fairly good from distances of 1000 miles and over.

20 meters. *Summer:* During the summer in the low part of the sunspot cycle, the 20-meter band is the best band for consistent daytime DX to all parts of the world. It should remain open from approximately sunrise to sunset. In addition, the seasonal increase in sporadic-*E* activity should make short-skip openings a rather frequent occurrence.

Winter: Although the hours of daylight are considerably fewer than during the summer, what daylight hours there are will be good for DX activity in the 20-meter band. Between 15 and 20 meters, there should be no lack of wintertime daylight DX activity to anywhere in the world. Because of higher normal critical frequencies, short-skip openings should be frequent.

Equinox: Again this is the best daytime band for DX activity to all parts of the world. From sunrise to sunset, openings should come fast and furious. At vernal and autumnal equinox, there are 12 hours between sunrise and sunset. This should be ample for adding QSL's. Short-skip openings from distances of 500 to 1000 miles and greater are frequent.

40 meters. *Summer:* In the summertime, because of greater thunderstorm activity, there is naturally more noise on most shortwave bands; as the frequency is lowered, this noise becomes more pronounced. In spite of increased noise levels in the 40-meter band, however, nighttime DX openings should be numerous and consistent, from sunset to sunrise, to all parts of the world. Daytime short-skip should be good to 1000 or 1500 miles out.

Winter: This band will open for DX around sunset, and will be good for DX to all parts of the world for a few hours, after which the MUF's fall below 7 mc to many areas of the world. On other circuits, however, particularly into or toward the southern hemisphere, the band may remain open all night, until after sunrise.

Equinox: The band should be good throughout the evening and night hours and up to sunrise for DX openings to many parts of the world. Short-skip variations are numerous, ranging from 100 miles to over 1000 miles out during the daylight hours.

80 meters. *Summer:* Generally fair DX is possible on this band at night to many areas of the world, although noise levels will be high. During the daylight hours, openings up to 500 miles and beyond will be likely, with short-distance openings likely on a 24-hour basis.

Winter: This will be the best late-night long-distance band during the winter low period. DX openings to many areas, particularly in an east-west direction, should be possible late at night up to an hour or so before sunrise. Short-skip openings, from several hundred to over 1000 miles should be possible to some areas of the world.

Equinox: DX openings to many areas of the world are expected to be fair to good during the evening and nighttime hours, up to sunrise. Daytime short-skip will vary considerably, from local openings to distances of 1000 miles or so.

160 meters. *Summer:* Nighttime DX is expected to be only poor to fair, although long-distance openings, particularly in a north-south direction are not impossible. During the daylight hours, although noise and absorption will be relatively high, some short-skip up to several hundred miles out can be expected.

Winter: In spite of minimum sunspot conditions, winter daytime critical frequencies are considerably above this band, ruling out short-skip of any significance. Around sunset, when critical frequencies begin to fall rapidly, the band will open. Late at night should afford the best chances for DX openings.

Equinox: Possibilities for nighttime DX openings are only fair, and then only when noise levels are down and propagation conditions normal. On the whole, though, expect heavy noise and weak signal strength. Some short-skip will be likely.

Chapter 11

BE YOUR OWN FORECASTER

SIDS AND STORMS

Defining a radio disturbance or an ionospheric storm is not always an easy matter. In general, a disturbance occurs in one of two forms—the one of short duration, usually referred to as a Sudden Ionospheric Disturbance (SID), and one of longer duration, lasting up to several days and referred to as a "storm" or a "disturbance."

The SID, as its name implies, is characterized by a sudden fadeout in the entire high-frequency spectrum on circuits lying entirely or partially in *daylight* regions of the world. Fortunately the SID, or Short Wave Fadeout (SWF) as it is also known, is of brief duration, seldom lasting more than an hour and usually closer to half an hour.

The Ionospheric Disturbance or Storm is generally of considerably longer duration than the SID, continuing from a period of a few hours to several days.

The Ionospheric Storm, because it lasts as long as it does, represents the most important type of disturbance to long-distance shortwave radio communication. The Ionospheric Storm is characterized by weak signal strength on frequencies that are normally well received, increased absorption, rapid fading, with the introduction sometimes of a particular kind of flutter fading. Noise levels increase; the MUF decreases. Conditions are bad in both the daylight and dark parts of the world. In cases where the disturbance is severe, a complete blackout occurs.

The effects of a disturbance can vary greatly, with conditions generally deteriorating as the auroral zones are approached. All types of radio disturbance, whether of long or short duration, are generally believed to be of solar origin.

IMPORTANCE OF FORECASTING

Airlines and shipping companies want to know as far in advance as possible the weather forecast to enable them to schedule their transportation facilities most effectively. Radio men, amateur and professional alike, are equally interested to learn about the radio weather forecast. With sufficient forewarning, the commercial communications companies, the radio amateurs, and the shortwave broadcasters can take steps to minimize the adverse effects of abnormal radio conditions.

For example, if the commercial communications company is advised of the impending onset of a radio disturbance, emergency measures can be taken immediately: first, highest-priority traffic can be moved immediately; extra transmitters can be put on the air to move as much traffic as possible before conditions deteriorate; traffic can be rerouted over paths which are less susceptible to disturbance than others. For example, during severe radio storms, the New York-London circuit usually "blacks out"; that is, radio communication is completely cut off. This is so because the path runs close to the Northern Auroral Zone, which adversely affects radio signals. During severe disturbances the Northern Auroral Zone spreads southward, enveloping a good part of this circuit and making it highly sensitive to storm conditions.

The further south we go, the less susceptible radio signals become to adverse storm effects. As a general rule we can say that the further we are from the auroral zone, the better off we are. This immediately suggests a method for literally getting around the disturbance.

If we establish an alternate circuit along a more southerly route—from New York to Tangier in Northwest Africa, for example, we can *relay* the signal from Tangier to London. Since the midpoint of the Tangier-London circuit lies considerably below the Northern Auroral Zone, even during most disturbances, traffic can generally be moved to London from New York, via Tangier, when the direct circuit to London is out because of an ionospheric storm. (See Fig. 11-1.)

At present, the Voice of America and two of the largest commercial U. S. communications companies maintain relay stations at Tangier. In addition most communications companies maintain alternate circuits in one form or another for emergencies that may arise out of deteriorating radio conditions.

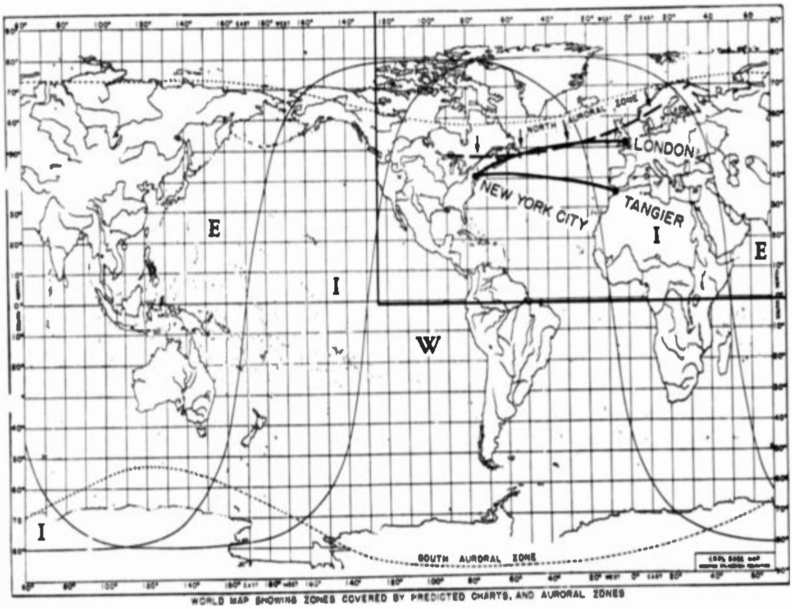

Fig. 11-1. During disturbance, the Northern Auroral Zone moves south, disrupting communications over the New York - London circuit, while the more southerly New York - Tangier circuit remains normal, away from the adverse effects of Northern Auroral Zone.

The radio amateur, too, is directly concerned with radio conditions. During a storm, for example, when east-west circuits in the higher latitudes are generally out, the amateur can content himself with north-south contacts. Quite often, conditions appear to *improve* on north-south circuits during severe storms. This rather strange phenomenon is due in part to the absence of QRM (interference) from stations that are out because of the storm, as well as the fact that signal levels on the north-south path have not changed much, resulting in an apparent increase in signal levels from the south.

During the early history of amateur radio, many amateurs spent many hours servicing their equipment, while all along the cause of their troubles was not in the receivers, but in the ionosphere.

FORECASTING METHODS

For a great many years scientists and engineers have worked on methods to develop and improve techniques of forecasting ionospheric disturbances. When one considers the drawbacks, the results have been impressive. First, the sun, which is believed to be primarily responsible for disturbances in the ionosphere, is over 90 million miles from the earth. Secondly, the ionosphere itself, which is the medium that becomes disturbed, has, up until the last few years, been beyond reach of direct measurement.

With rockets and satellites, considerable progress has been made toward solving some of the problems in the ionosphere. A great deal, however, is not known.

Current forecasting techniques are based almost solely on statistical relationships between activity on the sun and unusual conditions in the earth's ionosphere. Among the most common of these statistical relationships are the following:

Large flares. The flare is a sudden cataclysmic explosion in the sun's atmosphere, blazing up suddenly to 10 or more times the normal brilliance of the sun and characterized by white-hot streamers and filaments shooting many thousands of miles into space; the area of such a flare can extend to a billion square miles, or more.

Generally the solar flare emits tremendous amounts of ultraviolet and x-ray radiation. Ultraviolet light is responsible for ionization in our ionosphere. When too much ultraviolet light strikes the ionosphere, it is overionized. X-rays appear to affect the *D* region of the ionosphere in a similar manner. This results in absorption of radio waves traveling in the lower regions of the ionosphere.

Since ultraviolet light travels with the speed of light, the effects of large flares are felt at the time of their observation. These effects are generally an SID. The duration of the SID depends on the duration of the flare. Usually, a flare builds to maximum intensity within 10 minutes of commencement, then decays slowly. Durations may differ, however, from a few minutes to several hours. The duration of the SID depends on the duration and intensity of the flare.

In addition to waves, the flare emits atomic particles, or corpuscles; these travel more slowly and reach the earth in from 1 to 4 days after the flare has been observed. These particles, if the bombardment is intense enough, cause great currents to circulate far above the earth. These, in turn, can cause magnetic and ionospheric storms, as well as aurora.

Although large flares can cause SID's and major magnetic and ionospheric storms regardless of their position on the sun, the probability that a disturbance will occur increases as the central zone of the sun is approached.

2. The development of radio astronomy in recent years has given forecasters another valuable tool for use in prediction services. Thus, observatories throughout the world have been set up to measure the radio noise emissions from the sun. These emissions occur in the VHF and UHF ranges and have been of considerable value in the evaluation of activity of certain regions on the sun.

3. A very good statistical relationship has been found to exist between ionospheric storm occurrence and the flare – SID – noise storm sequence. When a large solar flare coincides in time with a major solar

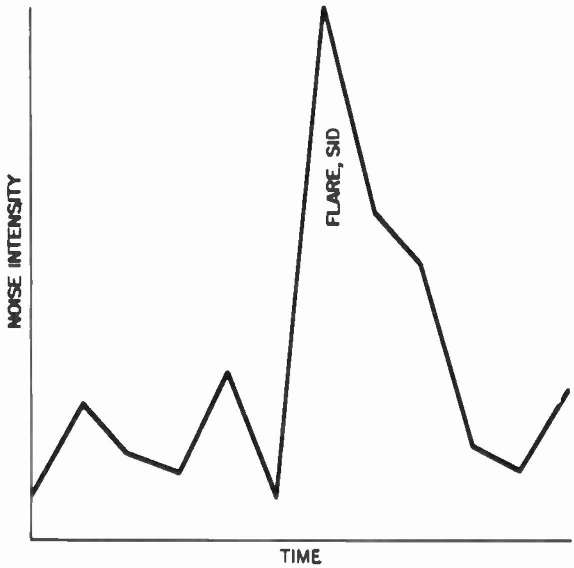

Fig. 11-2. When a large solar flare coincides in time with an SID, and a major solar radio noise outburst as shown above, the probability of a disturbance in from one to four days is high.

radio noise outburst and a severe SID, the probability of a disturbance occurring in from 1 to 4 days may be great. (See Fig. 11-2.)

4. One of the most reliable aids in forecasting is the 27-day recurrence tendency. During certain years of the sunspot cycle, magnetic and ionospheric storms show a strong tendency to recur. This tendency is most pronounced during years of minimum sunspot activity, and in particular from about 3 years before to about 1 year after sunspot minimum. Since the minimum of the last sunspot cycle was reached in 1954, the 27-day recurrence will probably be most effective from

approximately 1961 to 1965, although there is no way of knowing now when the next sunspot minimum will occur, except on a statistical basis.

The interval of 27 days corresponds to the average period of one solar rotation as viewed from the earth. A series of recurring storms may last for several months to several years. These recurrent disturbances are never as severe as the great storms caused by the largest solar flares. But they make up in duration for what they lack in intensity. Whereas flare-caused storms last from 1 to 2 days, recurring storms can continue up to 5 days. One other characteristic of recurring storms is their apparent lack of correlation with particular solar occurrences, such as flares, SID's, noise; although 27-day storms behave in a generally consistent manner, there has not yet been any definite identification of the solar sources of recurrent storms.

5. From time to time, relatively inactive areas on the sun suddenly exhibit a phenomenally rapid increase in activity, brightness, size. Such increase, especially when it occurs near the center of the sun, can be associated with a disturbance occurring 1 or 2 days later.

6. Observation of an area of high activity can sometimes be made as it rotates onto the east limb (the sun rotates from east to west) of the sun. This activity is characterized by emissions in the sun's corona, surges, prominences, or increased noise outbursts. (See Fig. 11-3.)

The above relationships are statistical. Consequently, disturbances may actually occur before or after they were expected, or even not at all. In the long run, however, the chances that a disturbance will occur, as discussed in items 1 and 6 in the foregoing are very good.

OTHER METHODS

Mr. John Nelson, Propagation Analyst for RCA Communications, Inc., has developed a method of short-term forecasts that is based almost exclusively on analysis of actual radio conditions. He has been able to analyze propagation trends and make short-term forecasts (covering the coming 24 hours) with over 90% accuracy over a period of years.

Work on a long-range forecast service, based on the position of the planets, is also being carried on. Although the long-range service shows promise, there has been a tendency toward overwarning (predicting more disturbances than actually occur). The belief at present is that a great deal of additional research is needed before this method can be used as an accurate and reliable method for forecasting ionospheric storms far in advance.

Neither Mr. Nelson's short- or long-term services are available to the general public at present.

FORECASTING SERVICES

The Central Radio Propagation Laboratory (CRPL) of the National Bureau of Standards (NBS) maintains the largest Radio Disturbance Warning Service in America.

The forecasts are based primarily on the statistical relationships discussed in the section headed Forecasting Methods. With observatories throughout the world reporting on solar activity, Bureau Forecasters

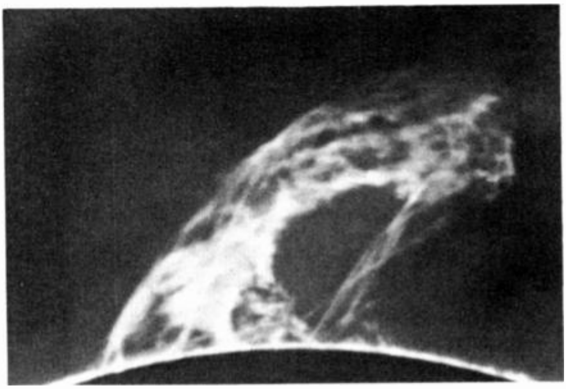

Fig. 11-3. Spectroheliogram of large solar prominence. *McMath-Hulbert Observatory, University of Michigan.*

are continually able to evaluate current radio conditions, as well as to predict their probable trend. Forecasts available to general users are:

The CRPL-J Report, issued each Wednesday by the NBS Washington offices—the North Atlantic Radio Warning Service—includes:

1. A day-by-day forecast of overall radio propagation conditions for the first 7 days after issue, giving expected daily quality on the CRPL radio quality scale (1 = useless, 9 = excellent).
2. Discussion of current solar activity as related to the forecast.
3. A review of propagation conditions during the previous week, based on immediately available reports; storm times are included.
4. In addition to the above, from time to time, there is included

general information which may be applied toward the maintenance of reliable shortwave radio communications over the North Atlantic transmission path.

Special Disturbance Warnings are issued by postcard on a nonscheduled basis whenever a solar event occurs which is expected to cause an ionospheric disturbance that was not covered in the regular J report.

Special CRPL Js Report. This supplementary report, issued to follow up the Special Disturbance Warning, includes background material that led to the issuance of the Special Warning, evaluation of its success, and revisions of the original J report, where these are necessary.

A special telegraphic summary of the Bureau's Special Disturbance Warning is available on a collect basis through regular federal or commercial communications channels. Requests for this special service must include a return telegraphic address.

In addition to the above, there is a service intended for general users of the ionosphere who are concerned with overall propagation conditions rather than over specific circuits, such as the North Atlantic and North Pacific. These reports, termed the *Jb Reports,* contain a forecast of geomagnetic conditions, the record of magnetic activity actually observed, and a record of forecasts previously issued for the North Atlantic and North Pacific. In addition there is a record of radio quality reported for North Atlantic and North Pacific paths.

The Jb reports are issued weekly, and are recommended to general radio users (radio amateurs) because they are less restrictive than the other services. These Jb reports are available *free of charge* from CRPL Radio Warning Services, Central Radio Propagation Laboratory, National Bureau of Standards, Boulder, Colorado.

A subscription to the three regular services listed above is available *free of charge* from North Atlantic Radio Warning Service, National Bureau of Standards, Box 178, Fort Belvoir, Virginia.

Similar services as they relate to North Pacific circuits can be obtained from North Pacific Radio Warning Service, National Bureau of Standards, Box 1119, Anchorage, Alaska.

The National Bureau of Standards radio stations at Beltsville, Maryland (WWV), and at Maui, Hawaii (WWVH), broadcast descriptions of up-to-the-minute propagation conditions, as well as short-term propagation predictions, several hours in advance. These forecasts consist of a letter and a number, transmitted in *International Morse Code.* The letter is a description of current radio quality, in terms either of normal conditions, N, unsettled conditions, U, and disturbed condi-

Fig. 11-4. Bright auroral arc with rayed structure (RA) extending from eastern to western

tions, W. The number is the forecast, covering the following six-hour period. It is given in terms of the CRPL quality (Q) index, as follows:

1 – Useless	4 – Poor to fair	7 – Good
2 – Very poor	5 – Fair	8 – Very good
3 – Poor	6 – Fair to good	9 – Excellent

The letter N would correspond to Q6-9; U would correspond to Q5, and W to Q1-4.

Thus, a forecast of U4 would mean that conditions *at present* are unsettled, and are *expected to become* poor to fair in the next six hours.

The WWV forecasts are revised 4 times daily, at 0500, 1200, 1700, and 2300 GMT. They are broadcast on 2.5, 5, 10, 15, 20, and 25 mc at 19½ and 49½ minutes past every hour. Each forecast is broadcast unchanged until the next one is issued.

The WWHV forecasts are revised at 1800 and 0200 GMT daily. They are broadcast at 9 and 39 minutes past the hour every hour on 5, 10, and 15 mc.

In addition to all of the above services that the NBS maintains, information on current radio propagation conditions, as well as general information about ionospheric conditions, disturbance forecasts, etc., can be obtained by telephone on a 24-hour daily basis by calling SOuth 5-6411, ext. 24253, in Washington, D.C., and ELmendorf 3-2211 in Anchorage, Alaska.

ACCURACY OF PRESENT WARNING SYSTEM

Discussions with Mr. James M. Weldon, Chief Forecaster for the North Atlantic Radio Warning Service of CRPL, indicate that the

horizon, directly overhead. Photographed July 8 and 9, 1958 at 00:25 EDT, Brownville, N.Y.
Photo by A. W. Starkweather.

NBS short-term forecasts are about 95% accurate. Forecast accuracy is rated by comparing predicted Q ratings on the CRPL 1-9 scale with conditions as observed over several typical circuits.

Considering the handicaps under which the forecaster works, accuracy of this magnitude is extremely fine.

Accuracy on long-term forecasts, up to 25 days in advance has not been nearly as good. Although these long-term forecasts have been about 80% accurate in forecasting good conditions, accuracy in forecasting disturbances is considerably lower. Since good conditions prevail most of the time, the accomplishment lies not in forecasting these but in predicting disturbances.

Great progress has been made in recent years. It is expected also that once the wealth of data compiled during the recent International Geophysical Year has been thoroughly analyzed, forecasting techniques will improve further.

DO-IT-YOURSELF FORECASTING

The amateur forecaster is really at an advantage during the years when the 27-day cycle can be applied. For during these periods he need only keep a log and be able to count to 27. Thus, a disturbance occurring on February 1, would recur on February 28, and again on March 27, unless it is leap year. The number of recurrences can not yet be forecast. The 27-day recurrence cycle will probably work best beginning in 1961; however, it may work right now, especially since the maximum of the 19th recorded sunspot cycle has already passed, and it is now heading toward the minimum. In addition to the 27-day cycle, there is the wealth of data that the NBS puts out. Draw your own conclusions from the literature, and from listening to WWV or WWVH.

Close observation of a particular circuit passing close to, but not through, the Northern Auroral Zone has sometimes yielded a clue that a disturbance was coming. During severe disturbances, the auroral zone moves southward, affecting circuits on which normal conditions generally prevail. The circuit with which good results were obtained here in New York is the BBC broadcasts to North America.

As the auroral zone begins to move southward, there is often a rather unique fading component superimposed on the BBC signal. It is called a *flutter fade,* and consists of an audio component of rather low frequency, generally varying from approximately 100 to 2000 cycles. In the early stages of a disturbance, this fading component is generally not severe, but as the disturbance develops, it usually becomes severe enough to render the transmission completely unintelligible. Auroral displays, as shown in Fig. 11-4, often accompany disturbances.

Often a *positive phase* will precede a severe disturbance. During this positive phase, conditions become supernormal. The signal strength is greater than usual on many circuits, and the reception of signals that are not usually heard becomes possible. This may indicate that a disturbance is close at hand.

Chapter 12

A LOOK AT THE FUTURE

Communication via shortwave radio frequencies in the bands ranging from 3 to 30 mc has grown progressively more difficult because the requirements in these ranges far exceed the available spectrum space, with demands for such space still on the rise. Civil, aeronautical, and military requirements all over the world have grown by leaps and bounds, with the need for interference-free channels more urgent than ever before.

Because of the chaotic situation existing in many bands of the shortwave spectrum, there is an urgent need for some kind of international sharing plan to be evolved, so that optimum use can be made of the shortwave spectrum.

During the past 30 years there have been a number of international conferences at which frequency allocation and management problems have been discussed in an attempt to evolve a pattern of systematic usage adequate to all parties with telecommunications requirements. The most recently held conferences were: The Atlantic City Telecommunications Convention of 1947, the Extraordinary Administrative Radio Conference (EARC), held at Geneva in 1951, and the International Telecommunications Convention, held at Buenos Aires in 1952.

At each of these conferences, attempts were made to allocate in an orderly manner specific groups of frequencies to various services making use of the shortwave spectrum. As a result, certain groups of frequencies were allocated to fixed services, others to broadcasting, still others for radio amateur use, etc.

Under Tables of Allocations (Article 5, Atlantic City Radio Regulations), blocs of frequencies were assigned to various services; some of these blocs were assigned internationally, others on a regional basis.

The international frequency picture during recent years has been further complicated by "out-of-band" usage; for example, fixed services operating in the broadcast bands.

THE GENEVA CONFERENCE

Another International Radio Conference began in Geneva, August 17, 1959 and will continue approximately 5 months, during which it is expected that problems of international broadcasting may be dealt with.

In all likelihood the radio conference will review the Radio Regulations, which cover all phases of radio in the shortwave spectrum, as well as the Tables of Frequency Allocations described above. It does not appear at the present time that major changes either in the Radio Regulations or the Tables of Allocations will be agreed upon; it is likely, therefore, that no changes will be made in the regulations or allocations governing amateur radio either.

In addition, the International Radio Conference is scheduled to discuss a draft plan for high-frequency broadcasting which has been prepared by a group in Geneva which was delegated the task by the EARC. Such a draft plan would assign *specific* broadcast frequencies to specific countries. Although such plans have been discussed previously, no generally acceptable formula has yet been found.

The United States has traditionally supported the concept of planned frequency usage in all bands, with the hope that a frequency list could be published on a basis that would reflect accurately the actual current use of the shortwave spectrum by the radio stations of all nations. It is with this attitude that the U. S. delegation entered the conference room at Geneva.

Unfortunately, the continuation of jamming does not appear to allow for the implementation of any plan which assigns specific frequencies to specific users, and a basic paradox exists in such a situation. On the one hand, a plan is designed to *assure* interference-free reception of programs in particular areas. Jamming on the other hand is deliberate man-made interference designed to *prevent* intelligible reception of certain programs in particular areas.

Under such circumstances, it does not appear likely that a broadcast plan will be agreed upon at the current conference unless a drastic, and at the present time unforeseen, change occurs in the international situation.

THE IGY

On July 1, 1957, there began one of the most exciting and imaginative scientific undertakings ever attempted in the history of mankind. Called the International Geophysical Year (IGY), it actually ran 18 months, ending December 31, 1958.

During the IGY, scientists from 66 countries participated in this monumental undertaking, designed to further mankind's scientific knowledge of the world we live in.

In particular, information concerning solar activity, cosmic rays, geomagnetism, ionospheric physics, aurora, gravity, oceanography, glaciology, meteorology, and seismology, as well as other related sciences, was gathered from hundreds of observatories located in all parts of the world—from the poles to the equator and on all continents.

From the very beginning, the success of the IGY was assured—the greatest cooperative scientific effort in history yielded vast quantities of data about our physical surroundings and offered an unparalleled opportunity to solve some of the basic mysteries concerning man's environment.

The program was scarcely one year old before it was decided that the efforts begun with the IGY could not end with it. Accordingly, it was agreed to extend the program, in a somewhat altered form, for another year; this program was called International Geophysical Co-operation—1959.

Although it will take many years before the reams of data submitted during the IGY will be fully analyzed and interpreted, some preliminary results have been received.

Essentially, readers of this book will be interested primarily in the IGY Upper Atmosphere Program, which involved studies in 5 closely interrelated areas of scientific inquiry, as follows: solar activity, cosmic rays, geomagnetism, ionospheric physics, and aurora.

Following is a brief summary of the programs in these areas and a discussion of preliminary findings:

Solar activity. The objectives of solar astronomers during the IGY were threefold: (1) they sought to devise better means of forewarning of the periods during which solar activity was expected to produce adverse geophysical effects; (2) they sought to make as many comprehensive measurements of solar phenomena as possible, so that (3) the observations of these phenomena might provide a better means of understanding solár activity as it relates to geophysical phenomena.

The solar activity program included intensive observations of solar flares, the sun's corona, radio noise from the sun, magnetic fields on the sun and the sun's atmosphere, among other things.

One of the first breakthroughs to occur involved rocket data sent back to earth during an SID. This remarkable information showed that, during the blackout, normal ion distribution in the layers above the absorbing *D* layer seemed to remain normal throughout the entire

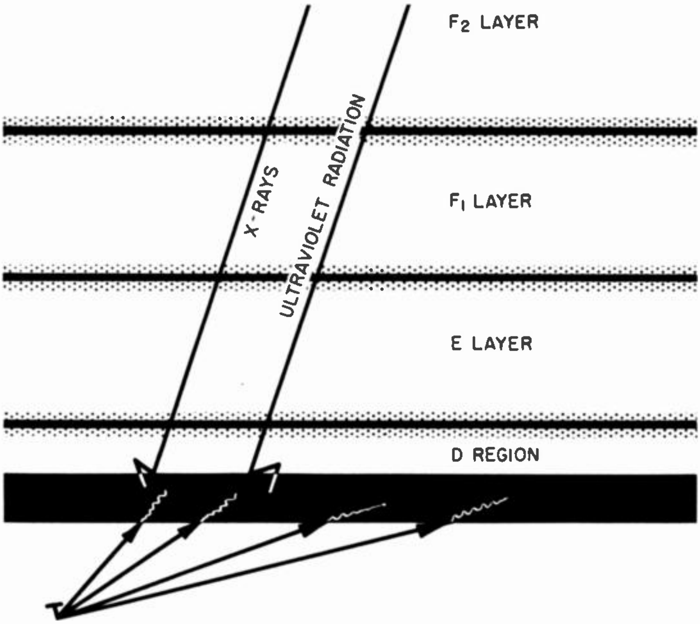

Fig. 12-1. Because of intense ionization in the *D* region, radio waves are "soaked up" and cannot penetrate to other layers of the ionosphere which remain normal during the SID.

blackout, giving further support to the theory that absorption of radio signals during such disturbed periods was due primarily to increased absorption in the lower layers. (See Fig. 12-1).

Another rocket experiment indicated that the absorbing layer formed at the lower parts of the ionosphere was probably caused by solar x-ray emission associated with solar flares.

Although the x-ray data have not been analyzed fully, it appears that x-ray energies are adequate to produce the absorption effects observed during SID's.

In this program, the use of rockets was of extreme value. Whenever a flare was reported, attempts were made to time rocket firings with the expected maximum of the flare so that observations could be made by the rocket at levels above the absorption region, during the periods of maximum flare activity.

Cosmic rays. Cosmic rays are electrically charged particles of enormous energies which constantly bombard the earth from every direction; they are influenced by the magnetic field of the earth, with the lower energy particles being deflected toward the geomagnetic poles and those of higher energy penetrating at lower latitudes.

Preliminary analysis of data supplied by the 20 United States cosmic-ray stations has already yielded some very interesting results. For example, rocket and balloon flights have shown that, during solar, magnetic, and auroral activity, there is an increase of relatively low-energy x-radiation which is believed to be caused by incoming auroral particles that create the x-rays by bombardment of other particles in the earth's atmosphere.

Other significant results indicate that cosmic-ray intensity appears to vary in an 11-year cycle, *opposite* in phase to the sunspot cycle, but lagging by about 1 year behind sunspot count. Cosmic-ray intensity measured during the IGY (sunspot maximum) was relatively low.

The investigation of cosmic-ray intensity has lead also to increased knowledge about magnetic fields in outer space.

Another surprising result of IGY investigation was the observation that there were significant *decreases* in cosmic-ray intensity during disturbances.

Geomagnetism. The magnetic field of the earth has been under observation on a routine basis for the past hundred years or so. It has been used for still longer periods in navigation and surveying. During the IGY, data on the earth's magnetic field were submitted by approximately 80 observatories located throughout the world.

It is believed that most of the earth's magnetic field is produced by electric currents circulating within the earth. The remainder of the field, thought to be about 5% of the whole, is thought to be generated by great currents ringing the earth in the upper regions of the atmosphere. The part of the field created within the earth is very stable, undergoing small changes in long periods of time. On the other hand, the part of the field generated by the earth's "ring currents" is subject to wide, and sometimes very rapid, fluctuations. It is this facet of geomagnetism with which the IGY was primarily concerned.

The basic objective of the IGY geomagnetism program was the

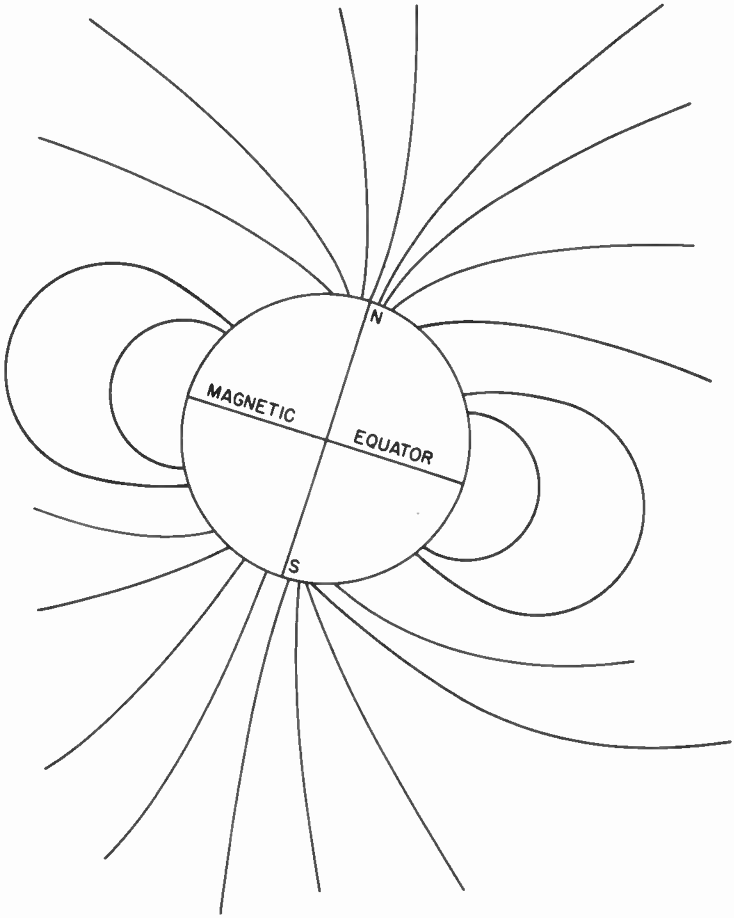

Fig. 12-2. IGY data indicated that the lines of force of the earth's magnetic field extended outward far thousands of miles into space. Scientists had believed this to be the case, but no proof was available.

recording of information concerning changes in the magnetic field of the earth and, in particular, changes that are taking place in the polar regions, the auroral zones, and at the geomagnetic equator. As a secondary objective, it was hoped that the IGY would yield correlating information concerning fluctuations of this nature which were connected with the entry into the atmosphere of the earth of abnormal solar radiation and high-energy corpuscles from the sun. (See Fig.

12-2.) Much of the data gathered is still in raw form. It will probably take several years to analyze it fully.

Ionospheric physics. The basis of the ionospheric physics program during the IGY was the increased use of ionospheric sounding equipment for the study of ionospheric characteristics, including studies of electron density, changes in critical frequency, virtual and actual ionosphere height determinations, the study of ionospheric structure at the geomagnetic poles and equator, and studies of ionospheric absorption. For these purposes, the network of U. S. sounding stations was expanded.

Some preliminary results of the ionospheric physics program follow: To determine variations in electron density in the ionosphere, highly complex data-reduction methods had to be developed. One method involves study of the behavior of radio signals from satellites as they pass through the ionosphere. Another method involves the solution of 40 simultaneous equations. These operations are performed on a digital computer. The computer is able to print out in a short time a record of true height values for specific values of electron density.

One interesting bit of data that has resulted from these studies is electron-density variations from day to day. Near sunrise, for example, it has been found that electron density increases rapidly at all heights of the ionosphere. Because of increased solar radiation, this increase would be expected. Behavior becomes more complicated at night. Around dusk, there is the expected drop in electron density, but afterward there is an increase. At some locations, nighttime electron density *exceeded* noon values. Since the thickness of the ionosphere appears to decrease at night, it is believed that compression of the ionosphere at night causes the electron density increase. Clearly, factors other than recombination and attachment are at work in the nighttime ionosphere.

New information about the outer atmosphere is obtained from the study of "whistlers," which are whistle-like sounds produced by lightning discharges and which are detected at very low frequencies. Whistlers travel thousands of miles outward along the earth's magnetic lines of force before returning to earth in the opposite polar hemisphere. Initial analysis of data indicates that ion density and molecular distribution are considerably greater at very high altitudes than had previously been suspected. As a matter of fact, there is increasing evidence to give credence to the theory that there may possibly be a very nebulous atmosphere extending the entire distance from the earth to the sun, and indeed, in all of interstellar space.

Although only a start has been made in gathering ionospheric data in sufficient quantity and considerably more work remains to be done, initial interpretation of data is prompting observers to start asking the right questions.

Aurora. There were 39 regular observation stations as well as hundreds of amateur observers reporting on auroral activity during the IGY. Since the IGY took place during a period of maximum solar activity, there were a number of extensive auroral displays, one of which was observed as far south as Havana, Cuba. All data observed were sent to the IGY data center at Cornell University where, under the able leadership of Dr. Carl Gartlein, they were put on punch cards for IBM machine analysis. Maps have been prepared which were previously unavailable, showing the location of the northern auroral zone in greater detail than has ever been possible.

Correlations made by English scientists have indicated that auroras occur simultaneously in both the northern and southern hemispheres—a fact previously suspected but not proved.

With the cooperation of radio amateurs, many data have been collected concerning auroral propagation, but have not yet been fully analyzed.

THE ROCKET PROGRAM

The use of rockets during the IGY contributed greatly in gathering data pertaining to the five fields of study discussed above. The use of the rocket as a research tool has meant that observations of the upper atmosphere could be made for the first time by direct observation with instruments and that radiation from the sun could be observed before it was absorbed in the high atmosphere. Thus, data were taken both by ground observations as well as by direct high-altitude rocket observations. The Nike-Hercules missile is illustrated in Fig. 12-3. Rockets such as this made many of the observations.

ARRL/IGY PROPAGATION RESEARCH PROJECT

Radio amateurs from all parts of the world cooperated during the IGY by observing and recording sporadic-E, meteor, scatter, and auroral propagation in the VHF ranges. In addition, observations of transequatorial scatter (the phenomenon which provides transmission from one hemisphere to the other on frequencies normally far above the MUF and which is restricted to sunspot maximum) and ground backscatter (the phenomenon whereby a signal is returned to earth by

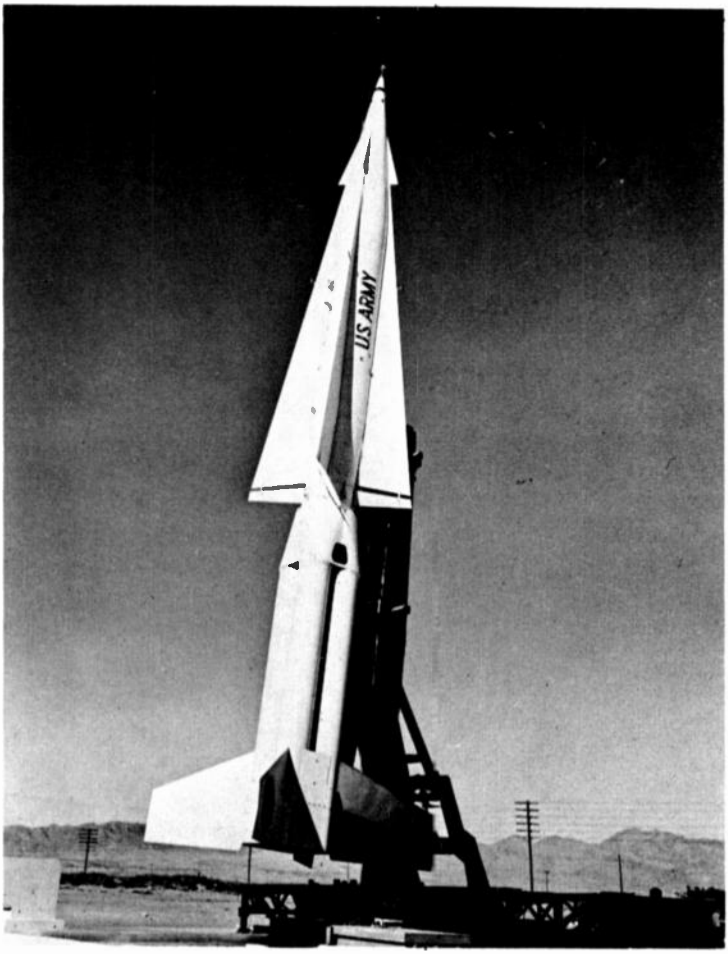

Fig. 12-3. The "Nike-Hercules," the U. S. Army's surface-to-air guided missile, on launcher at White Sands Proving Ground, January, 1957.

the ionosphere and is scattered backward by the ground so that the signal can be received at the original transmitting location) contributed greatly to our knowledge of the ionosphere.

The program in America was directed by the ARRL, with observations confined primarily to the 6- and 2-meter bands; although precise quantitative data were not generally provided by most amateur stations, the wide distribution of observing stations was of great value.

The enthusiasm shown in the ARRL/IGY project was typical of the amateur approach to radio, and again showed why amateurs have been first in utilizing practically all known means of long-distance communication.

PROJECT ARGUS

Late in the summer of 1958, the USS Norton Sound, a guided-missile launcher, fired a three-stage rocket into the skies above the South Atlantic. Three days later, on August 30, another three-stage rocket was fired. This was followed by a third on September 6.

Each of the Norton Sound's rockets carried a small atomic warhead which was detonated in the upper regions of the ionosphere, more than

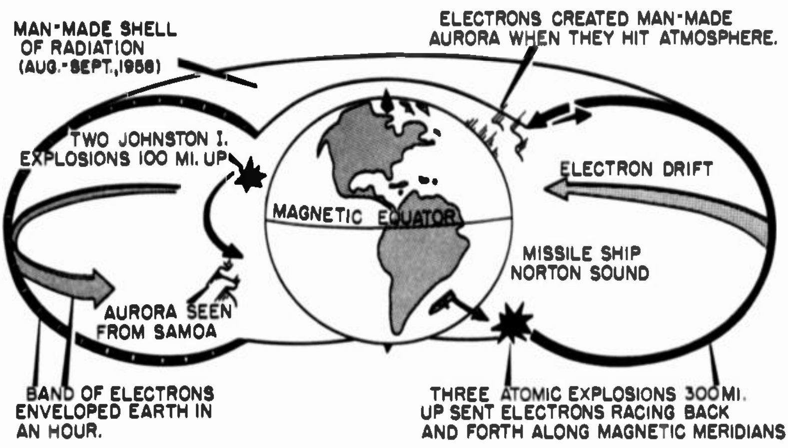

Fig. 12-4. Project Argus. After *Time Magazine*

300 miles above the surface of the earth. What has been called one of the most significant experiments in history—Project Argus—had been concluded successfully. Figure 12-4 illustrates graphically some of its findings.

The explosions sent enormous bursts of electrons into the earth's magnetic field. These particles were trapped and carried along lines of magnetic force. The motion of these electrons also caused them to move in an eastward direction, and within an hour after the launching, a shell of man-made radiation girdled a large part of the atmosphere high above the earth.

In addition to providing priceless data about the earth's magnetic field, the experiment succeeded in creating an aurora, caused a limited ionospheric disturbance, and created what amounted to an artificial ionosphere. The physical effects of Argus persisted for several months; the door to man's eventual control of the ionosphere had been opened.

CONCLUSIONS

Data taken during the IGY are now being analyzed. It will be years before all the results are in. Meanwhile, we have learned more about our physical surroundings in these 18 months than we would have in many years. The IGY, if it proves nothing else, has shown that men, working together, can conquer their environment.

There is a great deal that we must still learn. The more we know, the more fundamental the questions become; but there have always been, and there probably will continue to be, questions to ask, and to answer. When one considers that it is only a little over 30 years since the discovery of the ionosphere, we have come an amazingly long way. But still, we have only scratched the surface. The work, however, has begun. First, there will be the remainder of the surface—then the interior. The work will continue, and the answers will be had.

Index

Rider

Global Time Conversion SIMPLIFIER

The Correct Time...any place in the world...by the Daiger Method.

How to Make a TIME CONVERSION

FIRST read carefully all Keys, Columnar Heads, and Notes.

1. Locate the 2 Places and their Space Numbers on the Lists.
2. Refer to the corresponding Space Numbers on the Chart.
3. Read the Time Conversion.

COLOR KEY

TODAY	TOMORROW	YESTERDAY

(All determined from Eastern Standard Time Zone.)

EXAMPLE

Problem: You are in New York City and the time is 1 am, January 15th. You wish to know the time in Honolulu.

Solution:

- Check the U. S. List of Places, and find that New York is in Space 1; Honolulu is in Space 6.
  (You note that on January 15th neither place has DST.)
- Find Space 1 on the Chart and look over to 1 am.
- Look down the vertical column under 1 am to Space 6
- You find that the time in Honolulu is 8 pm, "yesterday", January 14th.
  ("Yesterday" because 8 pm is in the Black Section.)

GLOBAL TIME CONVERSION SIMPLIFIER CHART

Zone	SPACE NO.	PLACE																								
R +5	1	WASHINGTON, D. C. (EST) NEW YORK CITY	1 am	2 am	3 am	4 am	5 am	6 am	7 am	8 am	9 am	10 am	11 am	NOON	1 pm	2 pm	3 pm	4 pm	5 pm	6 pm	7 pm	8 pm	9 pm	10 pm	11 pm	MIDNT
S +6	2	CHICAGO (CST)	MIDNT	1 am	2 am	3 am	4 am	5 am	6 am	7 am	8 am	9 am	10 am	11 am	NOON	1 pm	2 pm	3 pm	4 pm	5 pm	6 pm	7 pm	8 pm	9 pm	10 pm	11 pm
T +7	3	DENVER (MST)	11 pm	MIDNT	1 am	2 am	3 am	4 am	5 am	6 am	7 am	8 am	9 am	10 am	11 am	NOON	1 pm	2 pm	3 pm	4 pm	5 pm	6 pm	7 pm	8 pm	9 pm	10 pm
U +8	4	LOS ANGELES (PST) Daylight Saving Time	10 pm 11 pm	11 pm MIDNT	MIDNT 1 am	1 am 2 am	2 am 3 am	3 am 4 am	4 am 5 am	5 am 6 am	6 am 7 am	7 am 8 am	8 am 9 am	9 am 10 am	10 am 11 am	11 am NOON	NOON 1 pm	1 pm 2 pm	2 pm 3 pm	3 pm 4 pm	4 pm 5 pm	5 pm 6 pm	6 pm 7 pm	7 pm 8 pm	8 pm 9 pm	9 pm 10 pm
V +9	5	DAWSON	9 pm	10 pm	11 pm	MIDNT	1 am	2 am	3 am	4 am	5 am	6 am	7 am	8 am	9 am	10 am	11 am	NOON	1 pm	2 pm	3 pm	4 pm	5 pm	6 pm	7 pm	8 pm
W +10	6	HAWAIIAN ISLANDS	8 pm	9 pm	10 pm	11 pm	MIDNT	1 am	2 am	3 am	4 am	5 am	6 am	7 am	8 am	9 am	10 am	11 am	NOON	1 pm	2 pm	3 pm	4 pm	5 pm	6 pm	7 pm
X +11	7	ALEUTIAN ISLANDS	7 pm	8 pm	9 pm	10 pm	11 pm	MIDNT	1 am	2 am	3 am	4 am	5 am	6 am	7 am	8 am	9 am	10 am	11 am	NOON	1 pm	2 pm	3 pm	4 pm	5 pm	6 pm
Y +12	8	HOWLAND ISLAND	6 pm	7 pm	8 pm	9 pm	10 pm	11 pm	MIDNT	1 am	2 am	3 am	4 am	5 am	6 am	7 am	8 am	9 am	10 am	11 am	NOON	1 pm	2 pm	3 pm	4 pm	5 pm
IDL	9		I	N	T	E	R	N	A	T	I	O	N	A	L		D	A	T	E		L	I	N	E	

INTERNATIONAL LIST OF PLACES

KEY

- The space number for a place on the LIST is the same space number which is used on the CHART.
- For some places, a TIME is given instead of a Space Number.
  Where a TIME like 10:26 am appears, the TIME at that place is 10:26 am when it is 1 am in Washington.
  1. Write in 10:26 am between 10 am and 11 am, in the first vertical column.
  2. Write in 11:26 am; 12:26 pm, across the horizontal line.

  As an EXAMPLE, Burma . . . 12:30 pm, is printed on the chart, between spaces 16 & 15.
- In each chart space—from left to right—along the horizontal line—a time is given for each hour of the day. The Time Conversion, or corresponding time—at any hour—for almost any place in the world—is found by looking up or down the vertical column, to the appropriate chart space, as shown on the Lists of Places.

PLACE	SPACE NO.
ADEN PROTECTORATE, Aden (NO DST)	21
ADMIRALTY Is., Lorengau (NO DST)	12
AFGHANISTAN, Kabul (NO DST)	10:26 am
ALBANIA, Tirone (NO DST)	23
ALGERIA, Algiers (NO DST)	23
ANDAMAN Is., Port Blair (NO DST)	12:30 pm
ANDORRA, Andorra la Vieja (NO DST)	23
ANGOLA, Luanda (NO DST)	23
ANTILLES, GREATER 2 Time Zones	
Puerto Rico & Possessions (NO DST) (Culebra Is., Mona Is., Vieques I.)	29
Other Islands (Separately Listed)	1
ANTILLES, LESSER (NO DST)	29
ARGENTINA, Buenos Aires (DST all year. Corrected space shown)	27
ASCENSION I., Georgetown (NO DST)	24
AUSTRALIA (3 Time Zones—NO DST)	
New South Wales, Canberra, Sydney	12
Northern Territory, Darwin	3:30 pm
Queensland, Brisbane	12
Southern Australia, Adelaide	3:30 pm
Victoria, Melbourne	12
Western Australia, Perth	14
AUSTRIA, Wien (Vienna) (NO DST)	23
AZORES Is., Ponta Delgada (DST 1st Sun. Apr.-1st Sun. Oct.)	26
BAHAMA Is., Nassau (NO DST)	1
BAHRAIN Is., Manama (NO DST)	19
BALEARIC Is., Palma (NO DST)	23
BARBADOS, Bridgetown (NO DST)	29
BASUTOLAND, Maseru (NO DST)	22
BECHUANALAND PROT., Mafeking (NO DST)	22
BELGIAN CONGO (2 Time Zones—NO DST)	
Leopoldville	23
Stanleyville	22
BELGIUM, Brussels (DST all year. Corrected space shown)	23
BERMUDA, Hamilton (NO DST)	29
BHUTAN, Bumthang, Punakha (NO DST)	17
BIKINI I., (Marshall Is.) (NO DST)	10
BISMARK ARCHIPELAGO, Rabaul (NO DST)	12
BOLIVIA, La Paz (NO DST)	29
BONIN Is. (NO DST)	12
BOOTHIA PEN. (NO DST)	2
BRAZIL (3 Time Zones—DST 1 Dec.-30 Apr.)	
Manaus	29
Rio Branco	1
Rio de Janeiro	27
Santos, Sao Paulo	27
Vitoria	27
BRITISH HONDURAS, Belize (DST ½ hr. 16 Oct.-Feb.)	2
BRUNEI, Brunei (NO DST)	14
BULGARIA, Sofia (NO DST)	22
BURMA, (NO DST) Akyab, Mandalay, Rangoon	12:30 pm
CAMBODIA, Phnom Penh (NO DST)	15
CAMEROONS (Br), Lagos (NO DST)	23
CAMEROONS (Fr), Yaounde (NO DST)	23

PLACE	SPACE NO.
GUIANA, NETH. (SURINAM) (NO DST)	28
GUINEA, Conakry (NO DST)	24
GUINEA, PORTUGESE, Bissau (NO DST)	25
GUINEA, SP. (RIO MUNI), St. Isobel (NO DST)	23
HAITI, Port au Prince (NO DST)	1
HONDURAS, Tegucigalpa (NO DST)	2
HONG KONG, Victoria (DST 1st Sun. Apr.-1st Sun. Nov.)	14
HOWLAND I. (NO DST)	8
HUNGARY, Budapest (NO DST)	23
ICELAND, Reykjavik (DST 5 Apr.-25 Oct.)	25
IFNI, Sidi Ifni (NO DST)	24
INDIA (NO DST) Bangalore, Bombay, Calcutta, Madras, New Delhi	17
INDOCHINA (NO DST)	15
INDONESIA (5 Time Zones—NO DST)	
BALI, Singaradja	1:30 pm
BORNEO, Bandjermasin, Pontianak	1:30 pm
CELEBES, Makassar	14
FLORES, Ende	14
JAVA, Djakarta	1:30 pm
MADURA I., Pamekasan	1:30 pm
MOLUCCA Is., Ternate, Morotai	2:30 pm
SOEMBA, Waikaio	14
SOEMBAWA, Soembawa	14
SUMATRA (2 Time Zones)	
Padang	12:30 pm
Palembang	15
TIMOR, Kupang	14
IRAN (Persia), (NO DST) Bushire, Tabriz, Teheran	20
IRAQ, Baghdad (NO DST)	21
IRELAND, (Eire), Dublin (DST 3rd Sun. Apr.-1st Sun. Oct.)	24
IRELAND, NORTHERN, Belfast (DST 3rd Sun. Apr.-1st Sun. Oct.)	24
ISRAEL, Tel Aviv (NO DST)	22
ITALY, Rome (NO DST)	23
IVORY COAST REP., Abidjan (NO DST)	24
IWO JIMA, Mt. Suribachi (NO DST)	12
JAMAICA, Kingston (NO DST)	1
JAPAN, Osaka, Tokyo (NO DST)	13
JOHNSTON I. (NO DST)	7
JORDON, Amman (NO DST)	22
KASHMIR (JAMMU) Srinagar (NO DST)	17
KENYA, Nairobi (NO DST)	21
KOREA (North) P'yongyang (NO DST)	13
KOREAN REPUBLIC, Pusan, Seoul, Taegu	
Civilian Time (DST May 3-Sept. 20)	2:30 pm
U.S. Military Time (NO DST) Same as Japan	13
KURILE Is. (Chishima Retto) (NO DST) Severo-Kuril'sk	13
KUWAIT, Kuwait (NO DST)	21
LABRADOR, Goose Bay (DST to last Sun. Sept.)	28
LACCADIVE Is.	17
LAOS, Vientiane (NO DST)	15

PLACE	SPACE NO.
PARAGUAY, Asuncion (NO DST)	29
PERU, Lima (DST 1st Sun. Nov.-1st Sun. Apr.)	1
PHILIPPINE REPUBLIC (NO DST) Batoan, Cebu, Monila, Quezon City	14
PHOENIX Is., Conton I. (NO DST)	7
PITCAIRN Is. (NO DST)	6
POLAND, Warsaw (DST May 31-Sept. 28)	23
POLYNESIA, FR., Papeete (NO DST)	6
PONDICHERY (NO DST)	17
PORTUGAL, Lisbon (DST 2:00 am on Sun. following 1st Sat. Apr. to 3:00 am Sun. following 1st Sat. Oct.)	24
PRINCE EDWARD I., Charlottetown	29
PUERTO RICO, San Juan (NO DST)	29
QATAR, Doha (NO DST)	21
REUNION I., St. Denis (NO DST)	19
RHODESIA & NYASALAND, FED. OF Salisbury, Zomba (NO DST)	22
RUANDA-URUNDI, Usuhbura (NO DST)	21
RUMANIA, Bucharest (NO DST)	22
RYUKYU Is. (Nansei Shoto), Naha (NO DST)	13
SAAR, Saarbrucken (DST all year. Corrected space shown)	23
ST. HELENA I., Jamestown (NO DST)	24
SAMOA (USA), Pago Pago (NO DST)	7
SAMOA, WESTERN (N.Z.), Apia (NO DST)	7
SAN MARINO, San Marino (NO DST)	23
SAO TOME & PRINCIPE (NO DST)	24
SARAWAK, Kuching (NO DST)	14
SARDINIA, Cagliari (NO DST)	23
SAUDI ARABIA, Jiddah (NO DST)	22
Dhahran (DST Apr. 10-Sept. 4)	19
No DST in other parts of Saudi Arabia (Space 21 gives approximate time for Mecca and for other parts of the country. Saudi Arabia keeps "Sun Time." Each day ends at sundown and all watches are set to 12 o'clock.)	
SCOTLAND, Edinburgh, Glasgow, Iona (DST 3rd Sun. Apr.-1st Sun. Oct.)	24
SEYCHELLES Is., Victoria (NO DST)	19
SHETLAN Is., Lerwick (NO DST)	24
SICILY, Palermo (NO DST)	23
SIERRA LEONE, Freetown (NO DST)	24
SIKKIM, Gangtok (NO DST)	17
SINGAPORE, Singapore (NO DST)	1:30 pm
SOCIETY Is., Papeete (NO DST)	6
SOLOMON Is. (Aust.), Sohano (NO DST)	11
SOLOMON Is. (British), Honiara (NO DST)	11
SOMALILAND (British), Hargeisa (NO DST)	21
SOMALILAND (French), Djibouti (NO DST)	21
SOMALIA, Mogadiscio (NO DST)	21
SOUTH GEORGIA I. (NO DST)	4:30 am
SOUTH ORKNEY Is. (NO DST)	27
SOUTH SANDWICH Is. (NO DST)	26
SOUTH SHETLAND Is.	29

M −12	10	MARSHALL ISLANDS	6 pm	7 pm	8 pm	9 pm	10 pm	11 pm	MIDNT	1 am	2 am	3 am	4 am	5 am	6 am	7 am	8 am	9 am	10 am	11 am	NOON	1 pm	2 pm	3 pm	4 pm	5 pm
L −11	11	NEW CALEDONIA	5 pm	6 pm	7 pm	8 pm	9 pm	10 pm	11 pm	MIDNT	1 am	2 am	3 am	4 am	5 am	6 am	7 am	8 am	9 am	10 am	11 am	NOON	1 pm	2 pm	3 pm	4 pm
K −10	12	MELBOURNE	4 pm	5 pm	6 pm	7 pm	8 pm	9 pm	10 pm	11 pm	MIDNT	1 am	2 am	3 am	4 am	5 am	6 am	7 am	8 am	9 am	10 am	11 am	NOON	1 pm	2 pm	3 pm
I −9	13	TOKYO	3 pm	4 pm	5 pm	6 pm	7 pm	8 pm	9 pm	10 pm	11 pm	MIDNT	1 am	2 am	3 am	4 am	5 am	6 am	7 am	8 am	9 am	10 am	11 am	NOON	1 pm	2 pm
H −8	14	PHILIPPINE ISLANDS	2 pm	3 pm	4 pm	5 pm	6 pm	7 pm	8 pm	9 pm	10 pm	11 pm	MIDNT	1 am	2 am	3 am	4 am	5 am	6 am	7 am	8 am	9 am	10 am	11 am	NOON	1 pm
G −7	15	THAILAND	1 pm	2 pm	3 pm	4 pm	5 pm	6 pm	7 pm	8 pm	9 pm	10 pm	11 pm	MIDNT	1 am	2 am	3 am	4 am	5 am	6 am	7 am	8 am	9 am	10 am	11 am	NOON
		Burma	12:30 pm	1:30 pm	2:30 pm	3:30 pm	4:30 pm	5:30 pm	6:30 pm	7:30 pm	8:30 pm	9:30 pm	10:30 pm	11:30 pm	12:30 am	1:30 am	2:30 am	3:30 am	4:30 am	5:30 am	6:30 am	7:30 am	8:30 am	9:30 am	10:30 am	11:30 am
F −6	16	STALINABAD	NOON	1 pm	2 pm	3 pm	4 pm	5 pm	6 pm	7 pm	8 pm	9 pm	10 pm	11 pm	MIDNT	1 am	2 am	3 am	4 am	5 am	6 am	7 am	8 am	9 am	10 am	11 am
	17	INDIA	11:30 am	12:30 pm	1:30 pm	2:30 pm	3:30 pm	4:30 pm	5:30 pm	6:30 pm	7:30 pm	8:30 pm	9:30 pm	10:30 pm	11:30 pm	12:30 am	1:30 am	2:30 am	3:30 am	4:30 am	5:30 am	6:30 am	7:30 am	8:30 am	9:30 am	10:30 am
E −5	18	WEST PAKISTAN	11 am	NOON	1 pm	2 pm	3 pm	4 pm	5 pm	6 pm	7 pm	8 pm	9 pm	10 pm	11 pm	MIDNT	1 am	2 am	3 am	4 am	5 am	6 am	7 am	8 am	9 am	10 am
D −4	19	STALINGRAD	10 am	11 am	NOON	1 pm	2 pm	3 pm	4 pm	5 pm	6 pm	7 pm	8 pm	9 pm	10 pm	11 pm	MIDNT	1 am	2 am	3 am	4 am	5 am	6 am	7 am	8 am	9 am
	20	IRAN	9:30 am	10:30 am	11:30 am	12:30 pm	1:30 pm	2:30 pm	3:30 pm	4:30 pm	5:30 pm	6:30 pm	7:30 pm	8:30 pm	9:30 pm	10:30 pm	11:30 pm	12:30 am	1:30 am	2:30 am	3:30 am	4:30 am	5:30 am	6:30 am	7:30 am	8:30 am
C −3	21	BAGHDAD; MOSCOW	9 am	10 am	11 am	NOON	1 pm	2 pm	3 pm	4 pm	5 pm	6 pm	7 pm	8 pm	9 pm	10 pm	11 pm	MIDNT	1 am	2 am	3 am	4 am	5 am	6 am	7 am	8 am
B −2	22	EGYPT; ISRAEL	8 am	9 am	10 am	11 am	NOON	1 pm	2 pm	3 pm	4 pm	5 pm	6 pm	7 pm	8 pm	9 pm	10 pm	11 pm	MIDNT	1 am	2 am	3 am	4 am	5 am	6 am	7 am
A −1	23	FRANCE; GERMANY	7 am	8 am	9 am	10 am	11 am	NOON	1 pm	2 pm	3 pm	4 pm	5 pm	6 pm	7 pm	8 pm	9 pm	10 pm	11 pm	MIDNT	1 am	2 am	3 am	4 am	5 am	6 am
Z 0	24	ENGLAND Greenwich Time	6 am	7 am	8 am	9 am	10 am	11 am	NOON	1 pm	2 pm	3 pm	4 pm	5 pm	6 pm	7 pm	8 pm	9 pm	10 pm	11 pm	MIDNT	1 am	2 am	3 am	4 am	5 am
		24 Hour Clock	0600	0700	0800	0900	1000	1100	1200	1300	1400	1500	1600	1700	1800	1900	2000	2100	2200	2300	2400	0100	0200	0300	0400	0500
N +1	25	ICELAND	5 am	6 am	7 am	8 am	9 am	10 am	11 am	NOON	1 pm	2 pm	3 pm	4 pm	5 pm	6 pm	7 pm	8 pm	9 pm	10 pm	11 pm	MIDNT	1 am	2 am	3 am	4 am
O +2	26	AZORES	4 am	5 am	6 am	7 am	8 am	9 am	10 am	11 am	NOON	1 pm	2 pm	3 pm	4 pm	5 pm	6 pm	7 pm	8 pm	9 pm	10 pm	11 pm	MIDNT	1 am	2 am	3 am
P +3	27	RIO de JANEIRO	3 am	4 am	5 am	6 am	7 am	8 am	9 am	10 am	11 am	NOON	1 pm	2 pm	3 pm	4 pm	5 pm	6 pm	7 pm	8 pm	9 pm	10 pm	11 pm	MIDNT	1 am	2 am
	28	NEWFOUNDLAND	2:30 am	3:30 am	4:30 am	5:30 am	6:30 am	7:30 am	8:30 am	9:30 am	10:30 am	11:30 am	12:30 pm	1:30 pm	2:30 pm	3:30 pm	4:30 pm	5:30 pm	6:30 pm	7:30 pm	8:30 pm	9:30 pm	10:30 pm	11:30 pm	12:30 am	1:30 am
Q +4	29	BERMUDA	2 am	3 am	4 am	5 am	6 am	7 am	8 am	9 am	10 am	11 am	NOON	1 pm	2 pm	3 pm	4 pm	5 pm	6 pm	7 pm	8 pm	9 pm	10 pm	11 pm	MIDNT	1 am

For the convenience of airline, steamship and communications personnel, in sending official messages, GREENWICH MEAN TIME is shown in Space 24.
For the convenience of the Armed Forces, and certain countries, conversions from the AM and PM System to the 24 Hour Clock System are shown in Space 24.
For your personal convenience, use blank spaces for names of places, Daylight Saving Time, and other data of special interest to you. See examples in spaces 4 and 15. Personalize your Simplifier.

Printed in U.S.A.

CANADA (6 Time Zones—DST OPTIONAL)
- Dawson (Yukon Terr.) (NO DST) ... 5
- Edmonton (Alberta) (NO DST) ... 3
- Fredericton (N.B.) (DST to Oct. 25) ... 29
- Halifax (N.S.) (DST to Oct. 25) ... 29
- Mantreal (Quebec) (DST to Oct. 25) ... 1
- Ottawa (Ont.) (DST to Oct. 25) ... 1
- Quebec (Que.) (DST to Oct. 25) ... 1
- Regina (Sask.) (DST to Oct. 25) ... 3
- St. John's (Newf.) (DST to Sept. 27) ... 28
- Toronto (Ont.) (DST to Oct. 25) ... 1
- Vancouver (Br. Col.) (DST to Sept. 27) ... 4
- Victoria (Br. Col.) (DST to Sept. 27) ... 4
- White Horse (Yukon Terr.) (NO DST) ... 5
- Winnipeg (Man.) (DST to Oct. 25) ... 2

CANAL ZONE, Balboa Heights (NO DST) ... 1
CANARY Is., La Polma (NO DST) ... 24
CAPE OF GOOD HOPE, Capetown (NO DST) ... 22
CAPE VERDE Is., Praia (NO DST) ... 26
CENTRAL AFR. REP., Bangui (NO DST) ... 23
CEYLON, Calombo (NO DST) ... 17
CHAD REP., Fort Lamy (NO DST) ... 23
CHANNEL Is., St. Heller (DST) ... 24
CHATHAM Is. (NO DST) ... 6:15 pm
CHILE, Santiago, Valparaiso (NO DST) ... 29
CHINA (NO DST) ... 14
COCOS Is. (NO DST) ... 12:30 pm
COLOMBIA, Bagata (NO DST) ... 1
COMORES Is. (Fr.) Dzaudzi (NO DST) ... 21
CONGO REP., Brazzaville (NO DST) ... 23
COOK Is., Avarua (NO DST) ... 7:30 pm
CORSICA, Ajaccia (NO DST) ... 23
COSTA RICA, San Jose (NO DST) ... 2
CRETE, Erakleian (NO DST) ... 22
CUBA, Havana (NO DST) ... 1
CYPRUS, Nicasia (NO DST) ... 22
CZECHOSLOVAKIA, Prague (NO DST) ... 23
DAHOMEY REP., Parto Novo (NO DST) ... 24
DENMARK, Capenhagen (NO DST) ... 23
DOMINICAN REP., Cuidad Trujillo ... 1
(DST Nav.-Jan.)
ECUADOR (NO DST) ... 1
Guayaquil, Quito
EGYPT, Caira (DST May 1st-Sept. 30) ... 22
EL SALVADOR, San Salvador (NO DST) ... 2
ENGLAND, Greenwich, London ... 24
(DST 3rd Sun. Apr.-1st Sun. Oct.)
ERITREA, Asmara (NO DST) ... 21
ESTONIA, Tallinn ... 21
ETHOPIA, Addis Ababa (NO DST) ... 21
FALKLAND Is. Part Stanley (NO DST) ... 29
FIJI Is. Suva (NO DST) ... 10
FINLAND, Helsinki (NO DST) ... 22
FORMOSA (TAIWAN), Taipei ... 14
(DST 1 Mar.-31 Oct.)
FRANCE, Paris ... 23
(DST all year. Carrected space shown)
FRANZ JOSEF LAND (NO DST) ... 19
GABON REP., Libreville (NO DST) ... 23
GALAPAGOS Is., El Pragresa (NO DST) ... 1
GAMBIA, Bathurst (NO DST) ... 24
GERMANY, EAST, Berlin (East) (NO DST) ... 23
GERMANY, WEST (NO DST) ... 23
FEDERAL REPUBLIC, Bann, Berlin (West)
Bad Hamburg v.d.H., Frankfurt /M
GHANA, Accra (NO DST) ... 24
GIBRALTAR (NO DST) ... 23
GILBERT & ELLICE Is., Tarawa (NO DST) ... 10
GOA, Pangim (NO DST) ... 17
GREECE, Athens (NO DST) ... 22
GREENLAND (3 Time Zones—NO DST)
- Angmagssalik ... 27
- Gadthaab ... 27
- Scoresby Sound ... 26
- Thule, Etah ... 29

GUADELOUPE Is. (Fr.) Basse Terre (NO DST) ... 29
GUAM, (Mariana Is.) Agana (NO DST) ... 12
GUATEMALA, Guatemala (NO DST) ... 2
GUIANA, BR., Georgetown (NO DST) ... 2:15 am
GUIANA, FR., Cayenne (NO DST) ... 29

LATVIA, Riga ... 21
LEBANON, Beirut (NO DST) ... 22
LEEWARD Is., Antiqua Is., St. John's ... 29
LIBERIA, Manrovia (NO DST) ... 5:16 am
Roberts Field ... 24
LIBYA, Bengasi, Tripoli (NO DST) ... 22
LIECHTENSTEIN, Vaduz ... 23
LITHUANIA, Vilna ... 21
LITTLE AMERICA (ANTARCTICA) ... 7
LOYALTY Is., Chepenehe ... 11
LUXEMBOURG, Luxembourg ... 23
(DST all year. Corrected space shown)
MACAO, Macao (NO DST) ... 14
MADEIRA Is. (DST 1st Sun. Apr.-1st Sun. Oct.) 25
MALAGASY REP., Tananarive (NO DST) ... 21
MALAYAN FED. (NO DST) ... 1:30 pm
Kuala Lumpur, Malacca, Penang
MALDIVE Is. Male (NO DST) ... 10:55 am
MALI FEDERATION (NO DST) ... 24
REP. OF SENEGAL, Dakar
SUDANESE REP., Bamako, Timbuktu
MALTA, Valletta (NO DST) ... 23
MANCHURIA, Mukden (Shenyang) ... 13
MARIANA Is., Saipan I. (NO DST) ... 12
MARQUESAS Is., Taiohae (NO DST) ... 6
MARSHALL Is., Eniwetok I., (NO DST) ... 10
MARTINIQUE I., Fort de France ... 29
MAURITANIAN ISLAMIC REP. (NO DST) ... 24
Nanakchatt
MAURITIUS I., Port Lauis (NO DST) ... 19
MEXICO (3 Time Zones)
- BAJA CALIF. NORTE, Mexicali ... 4
  (DST last Sun. Apr.-1st Sun. Sept.)
- BAJA CALIF. SUR, La Paz (NO DST) ... 3
- Guaymas (NO DST) ... 3
- Mexica City, Tapachula (NO DST) ... 2

MIDWAY Is., (NO DST) ... 7
MONACO, Manaca (DST) ... 23
MONGOLIA (2 Time Zones—NO DST)
- Ulaan Gaam ... 15
- Ulan Batar ... 14

MOROCCO, Tangier, Casablanca (NO DST) 24
MOZAMBIQUE, Lourenca Marques (NO DST) 2?
NAURU I. (NO DST) ... 5:30 pm
NEPAL, Katmandu (NO DST) ... 17
NETHERLANDS, Amsterdam ... 23
(DST all year. Carrected space shown)
NETHERLANDS ANTILLES
(NO DST) ... 1:30 am
Aruba I., Oranjestad
Banaire I., Kralendijk
Curacaa I., Willemstad
NEW CALEDONIA, Naumea (NO DST) ... 11
NEWFOUNDLAND (DST to last Sun. Sept.) 28
NEW GUINEA, NETH., Hallandia
(NO DST) ... 3:30 pm
NEW GUINEA, TERR. Of, (PAPUA) (NO DST) 12
Madang, Part Moresby
NEW HEBRIDES, Vila (NO DST) ... 11
NEW ZEALAND, Wellingtan ... 10
(½ hr. DST all yr. Carrected space shawn.)
NICARAGUA, Managua (DST) ... 2
NICOBAR Is., Part Blair (NO DST) ... 12:30 pm
NIGER REP., Niamey (NO DST) ... 24
NIGERIA, Lagos (NO DST) ... 23
NORFOLK I. (NO DST) ... 5:30 pm
NORTH BORNEO, Jesseltan (NO DST) ... 14
NORWAY, Osla (DST May 31-Sept. 20) ... 23
NOVA SCOTIA, Halifax ... 29
(DST last Sun. April-last Sun. Oct.)
OKINAWA Is., Naha (NO DST) ... 13
OMAN SULTANATE (NO DST) ... 19
Muscat, Nizwa
ORKNEY Is., Kirkwall (NO DST) ... 24
PAKISTAN (NO DST) ... 16
- EAST PAKISTAN, Chittagang ... 16
- WEST PAKISTAN, Karachi ... 18

PALESTINE (Gaza Area) Gaza (NO DST) ... 22
PALMER PEN. (ANTARCTICA) (NO DST) ... 29
PANAMA, Colon, Panama (NO DST) ... 1

SOUTH WEST AFRICA, Windhoek (NO DST) 22
SPAIN, Madrid ... 23
(DST all year. Corrected space shown.)
SPANISH WEST AFRICA (RIO de ORO)(NO DST) 24
Villa Cisneros (NO DST)
SUDAN, Khartoum (NO DST) ... 22
SURINAM, Paramaribo (NO DST) ... 28
SVALBARD (Spitsbergen) (NO DST) ... 23
SWAZILAND, Mbabane (NO DST) ... 22
SWEDEN, Stockholm (NO DST) ... 23
SWITZERLAND, Bern, Geneva (NO DST) ... 23
SYRIA, Damascus (DST 8 May-30 Sept.) ... 22
TAHITI I. (Society Is.) (NO DST) ... 6
TAIWAN (FORMOSA) ... 14
(DST Zero hour 1 Apr. ta 2400 hours 30 Sept.)
TANGANYIKA, Dar es Salaam (NO DST) ... 21
TASMANIA, Habart (NO DST) ... 12
THAILAND (SIAM), Bangkok (NO DST) ... 15
TIBET, Lhasa (NO DST) ... 14
TOGOLAND (French), Lame (NO DST) ... 24
TONGA Is., Nukualafa ... 6:20 pm
(DST Oct.-Mar.)
TRIESTE (NO DST) ... 23
TRINIDAD, Port-af-Spain (DST) ... 29
TRUCIAL OMAN, Sharja (NO DST) ... 19
TRUK I. (Caraline Is.) (NO DST) ... 11
TUNISIA, Tunis (NO DST) ... 23
TURKEY, Ankara (NO DST) ... 22
UGANDA, Entebbe (NO DST) ... 21
UNION OF SOUTH AFRICA (NO DST) ... 22
Capetown, Jahannesburg, Pretoria
UNION OF SOVIET SOCIALIST REPUBLICS (11 Time Zones)
(DST all year. Corrected spaces shown.)
- Alma-Ata, KAZAKH (SSR) ... 16
- Ashkhabad, TURKMEN (SSR) ... 18
- Baku, AZERBAIDZHAN (SSR) ... 19
- Chita (RSFSR) ... 13
- Frunze, KIRGHIZ (SSR) ... 16
- Irkutsk (RSFSR) ... 14
- Kiev, UKRAINE (SSR) ... 21
- Kishinev, MOLDAVIA (SSR) ... 21
- Magadan (RSFSR) ... 11
- Minsk, BYELORUSSIA (SSR) ... 21
- Moscaw ... 21
- Murmansk (Kal'skiy Peninsula) ... 21
- Petrapavlavsk (Kamchatka Pen.) ... 10
- Petrazavodsk, KARELIA (SSR) ... 21
- Riga, LATVIA (SSR) ... 21
- Stalinbad, TADZHIK (SSR) ... 16
- Tallinn, ESTONIA (SSR) ... 21
- Tashkent, UZBEK (SSR) ... 16
- Tiflis, GEORGIA (SSR) ... 19
- Tamsk (RSFSR) ... 15
- Uelen (Chukatskiv Pen.) ... 7
- Vilna, LITHUANIA (SSR) ... 21
- Vladivastak (RSFSR) ... 12
- Yalta (Crimean Peninsula) ... 21
- Yerevan, ARMENIA (SSR) ... 19

UNITED ARAB REP. (See separate listings)
UNITED KINGDOM (See separate listings)
UNITED STATES OF AMERICA
(See spaces 1 ta 4)
UPPER VOLTA, Ouagadougou ... 24
URUGUAY, Mantevideo ... 27
(½ hr. DST all yr. Corrected space shawn)
VATICAN CITY, Papacy (NO DST) ... 23
VENEZUELA (NO DST) ... 1:30 am
(Caracas, Maracaiba)
VIETNAM, NORTH, Hanoi (NO DST) ... 15
VIETNAM, REP., Saigon (NO DST) ... 15
VIRGIN Is. (U.S.A.), (NO DST) ... 29
Charlotte Amalie
VOLTAIC REP., Ouagadougou (NO DST) ... 24
WAKE ISLAND (NO DST) ... 10
Lat. 19°18′ N; Lang. 166°35′ E.
WALES, Cardiff ... 24
(DST 3rd Sun. Apr.-1st Sun. Oct.)
WINDWARD Is. (Grenada I.) St. Gearge's ... 29
YEMEN, San'a ... 22
Space 21 gives appraximate time.)
(See Note under Saudi Arabia)
YUGOSLAVIA, Belgrade (NO DST) ... 23
ZANZIBAR, Zanzibar (NO DST) ... 21

Other Rider Books!

ELECTRONIC TECHNOLOGY SERIES

edited by Alex. Schure, Ph.D., Ed.D.

An economically priced series of books devoted to the explanation of the basic concepts and principles of individual phases of electronic technology. Each book deals with a specialized subject; groups of these books form broad categories in the study of electronic technology.

Aimed for use by students in technical institutes, junior colleges, adult education classes, vocational schools teaching electronic technology, operators of communication equipments such as radio amateurs, commercial ship and broadcast station operators, electronics laboratory technicians, and experimenters who desire a more than casual understanding of the subjects covered.

Soft Covers, 5½ x 8½", illus.

RC & RL TIME CONSTANT
#166 .... $ .90

F-M LIMITERS & DETECTORS
#166-2 .... $ .90

FREQUENCY MODULATION
#166-3 .... $ .90

CRYSTAL OSCILLATORS
#166-4 .... $1.25

A-M DETECTORS
#166-5 .... $1.25

LIMITERS & CLIPPERS
#166-6 .... $1.25

MULTIVABRATORS
#166-7 .... $ .90

R-F TRANSMISSION LINES
#166-8 .... $1.25

AMPLITUDE MODULATION
#166-9 .... $1.25

BLOCKING OSCILLATORS
#166-10 .... $1.25

WAVE PROPAGATION
#166-11 .... $1.25

SUPERHETERODYNE CONVERTERS & I-F AMPLIFIERS
#166-12 .... $ .90

L-C OSCILLATORS
#166-13 .... $1.25

ANTENNAS
#166-14 .... $1.50

INVERSE FEEDBACK
#166-15 .... $ .90

RESONANT CIRCUITS
#166-16 .... $1.25

ELECTROSTATICS
#166-17 .... $1.35

D-C CIRCUIT ANALYSIS
#166-8 .... $1.35

A-C CIRCUIT ANALYSIS
#166-19 .... $1.80

VACUUM TUBE RECTIFIERS
#166-21 .... $1.50

VACUUM TUBE CHARACTERISTICS
#166-22 .... $1.80

IMPEDANCE MATCHING
#166-23 .... $2.90

GAS TUBES
#166-24 .... $1.50

R-F AMPLIFIERS
#166-27 .... $2.40

VIDEO AMPLIFIERS
#166-28 .... $1.80

LOW-FREQUENCY AMPLIFIERS
#166-30 .... $1.80

LOW-FREQUENCY AMPLIFIER SYSTEMS
#166-31 .... $1.80

PHOTOTUBES
#166-33 .... $1.80

Other titles coming soon . . .

MAGNETISM & ELECTROMAGNETISM
ADVANCED MAGNETISM & ELECTROMAGNETISM
TRANSISTOR FUNDAMENTALS
MAGNETIC AMPLIFIERS
MICROWAVE TUBES
ELECTRON OPTICS
WAVEGUIDES
TRANSMITTING TUBES
MICROWAVE ANTENNAS
TRANSFORMERS
FILTERS & ATTENUATORS
MICROWAVE OSCILLATORS

JOHN F. RIDER PUBLISHER, INC., 116 WEST 14th ST., N. Y. 11, N. Y.